



HAL
open science

Removal of organic pollutants from water by electro-Fenton and electro-Fenton like processes

Heng Lin

► **To cite this version:**

Heng Lin. Removal of organic pollutants from water by electro-Fenton and electro-Fenton like processes. Geophysics [physics.geo-ph]. Université Paris-Est, 2015. English. NNT : 2015PESC1058 . tel-01336262

HAL Id: tel-01336262

<https://theses.hal.science/tel-01336262v1>

Submitted on 22 Jun 2016

HAL is a multi-disciplinary open access archive for the deposit and dissemination of scientific research documents, whether they are published or not. The documents may come from teaching and research institutions in France or abroad, or from public or private research centers.

L'archive ouverte pluridisciplinaire **HAL**, est destinée au dépôt et à la diffusion de documents scientifiques de niveau recherche, publiés ou non, émanant des établissements d'enseignement et de recherche français ou étrangers, des laboratoires publics ou privés.

Joint PhD degree in Environmental Science & Technology



WUHAN UNIVERSITY

Docteur de l'Université Paris-Est

Spécialité : Science et Technique de l'Environnement

PhD degree of Wuhan University

Speciality: Environmental Engineering

Thèse de doctorat d'université – PhD thesis

Heng LIN

Removal of organic pollutants from water by indirect electro-oxidation using hydroxyl ($\cdot\text{OH}$) and sulfate ($\text{SO}_4^{\cdot-}$) radical species

Élimination des polluants organiques de l'eau par électrochimie indirecte basée sur les radicaux hydroxyles ($\cdot\text{OH}$) and sulfate ($\text{SO}_4^{\cdot-}$)

To be defended on **May 29, 2015**

In front of the PhD committee

| | | |
|------------------------------|-------------|-------------------------------|
| Prof. Ignacio SIRES SADORNIL | Reviewer | Barcelona University - Spain |
| Prof. Zhihui AI | Reviewer | Central China Normal Univ. |
| Prof. Mehmet A. OTURAN | Promotor | Université Paris-Est - France |
| Prof. Hui ZHANG | Co-promotor | Wuhan University - China |
| Dr. Nihal OTURAN | Examiner | Université Paris-Est - France |
| Prof. Feng WU | Examiner | Wuhan University - China |

Acknowledgements

I would like to thank gratefully to my supervisors Prof. Mehmet A. Oturan and Prof. Hui Zhang for giving me the chance to conduct the thesis work. It is my pleasure to work with Prof. Mehmet A. Oturan and Prof. Hui Zhang and I learned a lot of things from them.

I would also like to thank Dr. Nihal Oturan for giving me precious advice and technical supports.

I wish to express my gratitude to Prof. Ignacio Sirés (Barcelona University, Spain) and Prof. Zhihui Ai (Central China Normal University, China) for reading and evaluating my thesis. I also wish to thank Dr Nihal Oturan (Université Paris-Est, France) and Professor Feng Wu (Wuhan University, China) for their acceptance to be part of thesis jury.

I also wish to thank all my colleagues in Advanced Oxidation Lab of Wuhan University and Laboratoire Géomatériaux et Environmental of Université Paris-Est for their kindness help.

Thank for the fund support of China Scholarship Council (CSC) affiliated with the Ministry of Education of P.R. China.

Finally, I would especially like to thank my parents for always been there with encouragement.

Table of contents

| | |
|--|------------|
| Acknowledgements..... | II |
| List of Abbreviations..... | I |
| Abstract..... | III |
| Chapter 1 Introduction..... | 1 |
| 1.1 Background..... | 2 |
| 1.2 Research goals and objective | 4 |
| 1.3 Structure of the thesis..... | 5 |
| Chapter 2 Literature review..... | 13 |
| 2.1 Artificial sweeteners..... | 14 |
| 2.1.1 Aspartame..... | 16 |
| 2.1.2 Saccharin | 17 |
| 2.1.3 Sucralose | 17 |
| 2.2 Synthetic dyes | 18 |
| 2.3 Advanced oxidation processes (AOPs) in dye removal | 20 |
| 2.3.1 Fenton process..... | 20 |
| 2.3.2 Electrochemical Advanced Oxidation Processes (EAOPs) based on Fenton's reaction..... | 22 |
| 2.3.3 Sulfate radical-based Fenton-like process | 27 |
| 2.4 Iron oxides applied in AOPs based on Fenton and Fenton-like process | 30 |
| 2.4.1 Goethite (α -FeOOH) | 31 |
| 2.4.2 Magnetite (Fe_3O_4) | 31 |
| Chapter 3 Treatment of aspartame (ASP) in aqueous solution by electro-Fenton process | 49 |
| 3.1 Introduction..... | 50 |
| 3.2 Materials and methods | 50 |
| 3.2.1 Chemicals..... | 50 |
| 3.2.2 Procedures and equipment | 51 |
| 3.2.3 High performance liquid chromatography (HPLC) analysis..... | 51 |
| 3.2.4 Ion chromatography (IC) analysis..... | 52 |
| 3.2.5 Total organic carbon (TOC) analysis..... | 52 |
| 3.2.6 Toxicity measurements..... | 52 |
| 3.3 Results and discussion | 53 |

| | |
|---|-----------|
| 3.3.1 Effect of catalyst concentration on ASP degradation | 53 |
| 3.3.2 Effect of applied current on ASP degradation | 56 |
| 3.3.3 Determination of absolute constants for oxidation of ASP by hydroxyl radicals... | 59 |
| 3.3.4 The effect of catalyst concentration and applied current on ASP mineralization ... | 60 |
| 3.3.5 Identification and evolution of carboxylic acids | 63 |
| 3.3.6 Identification and evolution of inorganic ions..... | 64 |
| 3.3.7 The evolution of solution toxicity with reaction time | 66 |
| 3.4 Conclusions..... | 67 |
| Chapter 4 Treatment of saccharin (SAC) in aqueous solution by electro-Fenton process | 72 |
| 4.1 Introduction..... | 73 |
| 4.2 Materials and methods | 73 |
| 4.2.1 Chemicals..... | 73 |
| 4.2.2 Electrochemical apparatus and procedures | 73 |
| 4.2.3 Analytical methods and procedures..... | 74 |
| 4.2.4 Toxicity measurements..... | 75 |
| 4.3 Results and discussion | 75 |
| 4.3.1 Effect of supporting electrolyte on the degradation SAC..... | 75 |
| 4.3.2 Effect of anode materials on the removal and mineralization of SAC | 79 |
| 4.3.3 Effect of Fe ²⁺ concentration on the removal of SAC | 81 |
| 4.3.4 Effect of applied current on the removal of SAC..... | 82 |
| 4.3.5 Determination of the rate constant of reaction between SAC and [•] OH..... | 84 |
| 4.3.6 The effect of Fe ²⁺ concentration and applied current on SAC mineralization | 85 |
| 4.3.7 Identification and evolution of short-chain carboxylic acids | 88 |
| 4.3.8 Evolution of SAC solution toxicity during electro-Fenton process | 90 |
| 4.4 Conclusions..... | 91 |
| Chapter 5 Electrochemical mineralization of sucralose in aqueous medium at ambient temperature by electro-Fenton process | 95 |
| 5.1 Introduction..... | 96 |
| 5.2 Materials and methods | 96 |
| 5.2.1 Chemicals..... | 96 |
| 5.2.2 Electrochemical apparatus and procedures | 96 |
| 5.2.3 Analytical methods and procedures..... | 97 |
| 5.2.4 Toxicity measurements..... | 98 |
| 5.3 Results and discussion | 98 |

| | |
|---|------------|
| 5.3.1 Effect of Fe ²⁺ concentration on the mineralization of sucralose | 98 |
| 5.3.2 Effect of current intensity on the mineralization of SUC aqueous solutions | 101 |
| 5.3.3 Mineralization current efficiency (MCE)..... | 102 |
| 5.3.4 Identification and evolution of short-chain carboxylic acids | 104 |
| 5.3.5 Identification and evolution of chloride ions | 106 |
| 5.3.6 The evolution of toxicity with reaction time | 107 |
| 5.4 Conclusions..... | 109 |
| Chapter 6 Decolorization of Orange II in water by electro/α-FeOOH/PDS process..... | 112 |
| 6.1 Introduction..... | 113 |
| 6.2 Materials and methods | 113 |
| 6.2.1 Chemicals..... | 113 |
| 6.2.2 Electrochemical apparatus and procedures | 114 |
| 6.2.3 Analytical methods and procedures..... | 115 |
| 6.2.4 Box-Behnken design (BBD) | 115 |
| 6.3 Results and discussion | 117 |
| 6.3.1 Decolorization of Orange II under different systems | 117 |
| 6.3.2 Effect of initial pH | 122 |
| 6.3.3 Response surface analysis | 124 |
| 6.3.4 Stability of α -FeOOH..... | 131 |
| 6.3.5 Changes in the UV-visible spectrum and mineralization efficiency of Orange II | 131 |
| 6.4 Conclusion | 133 |
| Chapter 7 Decolorization of Orange II in water by electro/Fe₃O₄/PDS process..... | 138 |
| 7.1 Introduction..... | 139 |
| 7.2 Materials and methods | 139 |
| 7.2.1 Materials..... | 139 |
| 7.2.2 Experimental | 139 |
| 7.2.3 Analysis..... | 140 |
| 7.3 Results and discussion | 142 |
| 7.3.1 Decolorization of Orange II under different systems | 142 |
| 7.3.2 Effect of initial pH | 147 |
| 7.3.3 Effect of current density | 148 |
| 7.3.4 Effect of PDS concentration..... | 149 |
| 7.3.5 Effect of Fe ₃ O ₄ dosage | 150 |
| 7.3.6 Stability of Fe ₃ O ₄ | 151 |

| | |
|---|------------|
| 7.3.7 The degradation pathway of Orange II..... | 153 |
| 7.3.8 The changes of TOC and toxicity with reaction time..... | 155 |
| 7.3.9 Electrical energy consumption estimation..... | 157 |
| 7.4 Conclusions..... | 158 |
| Chapter 8 General conclusion and future perspectives | 162 |
| 8.1 General conclusion..... | 163 |
| 8.2 Future prespectives | 164 |
| Publications | 166 |

List of Abbreviations

| | |
|-----------|--|
| 2,4-DP | 2-(2,4-dichlorophenoxy)-propionic acid |
| 2,4,5-T | 2,4,5-trichlorophenoxyacetic acid |
| 2,4,5-TCP | 2,4,5-trichlorophenol |
| 4-NP | 4-nitrophenol |
| AAS | Atomic absorption spectroscopy |
| ACF | Activated carbon fiber |
| AOPs | Advance oxidation processes |
| ANOVA | Analysis of Variance |
| ASP | Aspartame |
| BA | Benzoic acid |
| BBD | Box-Behnken design |
| BDD | Boron-doped diamond |
| BPA | Bisphenol A |
| CA | Clofibric acid |
| CV | Coefficient of variation |
| DSA | Dimensionally stable anode |
| DC | Direct current |
| DO | Dissolved oxygen |
| EAOPs | Electrochemical advanced oxidation processes |
| EC | Electrochemical |
| EE/O | Electrical energy consumption per order of magnitude |
| EFO | Electro-Fe(II)/Oxone |
| EI | Electronimpact |
| E.U. | European Union |
| GC–MS | Gas chromatography–mass spectrometry |
| GDEs | Gas diffusion electrodes |
| HPLC | High performance liquid chromatography |

| | |
|-----------|--|
| IC | Ion chromatography |
| k_{app} | Apparent rate constant values |
| MCE | Mineralization current efficiency |
| MLSS | Mixed liquor suspended solids |
| NDIR | Non dispersive infra-red absorption detector |
| OUR | Oxygen uptake rate |
| PDS | Peroxydisulfate |
| PMS | Peroxymonosulfate |
| PPCPs | Pharmaceuticals and personal care products |
| PS | Persulfate |
| RhB | Rhodamine B |
| RSM | Response surface methodology |
| RVC | Reticulated vitreous carbon |
| SAC | Saccharin |
| SCP | Sulfachloropyridazine |
| SMM | Sulfamonomethoxine |
| SOUR | Specific oxygen uptake rate |
| SUC | Sucralose |
| TCE | Trichloroethylene |
| TOC | Total organic carbon |
| t_R | Retention time |
| UV | Ultraviolet |
| XPS | X-ray photoelectron spectroscopy |
| XRD | X-ray diffraction |

Abstract

In recent years, more and more refractory and toxic organic contaminants are detected in wastewater, surface water and ground water. Many of these organic pollutants can hardly be degraded by conventional water treatments. Advanced oxidation processes (AOPs), which based on in situ generation of strong oxidants, mainly the generation of hydroxyl radicals ($\cdot\text{OH}$), have been applied to treat various non-biodegradable organic compounds in water. Conventional Fenton technology is a promising AOP for the treatment of organic contaminants in water. In Fenton process, hydroxyl radical, which is the second strongest oxidant (after fluorine), is formed through Fenton's reaction and then degrade organic pollutants. Similar to conventional Fenton process, transition metal ions (Fe^{2+} , Co^{2+} , Ag^+ , etc.) can also activate persulfate (PS) and generate sulfate radicals ($\text{SO}_4^{\cdot-}$). Sulfate radical is a powerful oxidant and can oxidize most of organic pollutants. This process is named Fenton-like process. There are some disadvantages existed in conventional Fenton and Fenton-like process. For example, a high concentration of Fe^{2+} is required and a large amount of iron sludge is generated. In order to solve these problems, electro-Fenton and sulfate radical-based electro-Fenton-like processes are developed. Fe^{2+} can be regenerated via cathodic reduction in electro-Fenton and electro-Fenton-like processes. Therefore, the Fe^{2+} concentration used in these processes is much lower than that in Fenton and Fenton-like processes. In this paper, electro-Fenton and sulfate radical-based electro-Fenton-like processes were used to degrade artificial sweeteners and azo dyes. The removal efficiency, the oxidation mechanism, degradation pathway and toxicity evolution of target pollutants were investigated.

(1) A detailed discussion on the oxidative degradation of artificial sweetener aspartame (ASP) in acidic aqueous solution containing catalytic amount of Fe^{2+} by using electro-Fenton process is reported. In electro-Fenton process, ASP could be completely removed in a 30 min reaction and the removal of ASP followed pseudo-first-order kinetics. The increase of Fe^{2+} concentration and applied current to certain extent could increase the removal efficiency of ASP, while further increasing the Fe^{2+} concentration and applied current could lead to the decrease of removal efficiency. Absolute rate constant of

hydroxylation reaction of ASP was determined as $(5.23 \pm 0.02) \times 10^9 \text{ M}^{-1} \text{ S}^{-1}$. When boron-doped diamond (BDD) electrode was used as anode, ASP could be completely mineralized in a 360 min treatment. Short-chain aliphatic acids such as oxalic, oxamic and maleic acid were identified as aliphatic intermediates in the electro-Fenton process. The bacteria luminescence inhibition showed the toxicity of ASP solution increased at the beginning of electrolysis, and then it declined until lower than the untreated ASP solution at the end of the reaction.

(2) The removal of artificial sweetener saccharin (SAC) in aqueous solution by electro-Fenton processes was performed. Experiments were carried out in an undivided cylindrical glass cell with a carbon-felt cathode and a DSA, Pt or boron-doped diamond (BDD) anode. The removal of SAC by electrochemically generated hydroxyl radicals followed pseudo-first order kinetics with all the anodes. The absolute rate constant of the SAC hydroxylation reaction was found as $(1.85 \pm 0.01) \times 10^9 \text{ M}^{-1} \text{ s}^{-1}$, which was determined by using the competition kinetic method. The comparative study of TOC removal efficiency during electro-Fenton treatment indicated a higher mineralization rate with BDD than Pt anode. Formation of oxalic, formic, and maleic acids were observed during electro-Fenton process. The evolution of toxicity of SAC and/or its reaction by-products based on the *V. fischeri* bacteria luminescence inhibition was studied.

(3) The removal of artificial sweetener sucralose (SUC) in aqueous solution by electro-Fenton processes was also performed in this study. Hydroxyl radical ($\cdot\text{OH}$), a highly powerful oxidizing agent, was generated catalytically via the electrochemically assisted Fenton's reaction in the bulk and water oxidation on the surface of anode. The effect of Fe^{2+} concentration and applied current on the mineralization of SUC was evaluated. A higher mineralization rate was obtained with BDD than that of Pt anode. Mineralization current efficiency (MCE) was calculated and better mineralization current efficiency was achieved at relatively short electrolysis time and low applied current. The concentration of the formed carboxylic acids and released inorganic ion was monitored by ion-exclusion chromatography and ion chromatography (IC). The toxicity of SUC and/or its reaction by-products was investigated based on the *V. fischeri* bacteria luminescence inhibition.

(4) The removal of Orange II by a novel electro/ α -FeOOH/peroxydisulfate process is reported in this study. In electro/ α -FeOOH/peroxydisulfate process, sulfate radicals were generated by activating peroxydisulfate (PDS) with goethite (α -FeOOH). When combined with electrochemical process, the Fe(III) on the surface of α -FeOOH converts to Fe(II) by cathodic reduction. The effect of initial pH on the decolorization of Orange II was investigated. Response surface methodology (RSM) based on Box-Behnken statistical experiment design (BBD) was applied to analyze the experimental variables. The positive and negative effects on the decolorization of Orange II were determined. The response surface methodology models were derived based on the results of the pseudo-first-order decolorization rate constant and the response surface plots were developed accordingly. The results indicated that the applied current showed a positive effect on the decolorization rate constant of Orange II. The interaction of α -FeOOH dosage and PDS concentration was significant. The ANOVA results confirmed that the proposed models were accurate and reliable for the analysis of the variables of EC/ α -FeOOH/PDS process.

(5) The decolorization of Orange II in aqueous solution by magnetite (Fe_3O_4) activated peroxydisulfate (PDS) oxidation in an electrochemical reactor (EC/ Fe_3O_4 /PDS process) was performed in this study. Various parameters were investigated to optimize the process, including initial pH, current density, PDS concentration and Fe_3O_4 dosage. The stability of Fe_3O_4 particles was observed by recycle experiments. The X-ray photoelectron spectroscopy (XPS) was applied to investigate the surface properties of Fe_3O_4 before and after reaction. GC-MS analysis was employed to identify the intermediate products and a plausible degradation pathway of Orange II was proposed. The change of acute toxicity during the treatment was investigated by activated sludge inhibition test. The TOC removal efficiency was 30.0% in a 90 min treatment.

Keywords: Electro-Fenton; Electro-Fenton-like process; Hydroxyl radicals; Sulfate radicals; Organic pollutants

Chapter 1 Introduction

1.1 Background

Water quality and availability is a challenging problem facing our society all over the world (Rivas *et al.* 2009; Bernal-Mart ínez *et al.* 2010). In recent years, more and more organic contaminants from contaminated soil, agricultural runoff, industrial wastewater and hazardous compounds storage leakage are detected in wastewater, surface water and ground water. The presence of these organic compounds in water poses serious threat to public health since most of them are toxic, endocrine disrupting, mutagenic or potentially carcinogenic to humans, animals and aquatic life in general (Babuponnusami and Muthukumar 2014). Many organic pollutants are considered as toxic and detrimental even when present at very low concentrations. Moreover, many organic contaminants cannot be eliminated by conventional physical separation methods or cannot be degraded by biological processes due to the recalcitrant nature of the pollutants present (P érez *et al.* 2002). Therefore, more powerful wastewater treatment methods are required.

Advance oxidation processes (AOPs) have been proved to be effective for the degradation of many toxic/persistent organic contaminants from aqueous medium such as coloring matters, pesticides, artificial sweeteners and pharmaceuticals and personal care products (Kim and Tanaka 2009; Wang *et al.* 2012; Calza *et al.* 2013; Janin *et al.* 2013; El-Ghenymy *et al.* 2014; Rodrigo *et al.* 2014; Wang *et al.* 2014). Moreover, AOPs have been successfully used as pretreatment methods to reduce the concentration of toxic organic compounds that recalcitrant to biological wastewater treatments (Stasinakis 2008). AOPs are based on the in-situ generation of hydroxyl radical ($\cdot\text{OH}$, $E^0(\cdot\text{OH}/\text{H}_2\text{O})= 2.80 \text{ V/SHE}$) (Evgenidou *et al.* 2007; Salazar *et al.* 2013; Oturan and Aaron, 2014), which is the second strongest oxidizing agent after fluorine (Mousset *et al.* 2014a). AOPs are especially efficient for degrading aromatic molecules due to the electrophilic aromatic substitution of hydroxyl radical which then lead to the opening of the aromatic ring (Brillas *et al.* 2009; Mousset *et al.* 2014b). The most commonly used AOPs for the removal of organic pollutants from water is based on the Fenton's reagent (an aqueous mixture of Fe^{2+} and H_2O_2 that produces hydroxyl radicals)

(Babuponnusami and Muthukumar 2012; Basturk and Karatas 2014). It has been used as an attractive and effective technology for the degradation of various organic pollutants (Hermosilla *et al.* 2009a; Hermosilla *et al.* 2009b; Zazo *et al.* 2009; Hermosilla *et al.* 2012) because of the lack of toxicity of the reagents, eventually leaving no residues and the simplicity of the technology (Sun *et al.* 2007; Nidheesh and Gandhimathi 2012). However, the conventional Fenton process has the disadvantages of requirement of high Fe^{2+} concentration and the formation of Fe sludge which limit its application (Nidheesh and Gandhimathi 2012).

Electro-Fenton process, in which H_2O_2 is produced electrochemically and Fe^{2+} can be regenerated throughout the process, overcomes these disadvantages of conventional Fenton process. Compared to the conventional Fenton process, the electro-Fenton process has the advantage of regeneration of Fe^{2+} and avoiding the storing and transport of the H_2O_2 . Moreover, electricity as a clean energy source is used in the process, so the overall process does not create secondary pollutants (Jiang and Zhang 2007; Brillas *et al.* 2009). The electro-Fenton process has been successfully applied in wastewater treatment and the process efficiency has been experimentally confirmed by different authors for the treatment of media containing pesticides (Oturán *et al.* 2009; Yatmaz and Uzman 2009; Abdessalem *et al.* 2010), herbicides (Kaichouh *et al.* 2004; Da Pozzo *et al.* 2005; Garc ía *et al.* 2014), synthetic dyes (Cruz-González *et al.* 2010; Ghoneim *et al.* 2011; Kourdali *et al.* 2014), pharmaceuticals (El-Ghenymy *et al.* 2013; Feng *et al.* 2014; Yahya *et al.* 2014), and so on.

As a strong oxidant, persulfate (PS) is another popular reagent in the wastewater treatment because it is more stable than H_2O_2 and it can be transported over a long distance without alteration. Similar to the conventional Fenton process, PS can be activated by transition metals to generate sulfate radicals ($\text{SO}_4^{\cdot-}$), which have a high standard redox potential ($E^0 = 2.6 \text{ V/SHE}$) (Shukla *et al.* 2010; Deng and Ezyse 2011) and can oxidize organic compounds into small molecules and carbon dioxide (Gayathri *et al.* 2010). This process is also named Fenton-like process (Fernandez *et al.* 2003; Fernandez *et al.* 2004).

Like conventional Fenton process, Fe^{2+} is hard to be regenerated after conversion

to Fe^{3+} in sulfate radical-based Fenton-like process, thus high concentration of Fe^{2+} is required and a large amount of iron sludge is produced. In order to solve this problem, electrochemical (EC) technology was combined with Fenton-like process (electro-Fenton-like process) and used to treat herbicide 2,4,5-trichlorophenoxyacetic acid (2,4,5-T) (Wang and Chu 2011), azo dye Orange II (Wu *et al.* 2012), bisphenol A (BPA) (Lin *et al.* 2013), clofibric acid (CA) (Lin *et al.* 2014) and landfill leachate (Zhang *et al.* 2014). However, the electro-Fenton-like processes mentioned above are all homogeneous oxidation processes. The removal of metal ions from the effluent requires additional separation and disposal (Zhong *et al.* 2011). Therefore, various kinds of solid catalysts instead of soluble metal ions have received much attention. Compared with soluble metal ions, solid catalyst can be recovered and reused without being lost along with the effluent. As a result, different kinds of iron metal oxides (such as magnetite and goethite) are employed in the electro-Fenton-like process in this study.

In this work, electro-Fenton and electro-Fenton-like processes in the presence of different oxidants and catalysts were studied. As an emerging contaminant, artificial sweeteners are an essential part of food technology as a group of discrete chemical substances that possess intense sweetness. Synthetic dyes are one of the most common toxic pollutants in the natural environment around the world. These two types of organic compounds were selected as model pollutants in this thesis work.

1.2 Research goals and objective

The objective of this work was to study the removal of target pollutants from water using electro-Fenton and electro-Fenton-like processes. The optimal oxidation conditions were identified and the oxidation mechanisms were examined. To meet these goals, the following specific objectives were defined:

1. Conduct experiments to investigate the effect of the operation parameters on the degradation and mineralization of artificial sweetener aspartame (ASP) by electro-Fenton process. The concentration of inorganic ions and carboxylic acid released during the treatment was monitored.

2. Conduct experiments to investigate the degradation and mineralization of artificial sweetener saccharin (SAC) using electro-Fenton process. The comparison among different anode materials on the degradation and mineralization was investigated. Moreover, the toxicity of SAC and its byproducts during electro-Fenton process was determined.

3. Conduct experiment to investigate the mineralization of artificial sweetener sucralose (SUC) using electro-Fenton process. The influence of the operation parameters on the mineralization of SUC was investigated. The Mineralization current efficiency (MCE) was calculated to evaluate the mineralization capacity.

4. Fe^{2+} was replaced by goethite to activate PS and degraded azo dye Orange II in sulfate radical-based electro-Fenton-like process. The response surface methodology models were derived based on the results of the pseudo-first-order decolorization rate constant and the response surface plots were developed accordingly.

5. Magnetite was used as heterogeneous catalyst to degrade Orange II in sulfate radical-based electro-Fenton-like process. The surface properties of Fe_3O_4 before and after reaction were investigated. The intermediates of Orange II during the treatment were identified and a plausible degradation pathway was proposed. The change of acute toxicity during the treatment was investigated.

1.3 Structure of the thesis

This dissertation is composed of eight chapters.

Chapter 1 is an introduction, including background information of electro-Fenton and electro-Fenton-like processes and the chosen organic pollutants, research objectives and organization of this thesis.

Chapter 2 presents a review of recent work related to this study. Four parts are described:

2.1 Artificial sweeteners

2.2 Synthetic dyes

2.3 Advanced oxidation processes (AOPs)

2.4 Iron metal oxides application in AOPs

The following three chapters are the presentation of experiments results related to electro-Fenton process.

Chapter 3 is entitled “Treatment of aspartame in aqueous solution by electro-Fenton process”. The removal of ASP in electro-Fenton process was investigated. The effect of Fe^{2+} concentration and applied current on the degradation and mineralization of ASP was evaluated. The absolute rate constant for the reaction between ASP and $\cdot\text{OH}$ was determined by using the competition kinetic method. The concentration of the formed carboxylic acids and released inorganic ion was monitored by ion-exclusion chromatography and ion chromatography (IC). The toxicity of ASP and/or its reaction byproducts was studied based on the *V. fischeri* bacteria luminescence inhibition.

Chapter 4 is entitled “Treatment of saccharin (SAC) in aqueous solution by electro-Fenton process”. The removal of artificial sweeteners saccharin (SAC) in aqueous solution by electro-Fenton processes was performed in this study. Different anode materials on the removal and mineralization of SAC were tested. The absolute rate constant of the SAC hydroxylation reaction was determined. The evolution of carboxylic acids was determined by ion-exchange chromatography. The evolution of toxicity of SAC and/or its reaction byproducts based on the *V. fischeri* bacteria luminescence inhibition was studied.

Chapter 5 is entitled “Treatment of sucralose (SUC) in aqueous solution by electro-Fenton process”. The removal of artificial sweeteners SUC in aqueous solution by electro-Fenton processes was carried out in this study. The effect of Fe^{2+} concentration and applied current on the mineralization of SUC was evaluated. The concentration of the formed carboxylic acids and released inorganic ion was monitored by ion-exchange chromatography and ion chromatography. The toxicity of SUC and/or its reaction byproducts was investigated based on the *V. fischeri* bacteria luminescence inhibition.

The following two chapters are the parts devoted to the experiments results of electro-Fenton-like process.

Chapter 6 is entitled “Decolorization of Orange II in water by

electro/ α -FeOOH/PDS process". In this section, the removal of Orange II by electro/ α -FeOOH/peroxydisulfate process was investigated. Response surface methodology (RSM) based on Box-Behnken statistical experiment design (BBD) was applied to analyze the experimental variables. The positive and negative effects on the decolorization of Orange II were determined. The response surface methodology models were derived based on the results of the pseudo-first-order decolorization rate constant and the response surface plots were developed accordingly.

Chapter 7 is entitled "Decolorization of Orange II in water by electro/Fe₃O₄/PDS process". In this chapter, the decolorization of Orange II was performed in aqueous solution by Fe₃O₄ activated peroxydisulfate (PDS) oxidation in an electrochemical reactor (EC/Fe₃O₄/PDS process) was performed. Various parameters were investigated to optimize the process. The surface properties of Fe₃O₄ before and after reaction was investigate. The intermediates of Orange II during the treatment were identified and the degradation pathway was proposed. The change of acute toxicity during the treatment was investigated.

Finally, the thesis manuscript ends with Chapter 8 entitled "General conclusions and perspectives".

References

- Abdessalem, A.K., Bellakhal, N., Oturan, N., Dachraoui, M. and Oturan, M.A. (2010). Treatment of a mixture of three pesticides by photo- and electro-Fenton processes. *Desalination* 250(1), 450-455.
- Babuponnusami, A. and Muthukumar, K. (2012). Advanced oxidation of phenol: A comparison between Fenton, electro-Fenton, sono-electro-Fenton and photo-electro-Fenton processes. *Chemical Engineering Journal* 183, 1-9.
- Babuponnusami, A. and Muthukumar, K. (2014). A review on Fenton and improvements to the Fenton process for wastewater treatment. *Journal of Environmental Chemical Engineering* 2(1), 557-572.
- Basturk, E. and Karatas, M. (2014). Advanced oxidation of Reactive Blue 181 solution: A comparison between Fenton and Sono-Fenton Process. *Ultrasonics Sonochemistry*

21(5), 1881-1885.

- Bernal-Martínez, L.A., Barrera-Díaz, C., Solís-Morelos, C. and Natividad, R. (2010). Synergy of electrochemical and ozonation processes in industrial wastewater treatment. *Chemical Engineering Journal* 165(1), 71-77.
- Brillas, E., Sirés, I. and Oturan, M.A. (2009). Electro-Fenton process and related electrochemical technologies based on Fenton's reaction chemistry. *Chemical Reviews* 109(12), 6570-6631.
- Calza, P., Sakkas, V.A., Medana, C., Vlachou, A.D., Dal Bello, F. and Albanis, T.A. (2013). Chemometric assessment and investigation of mechanism involved in photo-Fenton and TiO₂ photocatalytic degradation of the artificial sweetener sucralose in aqueous media. *Applied Catalysis B: Environmental* 129, 71-79.
- Cruz-González, K., Torres-López, O., García-León, A., Guzmán-Mar, J.L., Reyes, L.H., Hernández-Ramírez, A. and Peralta-Hernández, J.M. (2010). Determination of optimum operating parameters for Acid Yellow 36 decolorization by electro-Fenton process using BDD cathode. *Chemical Engineering Journal* 160(1), 199-206.
- Da Pozzo, A., Merli, C., Sirés, I., Garrido, J., Rodríguez, R. and Brillas, E. (2005). Removal of the herbicide amitrole from water by anodic oxidation and electro-Fenton. *Environmental Chemistry Letters* 3(1), 7-11.
- Deng, Y. and Ezyske, C.M. (2011). Sulfate radical-advanced oxidation process (SR-AOP) for simultaneous removal of refractory organic contaminants and ammonia in landfill leachate. *Water Research* 45(18), 6189-6194.
- El-Ghenymy, A., Cabot, P.L., Centellas, F., Garrido, J.A., Rodríguez, R.M., Arias, C. and Brillas, E. (2013). Mineralization of sulfanilamide by electro-Fenton and solar photoelectro-Fenton in a pre-pilot plant with a Pt/air-diffusion cell. *Chemosphere* 91(9), 1324-1331.
- El-Ghenymy, A., Centellas, F., Garrido, J.A., Rodríguez, R.M., Sirés, I., Cabot, P.L. and Brillas, E. (2014). Decolorization and mineralization of Orange G azo dye solutions by anodic oxidation with a boron-doped diamond anode in divided and undivided tank reactors. *Electrochimica Acta* 130, 568-576.
- Evgenidou, E., Konstantinou, I., Fytianos, K., Poullos, I. and Albanis, T. (2007).

- Photocatalytic oxidation of methyl parathion over TiO₂ and ZnO suspensions. *Catalysis Today* 124(3–4), 156-162.
- Feng, L., Oturan, N., van Hullebusch, E.D., Esposito, G. and Oturan, M.A. (2014). Degradation of anti-inflammatory drug ketoprofen by electro-oxidation: comparison of electro-Fenton and anodic oxidation processes. *Environmental Science and Pollution Research*, 21(14), 8406-8416.
- Fernandez, J., Maruthamuthu, P., Renken, A. and Kiwi, J. (2004). Bleaching and photobleaching of Orange II within seconds by the oxone/Co²⁺ reagent in Fenton-like processes. *Applied Catalysis B: Environmental* 49(3), 207-215.
- Fernandez, J., Nadtochenko, V. and Kiwi, J. (2003). Photobleaching of Orange II within seconds using the oxone/Co²⁺ reagent through Fenton-like chemistry. *Chemical Communications* 18, 2382-2383.
- García, O., Isarain-Chávez, E., El-Ghenymy, A., Brillas, E. and Peralta-Hernández, J.M. (2014). Degradation of 2,4-D herbicide in a recirculation flow plant with a Pt/air-diffusion and a BDD/BDD cell by electrochemical oxidation and electro-Fenton process. *Journal of Electroanalytical Chemistry* 728, 1-9.
- Gayathri, P., Praveena Juliya Dorathi, R. and Palanivelu, K. (2010). Sonochemical degradation of textile dyes in aqueous solution using sulphate radicals activated by immobilized cobalt ions. *Ultrasonics Sonochemistry* 17(3), 566-571.
- Ghoneim, M.M., El-Desoky, H.S. and Zidan, N.M. (2011). Electro-Fenton oxidation of Sunset Yellow FCF azo-dye in aqueous solutions. *Desalination* 274(1–3), 22-30.
- Hermosilla, D., Cortijo, M. and Huang, C.P. (2009a). Optimizing the treatment of landfill leachate by conventional Fenton and photo-Fenton processes. *Science of The Total Environment* 407(11), 3473-3481.
- Hermosilla, D., Cortijo, M. and Huang, C.P. (2009b). The role of iron on the degradation and mineralization of organic compounds using conventional Fenton and photo-Fenton processes. *Chemical Engineering Journal* 155(3), 637-646.
- Hermosilla, D., Merayo, N., Ordóñez, R. and Blanco, Á. (2012). Optimization of conventional Fenton and ultraviolet-assisted oxidation processes for the treatment of reverse osmosis retentate from a paper mill. *Waste Management* 32(6), 1236-1243.

- Janin, T., Goetz, V., Brosillon, S. and Plantard, G. (2013). Solar photocatalytic mineralization of 2,4-dichlorophenol and mixtures of pesticides: Kinetic model of mineralization. *Solar Energy* 87, 127-135.
- Jiang, C.-c. and Zhang, J.-f. (2007). Progress and prospect in electro-Fenton process for wastewater treatment. *Journal of Zhejiang University SCIENCE A* 8(7), 1118-1125.
- Kaichouh, G., Oturan, N., Oturan, M., El Kacemi, K. and El Hourch, A. (2004). Degradation of the herbicide imazapyr by Fenton reactions. *Environmental Chemistry Letters* 2(1), 31-33.
- Kim, I. and Tanaka, H. (2009). Photodegradation characteristics of PPCPs in water with UV treatment. *Environment International* 35(5), 793-802.
- Kourdali, S., Badis, A. and Boucherit, A. (2014). Degradation of direct yellow 9 by electro-Fenton: Process study and optimization and, monitoring of treated water toxicity using catalase. *Ecotoxicology and Environmental Safety* 110, 110-120.
- Lin, H., Wu, J. and Zhang, H. (2013). Degradation of bisphenol A in aqueous solution by a novel electro/Fe³⁺/peroxydisulfate process. *Separation and Purification Technology* 117, 18-23.
- Lin, H., Wu, J. and Zhang, H. (2014). Degradation of clofibric acid in aqueous solution by an EC/Fe³⁺/PMS process. *Chemical Engineering Journal* 244, 514-521.
- Mousset, E., Oturan, N., van Hullebusch, E.D., Guibaud, G., Esposito, G. and Oturan, M.A. (2014a). Influence of solubilizing agents (cyclodextrin or surfactant) on phenanthrene degradation by electro-Fenton process – Study of soil washing recycling possibilities and environmental impact. *Water Research* 48, 306-316.
- Mousset, E., Oturan, N., van Hullebusch, E.D., Guibaud, G., Esposito, G. and Oturan, M.A. (2014b) Treatment of synthetic soil washing solutions containing phenanthrene and cyclodextrin by electro-oxidation. Influence of anode materials on toxicity removal and biodegradability enhancement. *Applied Catalysis B: Environmental* 160–161, 666-675.
- Nidheesh, P.V. and Gandhimathi, R. (2012). Trends in electro-Fenton process for water and wastewater treatment: An overview. *Desalination* 299, 1-15.
- Oturan, N., Sirés, I., Oturan, M.A. and Brillas, E. (2009). Degradation of pesticides in

- aqueous medium by electro-Fenton and related methods. A review. *Journal of Environmental Engineering and Management* 19(5), 235-255.
- Pérez, M., Torrades, F., García-Hortal, J.A., Domènech, X. and Peral, J. (2002). Removal of organic contaminants in paper pulp treatment effluents under Fenton and photo-Fenton conditions. *Applied Catalysis B: Environmental* 36(1), 63-74.
- Rivas, J., Gimeno, O. and Beltrán, F. (2009). Wastewater recycling: Application of ozone based treatments to secondary effluents. *Chemosphere* 74(6), 854-859.
- Rodrigo, M.A., Oturan, N. and Oturan, M.A. (2014) Electrochemically assisted remediation of pesticides in soils and water: A Review. *Chemical Reviews* 114(17), 8720-8745.
- Salazar, C., Sirés, I., Zaror, C. and Brillas, E. (2013). Treatment of a mixture of chloromethoxyphenols in hypochlorite medium by electrochemical AOPs as an alternative for the remediation of pulp and paper mill process waters. *Electrocatalysis* 4(4), 212-223.
- Shukla, P.R., Wang, S., Ang, H.M. and Tadé M.O. (2010). Photocatalytic oxidation of phenolic compounds using zinc oxide and sulphate radicals under artificial solar light. *Separation and Purification Technology* 70(3), 338-344.
- Stasinakis, A. (2008). Use of selected advanced oxidation processes (AOPs) for wastewater treatment—a mini review. *Global NEST Journal* 10(3), 376-385.
- Sun, J.-H., Sun, S.-P., Fan, M.-H., Guo, H.-Q., Qiao, L.-P. and Sun, R.-X. (2007). A kinetic study on the degradation of p-nitroaniline by Fenton oxidation process. *Journal of Hazardous Materials* 148(1–2), 172-177.
- Wang, A., Guo, W., Hao, F., Yue, X. and Leng, Y. (2014). Degradation of Acid Orange 7 in aqueous solution by zero-valent aluminum under ultrasonic irradiation. *Ultrasonics Sonochemistry* 21(2), 572-575.
- Wang, Y., Zhang, H., Chen, L., Wang, S. and Zhang, D. (2012). Ozonation combined with ultrasound for the degradation of tetracycline in a rectangular air-lift reactor. *Separation and Purification Technology* 84, 138-146.
- Wang, Y.R. and Chu, W. (2011). Degradation of 2,4,5-trichlorophenoxyacetic acid by a novel Electro-Fe(II)/Oxone process using iron sheet as the sacrificial anode. *Water*

Research 45(13), 3883-3889.

Wu, J., Zhang, H. and Qiu, J. (2012). Degradation of Acid Orange 7 in aqueous solution by a novel electro/ Fe^{2+} /peroxydisulfate process. *Journal of Hazardous Materials* 215–216, 138-145.

Yahya, M.S., Oturan, N., El Kacemi, K., El Karbane, M., Aravindakumar, C.T. and Oturan, M.A. (2014) Oxidative degradation study on antimicrobial agent ciprofloxacin by electro-fenton process: Kinetics and oxidation products. *Chemosphere* 117, 447-454.

Yatmaz, H.C. and Uzman, Y. (2009) Degradation of pesticide monochrotophos from aqueous solutions by electrochemical methods. *International Journal of Electrochemical Science* 4, 614-626.

Zazo, J.A., Casas, J.A., Mohedano, A.F. and Rodriguez, J.J. (2009). Semicontinuous Fenton oxidation of phenol in aqueous solution. A kinetic study. *Water Research* 43(16), 4063-4069.

Zhang, H., Wang, Z., Liu, C., Guo, Y., Shan, N., Meng, C. and Sun, L. (2014). Removal of COD from landfill leachate by an electro/ Fe^{2+} /peroxydisulfate process. *Chemical Engineering Journal* 250, 76-82.

Zhong, X., Royer, S., Zhang, H., Huang, Q., Xiang, L., Valange, S. and Barrault, J. (2011). Mesoporous silica iron-doped as stable and efficient heterogeneous catalyst for the degradation of C.I. Acid Orange 7 using sono-photo-Fenton process. *Separation and Purification Technology* 80(1), 163-171.

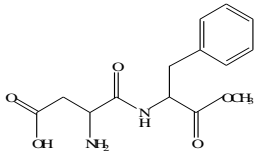
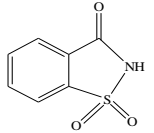
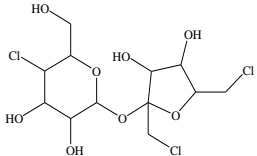
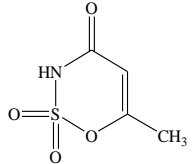
Chapter 2 Literature review

2.1 Artificial sweeteners

Artificial sweeteners are one of the most important and interesting classes of emerging contaminants. Artificial sweeteners have been classified as nutritive and non-nutritive depending on whether they are a source of calories (Whitehouse *et al.* 2008). The nutritive sweeteners include the monosaccharide polyols (e.g. sorbitol, mannitol, and xylitol) and the disaccharide polyols (e.g. maltitol and lactitol). They are approximately equivalent to sucrose in sweetness (Dills Jr 1989). The non-nutritive sweeteners, better known as artificial sweeteners, include substances from several different chemical classes that interact with taste receptors and typically exceed the sweetness of sucrose by a factor of 30 to 13,000 times (Whitehouse *et al.* 2008). The most popular artificial sweeteners are aspartame (ASP), saccharin (SAC), sucralose (SUC) and acesulfame. The chemical structure and main characteristics of these commonly used artificial sweeteners were presented in Table 2-1.

Artificial sweeteners are water contaminants that are highly specific to wastewater. Different from other emerging trace contaminants, such as pharmaceuticals and personal care products (PPCPs), artificial sweeteners have been considered in environmental sciences only recently (Loos *et al.* 2009; Mead *et al.* 2009; Richardson 2010; Richardson and Ternes 2011; Lange *et al.* 2012). Excretion after human consumption is one of the major source of artificial sweeteners in the environment (Kokotou *et al.* 2012). The artificial sweeteners can also enter into wastewater treatment plants from households and industries and they eventually reside in the receiving environmental bodies from effluents (Houtman 2010).

Table 2-1 The chemical structure and main characteristics of some commonly used artificial sweeteners

| Name | Chemical structure | Molecular formula | Molecular weight (g/mol) | CAS number | Water solubility (g/L) | Number of times sweeter than sucrose |
|------------|--|-----------------------|-----------------------------|------------|------------------------|---|
| Aspartame |  | $C_{14}H_{18}N_2O_5$ | 394.31 | 22839-47-0 | ~10 (25 °C) | 200 |
| Saccharin |  | $C_7H_5NO_3S$ | 183.18 | 81-07-2 | 4 | 200-700 |
| Sucralose |  | $C_{12}H_{19}Cl_3O_8$ | 397.63 | 56038-13-2 | 283 (20 °C) | 600 |
| Acesulfame |  | $C_4H_5NO_4S$ | 163.15 | 33665-90-6 | 270 (20 °C) | 200 |

Artificial sweeteners are extensively tested for potential adverse health effects on humans because they are used as food additives (Schiffman and Gatlin 1993; Kroger *et al.* 2006; En Humanos and Revisión 2009). Although the measured concentrations of some artificial sweeteners range up to microgram per liter levels in surface water, groundwater and drinking water, there is a huge safety margin regarding potential adverse health effects (Lange *et al.* 2012). Acceptable daily intake value of artificial sweeteners is 5 mg/kg of body weight per day and are thus three to four orders of magnitude above the maximum possible daily human intake by drinking water. Adverse human health effects for the application of artificial sweeteners have been reported in several studies (Lange *et al.* 2012; Toth *et al.* 2012). The long-term health effects resulting from the chronic exposure to low levels of these compounds are largely unknown (Mawhinney *et al.* 2011).

2.1.1 Aspartame

Aspartame, the best known of the various artificial sweeteners, is a dipeptide methyl ester (Table. 1), namely N-L- α -aspartyl-L-phenylalanine methyl ester. It was discovered by J. Schlatter in 1965 and commercialized by Searle & Co. under the brand name NutrasweetTM (Galletti *et al.* 1995). As the “first generation” sweeteners (Berset and Ochsenbein 2012), ASP is a white dipeptide, crystalline, low-caloric sweetener, which is 180-200 times sweeter than sucrose (Conceição *et al.* 2005). ASP is relatively stable in its dry form. When pH below 3.0, it is unstable and is hydrolyzed to aspartylphenylalanine. Above pH 6.0, it is transformed to 5-benzyl-3,6-dioxo-2-piperazine acetic acid (Sardesai and Waldshan 1991; Kokotou *et al.* 2012). ASP was found in all of the surface waters at a concentration up to 0.21 mg/L in Tianjin, China (Gan *et al.* 2013). The risks of ASP ingestion would be in the toxicity of its metabolism products. One of its metabolites is methanol which can cause acidoses and blindness (Conceição *et al.* 2005). ASP was rarely degraded by AOPs and it was treated by electro-Fenton process for the first time in this study.

2.1.2 Saccharin

Saccharin (SAC), one of the “first generation” artificial sweeteners, was discovered accidentally by Fahlberg and Remsen at Johns Hopkins University in 1879 when they were studying the oxidation of o-toluene-sulfonamides (Bruno *et al.* 2014). SAC is about 200-700 times sweeter than sucrose (Assumpção *et al.* 2008; Lange *et al.* 2012). Nowadays SAC is approved in more than 90 countries and is widely applied in many pharmaceutical and dietary products (Filho *et al.* 2003). For example, in the European Union (E.U.) SAC is used as an additive in animal feed for piglets, pigs, bovines and calves, and it is also the major degradation by-product of certain sulfonylurea herbicides (Buerge *et al.* 2010; Kokotou *et al.* 2012). SAC was slowly absorbed and not metabolized by the human organism, so it is consequently an appropriate artificial sweetener for diabetics (Filho *et al.* 2003). SAC has been detected in municipal wastewaters and in rivers in many countries, such as Germany, Switzerland and China (Gan *et al.* 2013; Van Stempvoort *et al.* 2011). For example, SAC was detected in surface waters and ranged from 50 ng/L to 0.21 mg/L in Tianjin, China (Gan *et al.* 2013). It is crucial to find efficient water treat technologies for the removal of SAC from aqueous media. In this work, electro-Fenton process was employed to degrade SAC in water.

2.1.3 Sucralose

Sucralose (SUC), which is a chlorinated disaccharide derived from sucrose, is one of the most popular artificial sweeteners and has shown increasing trend of consumption (Toth *et al.* 2012). SUC is about 600 times sweeter than the parent molecule, sucrose (Grotz and Munro 2009; Sharma *et al.* 2014). Nowadays, SUC is approved in more than 80 countries and is used widely in food products and pharmaceuticals (Sharma *et al.* 2014). SUC is not metabolized by the human body due to the orientation of the glycosidic linkage, and consequently, up to 92% of the consumed SUC is excreted unchanged in both urine and feces (Sharma *et al.* 2014; Toth *et al.* 2012). SUC assesses potential adverse effects on health, since it provokes symptoms, such as, increase in

blindness, mineralization of pelvic area and epithelial hyperplasia (Calza *et al.* 2013). Nowadays, SUC has been detected in wastewaters and rivers in many countries, such as America, France, Italy and China (Calza *et al.* 2013; Gan *et al.* 2013). Recently, SUC is considered as an emerging contaminant the by Environmental Protection Agency (EPA) due to its occurrence in environmental waters and persistence (half-life up to several years) (Richardson 2011; Richardson and Ternes 2011; Calza *et al.* 2013). Unfortunately, SUC is hard to degrade by conventional wastewater treatments processes (Labare and Alexander 1994; Torres *et al.* 2011; Sharma *et al.* 2014). It is crucial to find more powerful water treat technologies for the removal of SUC from polluted effluents.

Different AOPs have been employed to remove SUC from water, including ozonation (Scheurer *et al.* 2010; Soh *et al.* 2011), ultraviolet (UV) irradiation (Soh *et al.* 2011), UV/H₂O₂ photooxidation (Keen and Linden 2013), photo-Fenton process (Calza *et al.* 2013) and TiO₂ photocatalysis process (Calza *et al.* 2013). When treated by 100 µM ozone, 6% SUC remained after 60 min (Soh *et al.* 2011). Since SUC does not have any evident sites for direct oxidation by ozone, the removal of SUC was mainly caused by hydroxyl radicals generated in the oxidative system (Soh *et al.* 2011; Sharma *et al.* 2014). In a photochemical reactor, SUC did not degrade after 5 h UV exposure (Soh *et al.* 2011) and it also did not decay significantly when UV light irradiation lasted for 24 h (Torres *et al.* 2011), because SUC has low molar extinction coefficient in the UV region (Sharma *et al.* 2014). When H₂O₂ was added to UV irradiation system, the removal of SUC was accelerated and 500 µg/L SUC could be almost totally removed when UV fluence was 4000 mJ/cm² (Keen and Linden 2013). When photo-Fenton and TiO₂ photocatalysis processes were introduced to treat SUC, the removal efficiency of 15 mg/L SUC were 97.1% and 88.9%, respectively (Calza *et al.* 2013). SUC was removed from aqueous media by electro-Fenton process for the first time in this study.

2.2 Synthetic dyes

Nowadays, there has been an increasing use of synthetic dyes in a large amount of industrial areas such as the textile, leather goods, pharmaceutical industry, food industry

and other chemical usages (Forgacs *et al.* 2004; Hai *et al.* 2007; Soon and Hameed 2011). In 1856, the world's first commercially synthetic dye was discovered accidentally by William Henry Perkin (Saratale *et al.* 2011). Such dyes are defined as colored substances which can give fibers a permanent color. This color is able to resist fading upon exposure to sweat, light, water and many chemicals, including oxidizing agents and microbial attack (Rai *et al.* 2005). More than ten thousand commercially available dyes were developed and used in manufacturing by the end of the 19th century (Robinson *et al.* 2001). The growth of the worldwide textile industry has been accompanied by a rise in pollution due to wastewater contaminated with dyestuff (Parikh and Madamwar 2005). The water consumption and the wastewater generation from the textile industry (dry processing mill and woven fabric finishing mills) depend on the processing operations employed during the conversion of fiber to textile fabric (Dhanve *et al.* 2008). The textile industry is one of the greatest generators of liquid effluent pollutants which attributed to the high quantities of water used in the dyeing processes. Moreover, the processing stages and types of synthetic dyes applied during this conversion determine the variable wastewater characteristics in terms of pH, dissolved oxygen, organic and inorganic chemical content (Banat *et al.* 1996). It is estimated that over 7×10^5 tons of textile dyes are discharged in such industrial effluents every year (Robinson *et al.* 2001; Brillas and Mart ínez-Huitle 2015).

Dyes can be classified as Acid, Basic, Direct, Vat, Sulfur, Reactive, Disperse, metal complexes, etc., including antraquinone, indigoide, triphenylmethyl, xanthene and phthalocyanine derivatives (Mart ínez-Huitle and Brillas 2009; Brillas and Mart ínez-Huitle 2015). Among these dyes, azo dyes, which are characterized by one or two azo-bonds ($-N=N-$), account for over 70% of all dyestuffs used worldwide (Salazar *et al.* 2012, Saratale *et al.* 2011; Brillas and Mart ínez-Huitle 2015), making them the largest group of synthetic colorants and the most common synthetic dyes released into the environment (Chang *et al.* 2001; Zhao and Hardin 2007; Saratale *et al.* 2009). Inappropriate disposal of these dyes contaminated waters consistently would result in an even widely contaminated range of environmental matrixes, including surface, ground, drinking water, and soils. Unfortunately, due to the characteristic of biological

resistance and chemical stability, azo dyes can hardly be treated using classical wastewater treatments (Ganesh *et al.* 1994; Razo-Flores *et al.* 1997). For this reason, many studies have been focused mainly on the removal of azo dyes from waters (Shu and Chang 2005; Lucas and Peres 2006; Habibi and Talebian 2007; Migliorini *et al.* 2011; Yu *et al.* 2013).

2.3 Advanced oxidation processes (AOPs) in dye removal

Advanced oxidation processes (AOPs) have been precisely defined as “near ambient temperature and pressure water treatment processes which involve the generation of a powerful oxidizing agent such as hydroxyl radical in solution in sufficient quantity to effective water purification” by Glaze *et al.* at 1987. AOPs mainly use chemical, photochemical or electrochemical techniques to generate hydroxyl radicals ($\cdot\text{OH}$) which are a highly powerful oxidizing agents ($E^0 = 2.80 \text{ V/SHE}$) and can bring about chemical degradation of organic pollutants (Zhang *et al.* 2007; Mollah *et al.* 2010). $\cdot\text{OH}$ is a non-selective and efficient oxidizing agent. It readily attacks a large number of organic chemicals and converts them to less complex and less harmful intermediate products. At sufficient contact time and proper operation conditions, it is practically possible to mineralize the target pollutant to CO_2 and H_2O , which are the most stable end-product of chemical oxidation (Ayoub *et al.* 2010). The advantage of AOPs overall chemical and biological processes is that they are “environmental-friendly” as they neither transfer pollutants from phase to the other (as in chemical precipitation, adsorption, and volatilization) nor produce massive amounts of hazardous sludge (Ince and Apikyan 2000). AOPs are considered as the promising processes for the wastewater treatment in 21st century (Munter 2001).

2.3.1 Fenton process

The Fenton’s chemistry started as early as the end of the nineteenth century, when Henry J. Fenton reported that H_2O_2 could be activated by Fe(II) salts to oxidize tartaric acid (Fenton 1894). In a century since then, Fenton and related reactions have become

of great interest for their relevance to biological chemistry, synthesis and the chemistry of natural waters (Pignatello *et al.* 2006). In the 1930s, Haber and Weiss showed that the catalytic decomposition of H₂O₂ by iron salts obeyed to a complex radical and chain mechanism (Haber and Weiss 1934). Since then, interests in Fenton process has been definitely renewed, and Fenton's reagent was applied to oxidize toxic organics originally appeared in the mid-1960s (Brillas *et al.* 2009).

The generally accepted mechanism of the Fenton process proposes that hydroxyl radicals are produced in accordance with Eq. (2-1) (Bautista *et al.* 2008; Oturan and Aaron 2014), while the catalyst is regenerated through Eq. (2-2), or from the reaction of Fe³⁺ with intermediate organic radicals (Eqs. (2-3)–(2-4)) (Walling 1975; Pignatello *et al.* 2006; Bautista *et al.* 2008). However, ferrous ions are consumed more rapidly than they are regenerated (Nidheesh and Gandhimathi 2012), and then high concentration of Fe²⁺ is required in Fenton process.



Nevertheless, a number of competitive reactions can also occur (Eqs (2-6)–(2-10)), which negatively affect the oxidation process (Bautista *et al.* 2008). The HO₂[•] radical formed in Eq. (2-7) is characterized by a lower oxidization power and, therefore, is significantly less reactive towards organic compounds (Rush and Bielski 1985; Trapido *et al.* 2009; Oturan and Aaron 2014).



Basically, the Fenton process possesses some important advantages for wastewater

treatment, such as easy implementation in existing plants, easy-to-handle and relatively inexpensive chemicals, no need for energy input, and so on (Bautista *et al.* 2008; Oturan and Aaron 2014). It has been employed to degrade various kinds of organic pollutants in water, for example, dyes (Muruganandham and Swaminathan 2004; Sun *et al.* 2009), landfill leachate (Deng and Englehardt 2006; Hermosilla *et al.* 2009) and phenol (Kavitha and Palanivelu 2004; Zazo *et al.* 2005).

However, Fenton process has some disadvantages which limit its application. Firstly, high concentration of Fe^{2+} is required and large amount of Fe sludge is formed (Chou *et al.* 1999). The treatment of the sludge-containing Fe ions at the end of the wastewater treatment is expensive and needs large amount of chemicals and manpower (Nidheesh and Gandhimathi 2012). Secondly, Fenton's reaction is limited by a narrow pH range (pH 2.5–3.5) because iron ions will be precipitated at higher pH values (Nidheesh and Gandhimathi 2012). Thirdly, as a liquid solution, the storing and transport of H_2O_2 are difficult. In order to solve these problems, Electrochemical advanced oxidation processes (EAOPs) based on Fenton's reaction was developed.

2.3.2 Electrochemical Advanced Oxidation Processes (EAOPs) based on Fenton's reaction

2.3.2.1 Fundamentals and categories

The electrochemical (EC) technology which based on the transfer of electrons, have received great attention for the prevention of pollution problems (Brillas *et al.* 2009; Oturan and Aaron 2014). The main advantage of EC technology is its environmental compatibility since the main reagent, electron, is a clean reagent. A large variety of EAOPs were developed by combining EC technology with AOPs in the last decade due to their environmental safety and compatibility (operating at mild conditions), versatility, high efficiency, and possibility of automation (Oturan and Aaron 2014). Among all the EAOPs, EAOPs based on Fenton's reaction chemistry are

eco-friendly methods and avoid some disadvantages in conventional Fenton process that have recently attracted great attention for water remediation (Nidheesh and Gandhimathi 2012). EAOPs based on Fenton's reaction chemistry can be generally divided into three categories.

The first one is electro-Fenton process. H_2O_2 is formed by the reduction of the dissolved oxygen on the cathode surface (Eq. (2-11)) in an electrolytic cell. H_2O_2 can then react with the externally added catalyst (Fe^{2+} or Fe^{3+}) to produce $\cdot\text{OH}$ (Eq. (2-1)). Moreover, Fe^{2+} which consumed in Fenton's reaction can be regenerated by cathodic reduction (Eq. (2-12)) in electro-Fenton process which reduces the required concentration of initial Fe^{2+} to an catalytic amount (Figure 2-1a).



Electro-Fenton process solves some problems existed in Fenton process. For example, higher degradation rate of organic pollutants is obtained because of the continuous regeneration of Fe^{2+} at the cathode and the on-site production of H_2O_2 avoids its dangerous transport and storage (Mart ínez-Huitle and Brillas 2009) and avoiding also the competition of wasting reactions (2-6), (2-7) and (2-10) (Oturán and Aaron 2014, Sirés *et al.* 2014).

The reporting cathode materials favored the electrogeneration of H_2O_2 were gas diffusion electrodes (GDEs) (Brillas *et al.* 1998; Panizza and Cerisola 2009; Barros *et al.* 2014; Yu *et al.* 2015), graphite (Yuan and Lu 2005; Yuan *et al.* 2006) and three-dimensional electrodes such as carbon-felt (Pimentel *et al.* 2008; Diagne *et al.* 2014; Olvera-Vargas *et al.* 2014), activated carbon fiber (ACF) (Wang *et al.* 2005; Lei *et al.* 2010; Wang *et al.* 2010a), reticulated vitreous carbon (RVC) (Xie and Li 2006; Mart ínez and Bahena 2009) and carbon sponge (Özcan *et al.* 2008). Among these cathode materials, carbon-felt has a high specific surface that favors the fast generation of Fenton's reagent (H_2O_2 and Fe^{2+}) and has applied widely (Brillas *et al.* 2009). The commonly used anode materials in electro-Fenton process were high oxygen overvoltage anodes (M), such as PbO_2 , dimensionally stable anodes (DSA), Pt and boron-doped diamond (BDD) anode. Organic pollutants can also be destroyed by

heterogeneous hydroxyl radicals $M(\cdot\text{OH})$ electro-generated on high oxygen overvoltage anodes (Eq. (2-13)).



Dirany *et al.* 2012 treated antibiotics sulfachloropyridazine (SCP) in aqueous solution using electro-Fenton process. When the applied current was 300 mA, the initial pH of 0.21 mM SCP solution was fixed at 3.0, SCP could be totally removed in 10 min. The mineralization efficiency of SCP was nearly 100% in a 360 min reaction (Table 2-2).

The second category is Fered-Fenton process or EF-Fere process. Both components of Fenton's reagent (H_2O_2 and Fe^{2+}) are added externally to the reactor. Fe^{3+} which formed in the Fenton's reaction can convert to Fe^{2+} via cathodic reduction (Eq. (2-12)) (Figure 2-1b). Zhang *et al.* 2007 degraded 4-nitrophenol (4-NP) in water by using Fered-Fenton process. The COD removal efficiency for 200 mg/L 4-NP was 70% in a 120 min reaction, while the COD removal efficiency was only 50% in Fenton process at the same concentration of Fenton's reagent (H_2O_2 and Fe^{2+}) (Table 2-2).

The third category is electrochemical peroxidation process. A sacrificial iron anode was used for Fe^{2+} electrogeneration from anodic dissolution via Eq. (2-14). H_2O_2 is externally added to the treated solution to degrade the organic pollutants with $\cdot\text{OH}$ from Fenton's reaction (Figure 2-1c). In electrochemical peroxidation process, the coagulation of $\text{Fe}(\text{OH})_3$ precipitate formed depending on the pH and the applied current can be an significant alternative route for the degradation of organic pollutants (Brillas *et al.* 2009).



Electrochemical peroxidation process was employed to treat hexachlorbenzene (HCB) in aqueous solution by Xie *et al.* (Xie *et al.* 2005). 96.96% of the initial HCB could be removed in 3 h (Table 2-2).

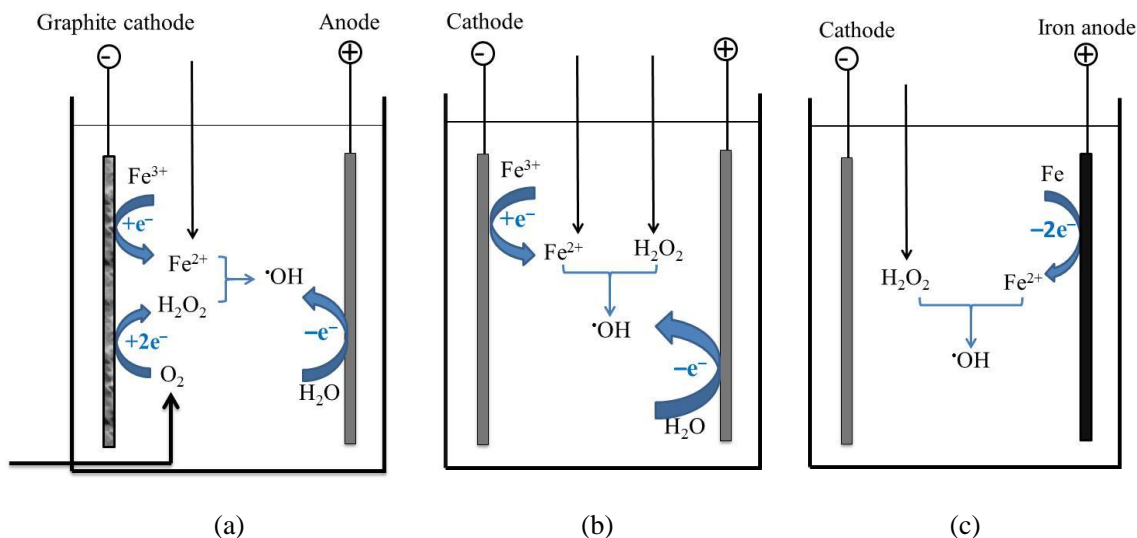


Figure 2-1 Schematic representation of different categories of EAOPs based on Fenton's reagent ((a) electro-Fenton process; (b) Fered Fenton process; (c) electrochemical peroxidation process;)

Table 2-2 Examples of different categories of EAOPs based on Fenton's reagent

| Categories | Compound | Typical condition | Corresponding results | Ref. |
|------------------------------|----------|---|--|---------------------------|
| Electro-Fenton | SCP | BDD anode, CF cathode, [SCP] ₀ = 0.21mM, [Fe ²⁺] = 0.2mM, I = 30 mA, pH ₀ 3.0 | 100% removal in 10 min and near 100 % TOC removal in 360 min | Dirany <i>et al.</i> 2012 |
| Fered-Fenton | 4-NP | Stainless steel cylinder cathode, RuO ₂ /IrO ₂ anode, [4-NP] ₀ = 200 mg/L, [H ₂ O ₂] = 9.12 mM, H ₂ O ₂ feeding time 60 min, Fe ²⁺ /H ₂ O ₂ = 0.05, I = 1.0 A, pH ₀ 5.0 | About 70% COD removal in a 120 min reaction | Zhang <i>et al.</i> 2007 |
| electrochemical peroxidation | HCB | Stainless steel electrode, gap between electrodes 6 cm, 30% H ₂ O ₂ concentration 500 mg/L, pH | 96.96% HCB removal in a 3 h reaction | Xie <i>et al.</i> 2005 |

2.5

2.3.2.2 Reactors for EAOPs based Fenton's reaction

Generally, the reactors in which EAOPs based Fenton's reaction were carried out

can be divided into two categories, i.e., the undivided cells and divided cells. Majority of researches were carried out in undivided electrochemical cells (Brillas *et al.* 1998; Mansour *et al.* 2015; Thirugnanasambandham *et al.* 2015; Zhang *et al.* 2015a). The major advantage of using undivided cells is that the electrolysis requires lower cell voltage because the voltage penalty of the separator of divided cells is avoided (Brillas *et al.* 2009). Nidheesh *et al.* 2014 degraded Rhodamine B (RhB) in a 1000 mL undivided cylindrical glass cell of 10.4 cm diameter containing 750 mL RhB solution (10 mg/L) by using electro-Fenton process. Two graphite plate with the same dimensions (5 × 5 cm) were used as anode and cathode. The results indicated RhB can be totally removed in a 180 min reaction.

However, reactive oxygen species and other weaker oxidants can also be generated at the anode in the undivided cell, which can complicate the electro-Fenton degradation process (Brillas *et al.* 2009). Therefore, it is harder to discuss the reaction mechanism in an undivided cell. Divided cells, in which cathode and anode are usually separated by membrane and salt bridge (Brillas *et al.* 2009) (Figure 2-2), are conducive to investigate the mechanism of cathodic Fenton process. Yuan *et al.* 2014 degraded 4-nitrophenol in a divided cell to investigate the mechanism of electro-Fenton process. Pozzo *et al.* 2005 employed an electrochemical cell divided by a cationic membrane to explore the production of hydrogen peroxide through the cathodic reduction of oxygen in acidic medium. Saltmiras and Lemley 2002 removed atrazine in a divided cell using anodic Fenton process in which ferrous ions were delivered via a sacrificial iron anode.

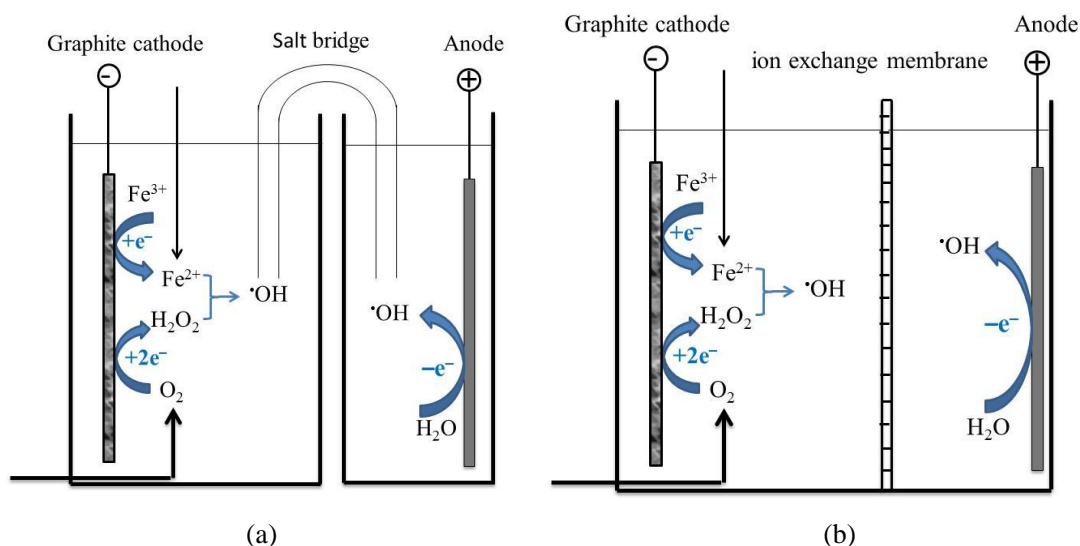


Figure 2-2 Schematic representation of electro-Fenton cells divided by salt bridge (a) and ion exchange membrane (b)

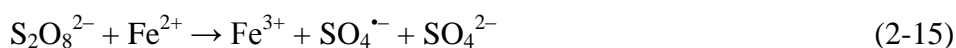
2.3.2.3 Improvements in electro-Fenton process

All the reactions mentioned above are homogeneous reactions, which have the disadvantages that the removal of metal ions from the effluent requires additional separation and disposal (Zhong *et al.* 2011). Therefore, various catalysts have been employed for the heterogeneous activation of H_2O_2 . Garrido-Ramírez *et al.* 2013 used nanostructured allophane clays supported with iron oxide ($AlSi_2Fe_6$) as iron source of Fenton's reaction to degrade atrazine in water by electro-Fenton process. 46 mM Atrazine could be totally removed in 8 h when the initial pH was 3.0. Iglesias *et al.* 2014 treated pesticide imidacloprid using a heterogeneous electro-Fenton system with ironalginate gel beads (EF-FeAB). The removal efficiency of 100 mg/L imidacloprid was 95% in a 120 min reaction.

2.3.3 Sulfate radical-based Fenton-like process

In recent years, activated persulfate (PS) oxidation is an emerging AOP for the treatment of organic pollutants (Rastogi *et al.* 2009; Tsitonaki *et al.* 2010). PS, which is discovered by M. Berthelot in 1878, is a stable oxidant with high aqueous solubility at ambient temperature (Cao *et al.* 2008). The commonly used PS in AOPs is

peroxydisulfate (PDS, $S_2O_8^{2-}$, $E^0 = 2.01$ V/SHE) and peroxymonosulfate (PMS, HSO_5^- , $E^0 = 1.82$ V/SHE). PS can be activated by transition metals (Fe^{2+} , Co^{2+} , Ag^+ , etc.) (Romero *et al.* 2010; Zhao *et al.* 2010; Pagano *et al.* 2012; Wang and Chu 2012; Long *et al.* 2013) to generate sulfate radicals ($SO_4^{\bullet-}$), which are promising in the treatment of organic contaminants in water ($E^0 = 2.6$ V/SHE) (Shukla *et al.* 2010; Cai *et al.* 2014; Wang *et al.* 2014). Transition metals activated PS process is similar to conventional Fenton process, so it also be named as Fenton-like process by Fernandez *et al.* (Fernandez *et al.* 2003; Fernandez *et al.* 2004). Compared to other transition metals, Fe^{2+} is inexpensive, nontoxic and effective, which has been widely used in catalytic oxidation process (Eq. (2-15) and (2-16)) (Wang and Chu 2011b; Li *et al.* 2015; Zhang *et al.* 2015b). Moreover, due to its unsymmetrical character, PMS might be more easily activated than PDS (Olmez-Hanci *et al.* 2011).



Similar to conventional Fenton process, there are some drawbacks encountered in sulfate radical-based Fenton-like process. For example, high ferrous ion dosage is required to activate PS due to the hard regeneration of Fe^{2+} . This results in large amount of iron sludge (Vicente *et al.* 2011). Like EAOPs based Fenton's reaction, electrochemical process was combined with Fenton-like process and solved these problems (electro-Fenton-like process) (Wang and Chu 2011a; Wu *et al.* 2012).

In sulfate radical-based electro-Fenton-like process, Fe^{2+} can be regenerated via cathodic reduction (Eq. (2-12)) of ferric iron ions. In addition, sulfate radicals could be produced via an electron transfer reaction (Eq. (2-17) and (2-18)) (Zhao *et al.* 2010; Zhou *et al.* 2011). Therefore, the degradation efficiency of organic pollutants was enhanced by coupling EC process and Fe^{2+} activated PS process.



According to different producing way of the PS and Fe^{2+} , electro-Fenton-like process can be divided into three categories.

In the first one, an iron electrode was used as anode and provided soluble ferrous

ions continuously through anodic oxidation (Eq. (2-14)). Once PS was added into the system, sulfate radicals were generated via the catalysis of ferrous ions (Eq. (2-17) or (2-18)) (Figure 2-3a).

Wang and Chu 2011a proposed an “electro-Fe(II)/Oxone (EFO)” process to degrade 2,4,5-trichlorophenoxyacetic acid (2,4,5-T). The EFO process demonstrated high 2,4,5-T removal efficiency and nearly completed the herbicide degradation within 10 min. Yuan *et al.* 2013 employed a similar system to degrade trichloroethylene (TCE). Cast gray iron was used as anode and provided Fe^{2+} , which could activate persulfate to generate sulfate radicals. 99% of 0.4 mM TCE could be transformed in a 20 min reaction time.

In the second category, both PS and Fe^{2+} are added externally to the reactor. Fe^{3+} which formed in Eq. (2-15) and (2-16) can transform to Fe^{2+} via cathodic reduction (Eq. (2-12)) (Figure 2-3b). Wu *et al.* 2012 chose azo dye Orange II as the target pollutant and treated it using an “electro/ Fe^{2+} /peroxydisulfate” process. 95% of 0.1 mM Orange II can be removed in a 60 min reaction with electrolyte concentration 0.1 M, Fe^{2+} concentration 1 mM, PDS concentration 12 mM, and current density (j) 16.8 mA/cm². “Electro/ Fe^{2+} /peroxydisulfate” process was also applied to the treatment of landfill leachate by Zhang *et al.* (Zhang *et al.* 2014). When PS concentration was 62.5 mM, Fe^{2+} concentration was 15.6 mM, j was 13.89 mA/cm² and initial pH 3.0, the COD removed by oxidation and coagulation was about 40% and 22%, respectively.

In the third category, Fe^{2+} is replaced by Fe^{3+} and added to the treated solution because Fe^{2+} has the disadvantage of easily oxidized to Fe^{3+} by air and ferrous solution should be stored under an acidic condition. Fe^{3+} was first reduced to Fe^{2+} (Eq. (2-12)) at the cathode and then activated PS to generate sulfate radicals. The regeneration of ferrous ions was enhanced by cathodic reduction (Eq. (2-12)) simultaneously (Figure 2-3c). “Electro/ Fe^{3+} /PDS” and “EC/ Fe^{3+} /PMS” processes were used to treat organic pollutants in water by our team (Lin *et al.* 2013, 2014). “Electro/ Fe^{3+} /PDS” was used to degrade bisphenol A (BPA) which is a known endocrine disrupter and industrial chemical (Staples *et al.* 1998; Cleveland *et al.* 2014; Olmez-Hanci *et al.* 2015). BPA could be nearly completely removed in a 60 min treatment time with initial BPA

concentration of 0.22 mM, Fe^{3+} concentration of 4 mM, PDS concentration of 20 mM, Na_2SO_4 concentration of 50 mM, initial pH value of 3.0 and the current density of 33.6 mA/cm^2 . The mineralization efficiency reached 94.3% in a 120 min reaction at the same condition (Lin *et al.* 2013). Clofibric acid (CA), which is the active metabolite of several widely used blood lipid regulators, was treated by “EC/ Fe^{3+} /PMS” process (Lin *et al.* 2014). When initial CA concentration was 50 mg/L, PMS concentration fixed at 20 mM, Fe^{3+} concentration was 2.00 mM, Na_2SO_4 concentration was 50 mM, initial pH was 4.0 and the current density was 33.6 mA/cm^2 , CA was completely removed after 60 min reaction.

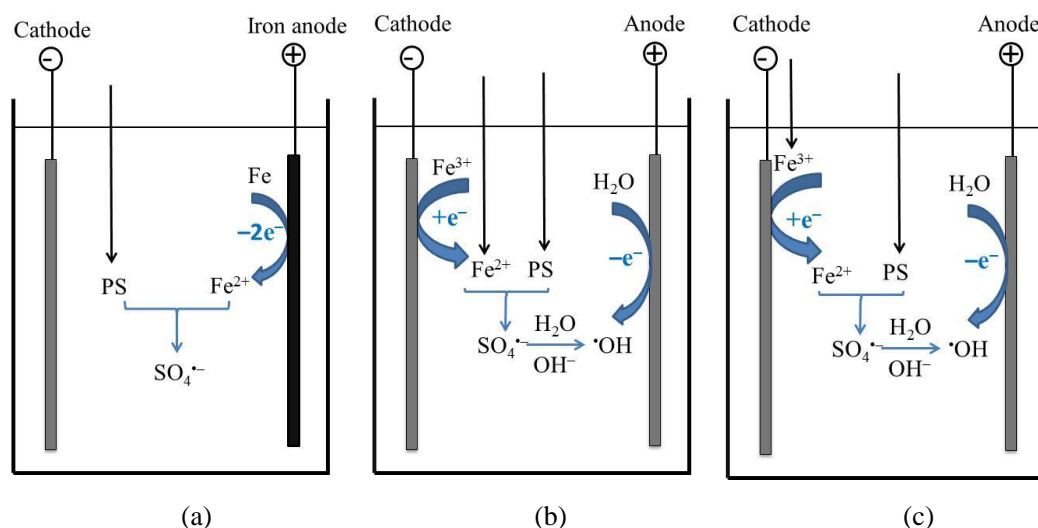


Figure 2-3 Schematic representation of different types of electro-Fenton-like processes: (a) The first category; (b) The second category; (c) The third category)

All the electro-Fenton-like processes mentioned above are homogeneous processes. They have the same drawbacks as homogeneous electro-Fenton processes. In this study, iron metal oxides were used to replace Fe^{2+} and activated PS.

2.4 Iron oxides applied in AOPs based on Fenton and Fenton-like process

Iron oxides are abundantly available minerals, presenting in the natural aqueous environment as suspended solid particles, and they also suspend in aerosol, clouds and fogs as fine particles (Hou *et al.* 2014; Rahim Pouran *et al.* 2014). Recently, iron oxides

are widely used in heterogeneous catalysis processes and constitute an attractive alternatives for the decontamination of soils, underground waters, sediments, and industrial effluents because they are natural, abundant, inexpensive, and environmentally friendly (Aredes *et al.* 2012; Xu *et al.* 2012; Rahim Pouran *et al.* 2014). Nowadays, several iron oxides and modified iron oxides are used to replace Fe^{2+} in AOPs based Fenton and Fenton-like process (He *et al.* 2005; Guo *et al.* 2010; Ji *et al.* 2013; He *et al.* 2014; Sun *et al.* 2014).

2.4.1 Goethite ($\alpha\text{-FeOOH}$)

Goethite, an iron oxyhydroxide mineral with chemical formula of $\alpha\text{-Fe}^{\text{III}}\text{O}(\text{OH})$, is a commonly used iron oxide among Fe(III) bearing minerals for heterogeneous Fenton and Fenton-like based AOPs due to its ability to operate in a wide range of pH, higher stability thermodynamically and being relatively low priced and environmentally friendly (Ortiz de la Plata *et al.* 2008; Wang *et al.* 2010b; Rahim Pouran *et al.* 2014; Sable *et al.* 2015). Goethite is also used in electro-Fenton process as a substitute of Fe^{2+} to react with H_2O_2 and form $\cdot\text{OH}$ through Fenton's reaction, avoiding the additional water pollution caused by the homogeneous catalyst. Expósito *et al.* 2007 applied goethite as active heterogeneous catalyst undergo Fenton's reaction with electrogenerated H_2O_2 in electro-Fenton process using aniline as the model pollutant. When initial aniline concentration was 100 mg/L, $\alpha\text{-FeOOH}$ dosage fixed at 1 g/L, Na_2SO_4 concentration was kept at 20 mM, initial pH was 3.0 and the applied current was 250 mA, the TOC removal efficiency of aniline was about 90% in a 25 h reaction.

2.4.2 Magnetite (Fe_3O_4)

Magnetite is a spinel iron oxide with chemical formula of $(\text{Fe}^{3+})_{\text{tet}}[\text{Fe}^{2+}\text{Fe}^{3+}]_{\text{oct}}\text{O}_4$ where Fe^{3+} cations occupy equally both octahedral and tetrahedral sites and Fe^{2+} cations are placed only in octahedral sites (Rahim Pouran *et al.* 2014). Magnetite has gained considerable attention than other iron oxides in AOPs based Fenton and Fenton-like process due to its unique characteristics: (i) The Fe(II) in its structure may play an

significant role as an electron donor to initiate the Fenton's reaction (Kwan and Voelker 2003; Moura *et al.* 2005; Hou *et al.* 2014); (ii) The octahedral site in the magnetite structure can easily accommodate both Fe(II) and Fe(III), which means that Fe(II) can be reversibly oxidized and reduced in the same structure (Moura *et al.* 2005); (iii) The production of more active systems by modification in the physico-chemical properties of the magnetite through isostructural substitution of iron by different transition metals (Moura *et al.* 2005; Hou *et al.* 2014); (iv) The magnetically easy separation of magnetite catalysts from the reaction system as a result of its magnetic property (Ai *et al.* 2011; Chun *et al.* 2012) and (v) Higher dissolution rate of magnetite compared to other iron oxides which lead to higher electron mobility in its spinel structure (Litter and Blesa 1992; Matta *et al.* 2008).

Chen *et al.* 2014 synthesized Fe₃O₄ nanoparticles (NPs) by the oxidation-precipitation method and investigated their catalytic properties by the peroxide oxidation of Orange II solution. After 60 min reaction, the decolorization efficiency of Orange II was 99.89% with initial Orange II concentration of 100 mg/L, Fe₃O₄ NPs dosage of 1.5 g/L, H₂O₂ concentration of 22 mM and initial pH value of 2.7. Yan *et al.* 2011 applied iron oxide magnetic nanoparticles (Fe₃O₄ MNPs) to activate PDS and degrade antibiotics sulfamonomethoxine (SMM) in aqueous solution. When initial SMM concentration was 0.06 mM, Fe₃O₄ MNPs dosage fixed at 2.40 mM, PDS concentration was 1.2 mM and initial pH was 6.8, SMM could be completely removed in a 15 min reaction.

References

- Ai, L., Zhang, C., Liao, F., Wang, Y., Li, M., Meng, L. and Jiang, J. (2011) Removal of methylene blue from aqueous solution with magnetite loaded multi-wall carbon nanotube: Kinetic, isotherm and mechanism analysis. *Journal of Hazardous Materials* 198, 282-290.
- Aredes, S., Klein, B. and Pawlik, M. (2012) The removal of arsenic from water using natural iron oxide minerals. *Journal of Cleaner Production* 29–30, 208-213.
- Assumpção, M.H.M.T., Medeiros, R.A., Madi, A. and Fatibello-Filho, O. (2008)

- Desenvolvimento de um procedimento biamperométrico para determinação de sacarina em produtos dietéticos. *Química Nova* 31, 1743-1746.
- Ayoub, K., van Hullebusch, E.D., Cassir, M. and Bermond, A. (2010). Application of advanced oxidation processes for TNT removal: A review. *Journal of Hazardous Materials* 178(1–3), 10-28.
- Banat, I.M., Nigam, P., Singh, D. and Marchant, R. (1996). Microbial decolorization of textile-dyecontaining effluents: A review. *Bioresource Technology* 58(3), 217-227.
- Barros, W.R.P., Franco, P.C., Steter, J.R., Rocha, R.S. and Lanza, M.R.V. (2014). Electro-Fenton degradation of the food dye amaranth using a gas diffusion electrode modified with cobalt (II) phthalocyanine. *Journal of Electroanalytical Chemistry* 722–723, 46-53.
- Bautista, P., Mohedano, A.F., Casas, J.A., Zazo, J.A. and Rodriguez, J.J. (2008). An overview of the application of Fenton oxidation to industrial wastewaters treatment. *Journal of Chemical Technology & Biotechnology* 83(10), 1323-1338.
- Berset, J.-D. and Ochsenbein, N. (2012). Stability considerations of aspartame in the direct analysis of artificial sweeteners in water samples using high-performance liquid chromatography–tandem mass spectrometry (HPLC–MS/MS). *Chemosphere* 88(5), 563-569.
- Brillas, E. and Martínez-Huitle, C.A. (2015) Decontamination of wastewaters containing synthetic organic dyes by electrochemical methods. An updated review. *Applied Catalysis B: Environmental* 166–167, 603-643.
- Brillas, E., Mur, E., Sauleda, R., Sánchez, L., Peral, J., Domènech, X. and Casado, J. (1998) Aniline mineralization by AOP's: anodic oxidation, photocatalysis, electro-Fenton and photoelectro-Fenton processes. *Applied Catalysis B: Environmental* 16(1), 31-42.
- Brillas, E., Sirés, I. and Oturan, M.A. (2009) Electro-Fenton process and related electrochemical technologies based on Fenton's reaction chemistry. *Chemical Reviews* 109(12), 6570-6631.
- Bruno, S.N.F., Cardoso, C.R., Maciel, M.M.A., Vokac, L. and da Silva Junior, A.I. (2014) Selective identification and quantification of saccharin by liquid

- chromatography and fluorescence detection. *Food Chemistry* 159, 309-315.
- Buerge, I.J., Keller, M., Buser, H.-R., Müller, M.D. and Poiger, T. (2010) Saccharin and other artificial sweeteners in soils: Estimated inputs from agriculture and households, degradation, and leaching to groundwater. *Environmental Science & Technology* 45(2), 615-621.
- Cai, C., Zhang, H., Zhong, X. and Hou, L. (2014) Electrochemical enhanced heterogeneous activation of peroxydisulfate by Fe-Co/SBA-15 catalyst for the degradation of Orange II in water. *Water Research* 66, 473-485.
- Calza, P., Sakkas, V.A., Medana, C., Vlachou, A.D., Dal Bello, F. and Albanis, T.A. (2013) Chemometric assessment and investigation of mechanism involved in photo-Fenton and TiO₂ photocatalytic degradation of the artificial sweetener sucralose in aqueous media. *Applied Catalysis B: Environmental* 129, 71-79.
- Cao, J., Zhang, W.-X., Brown, D.G. and Sethi, D. (2008) Oxidation of lindane with Fe (II)-activated sodium persulfate. *Environmental Engineering Science* 25(2), 221-228.
- Chang, J.-S., Chou, C., Lin, Y.-C., Lin, P.-J., Ho, J.-Y. and Lee Hu, T. (2001) Kinetic characteristics of bacterial azo-dye decolorization by *Pseudomonas luteola*. *Water Research* 35(12), 2841-2850.
- Chen, K., Wang, G.-H., Li, W.-B., Wan, D., Hu, Q. and Lu, L.-L. (2014). Application of response surface methodology for optimization of Orange II removal by heterogeneous Fenton-like process using Fe₃O₄ nanoparticles. *Chinese Chemical Letters* 25(11), 1455-1460.
- Chou, S., Huang, Y.-H., Lee, S.-N., Huang, G.-H. and Huang, C. (1999) Treatment of high strength hexamine-containing wastewater by electro-Fenton method. *Water Research* 33(3), 751-759.
- Chun, J., Lee, H., Lee, S.-H., Hong, S.-W., Lee, J., Lee, C. and Lee, J. (2012) Magnetite/mesocellular carbon foam as a magnetically recoverable fenton catalyst for removal of phenol and arsenic. *Chemosphere* 89(10), 1230-1237.
- Cleveland, V., Bingham, J.-P. and Kan, E. (2014) Heterogeneous Fenton degradation of bisphenol A by carbon nanotube-supported Fe₃O₄. *Separation and Purification Technology* 133, 388-395.

- Conceição, M.M., Fernandes Jr, V.J., Souza, A.G., Nascimento, T.G., Aragão, C.F.S. and Macedo, R.O. (2005) Study of thermal degradation of aspartame and its products of conversion in sweetener using isothermal thermogravimetry and HPLC. *Thermochimica Acta* 433(1–2), 163-169.
- Deng, Y. and Englehardt, J.D. (2006) Treatment of landfill leachate by the Fenton process. *Water Research* 40(20), 3683-3694.
- Dhanve, R.S., Shedbalkar, U.U. and Jadhav, J.P. (2008) Biodegradation of diazo reactive dye Navy blue HE2R (Reactive blue 172) by an isolated *Exiguobacterium* sp. RD3. *Biotechnology and Bioprocess Engineering* 13(1), 53-60.
- Diagne, M., Sharma, V., Oturan, N. and Oturan, M. (2014) Depollution of indigo dye by anodic oxidation and electro-Fenton using B-doped diamond anode. *Environmental Chemistry Letters* 12(1), 219-224.
- Dills Jr, W.L. (1989) Sugar alcohols as bulk sweeteners. *Annual review of nutrition* 9(1), 161-186.
- Dirany, A., Sirés, I., Oturan, N., Özcan, A. and Oturan, M.A. (2012) Electrochemical treatment of the antibiotic sulfachloropyridazine: Kinetics, reaction pathways, and toxicity evolution. *Environmental Science & Technology* 46(7), 4074-4082.
- En Humanos, T.d.I.S. and Revisión, U. (2009) Toxicity of sucralose in humans: A review. *International Journal of Morphology* 27(1), 239-244.
- Expósito, E., Sánchez-Sánchez, C.M. and Montiel, V. (2007). Mineral iron oxides as iron source in electro-Fenton and photoelectro-Fenton mineralization processes. *Journal of the Electrochemical Society* 154(8), 116-122.
- Fenton, H. (1894) LXXIII.—Oxidation of tartaric acid in presence of iron. *Journal of the Chemical Society, Transactions* 65, 899-910.
- Fernandez, J., Maruthamuthu, P., Renken, A. and Kiwi, J. (2004) Bleaching and photobleaching of Orange II within seconds by the oxone/Co²⁺ reagent in Fenton-like processes. *Applied Catalysis B: Environmental* 49(3), 207-215.
- Fernandez, J., Nadtochenko, V. and Kiwi, J. (2003) Photobleaching of Orange II within seconds using the oxone/Co²⁺ reagent through Fenton-like chemistry. *Chemical Communications* (18), 2382-2383.

- Filho, J.C., Santini, A.O., Nasser, A.L.M., Pezza, H.R., Eduardo de Oliveira, J., Melios, C.B. and Pezza, L. (2003). Potentiometric determination of saccharin in commercial artificial sweeteners using a silver electrode. *Food Chemistry* 83(2), 297-301.
- Forgacs, E., Cserháti, T. and Oros, G. (2004) Removal of synthetic dyes from wastewaters: a review. *Environment International* 30(7), 953-971.
- Galletti, G.C., Chiavari, G. and Bocchini, P. (1995) Thermal decomposition products of aspartame as determined by pyrolysis-gas chromatography/mass spectrometry. *Journal of Analytical and Applied Pyrolysis* 32, 137-151.
- Gan, Z., Sun, H., Feng, B., Wang, R. and Zhang, Y. (2013) Occurrence of seven artificial sweeteners in the aquatic environment and precipitation of Tianjin, China. *Water Research* 47(14), 4928-4937.
- Ganesh, R., Boardman, G.D. and Michelsen, D. (1994) Fate of azo dyes in sludges. *Water Research* 28(6), 1367-1376.
- Garrido-Ramírez, E.G., Mora, M.L., Marco, J.F. and Ureta-Zañartu, M.S. (2013) Characterization of nanostructured allophane clays and their use as support of iron species in a heterogeneous electro-Fenton system. *Applied Clay Science* 86, 153-161.
- Glaze, W.H., Kang, J.-W. and Chapin, D.H. (1987). The Chemistry of water treatment processes involving ozone, hydrogen peroxide and ultraviolet radiation. *Ozone: Science & Engineering* 9(4), 335-352.
- Grotz, V.L. and Munro, I.C. (2009) An overview of the safety of sucralose. *Regulatory Toxicology and Pharmacology* 55(1), 1-5.
- Guo, L., Chen, F., Fan, X., Cai, W. and Zhang, J. (2010) S-doped α -Fe₂O₃ as a highly active heterogeneous Fenton-like catalyst towards the degradation of acid orange 7 and phenol. *Applied Catalysis B: Environmental* 96(1–2), 162-168.
- Haber, F. and Weiss, J. (1934) The catalytic decomposition of hydrogen peroxide by iron salts. *Proceedings of the Royal Society of London. Series A, Mathematical and Physical Sciences* 147(861), 332-351.
- Habibi, M.H. and Talebian, N. (2007) Photocatalytic degradation of an azo dye X6G in water: A comparative study using nanostructured indium tin oxide and titanium oxide thin films. *Dyes and Pigments* 73(2), 186-194.

- Hai, F.I., Yamamoto, K. and Fukushi, K. (2007) Hybrid treatment systems for dye wastewater. *Critical Reviews in Environmental Science and Technology* 37(4), 315-377.
- He, J., Ma, W., Song, W., Zhao, J., Qian, X., Zhang, S. and Yu, J.C. (2005). Photoreaction of aromatic compounds at α -FeOOH/H₂O interface in the presence of H₂O₂: evidence for organic-goethite surface complex formation. *Water Research* 39(1), 119-128.
- He, J., Yang, X., Men, B., Bi, Z., Pu, Y. and Wang, D. (2014) Heterogeneous Fenton oxidation of catechol and 4-chlorocatechol catalyzed by nano-Fe₃O₄: Role of the interface. *Chemical Engineering Journal* 258, 433-441.
- Hermosilla, D., Cortijo, M. and Huang, C.P. (2009) Optimizing the treatment of landfill leachate by conventional Fenton and photo-Fenton processes. *Science of The Total Environment* 407(11), 3473-3481.
- Hou, L., Zhang, Q., Jérôme, F., Duprez, D., Zhang, H. and Royer, S. (2014) Shape-controlled nanostructured magnetite-type materials as highly efficient Fenton catalysts. *Applied Catalysis B: Environmental* 144, 739-749.
- Houtman, C.J. (2010) Emerging contaminants in surface waters and their relevance for the production of drinking water in Europe. *Journal of Integrative Environmental Sciences* 7(4), 271-295.
- Iglesias, O., Gómez, J., Pazos, M. and Sanromán, M.Á. (2014) Electro-Fenton oxidation of imidacloprid by Fe alginate gel beads. *Applied Catalysis B: Environmental* 144, 416-424.
- Ince, N.H. and Apikyan, I.G. (2000) Combination of activated carbon adsorption with light-enhanced chemical oxidation via hydrogen peroxide. *Water Research* 34(17), 4169-4176.
- Ji, F., Li, C., Wei, X. and Yu, J. (2013) Efficient performance of porous Fe₂O₃ in heterogeneous activation of peroxymonosulfate for decolorization of Rhodamine B. *Chemical Engineering Journal* 231, 434-440.
- Kavitha, V. and Palanivelu, K. (2004) The role of ferrous ion in Fenton and photo-Fenton processes for the degradation of phenol. *Chemosphere* 55(9),

1235-1243.

- Keen, O.S. and Linden, K.G. (2013). Re-Engineering an artificial sweetener: Transforming sucralose residuals in water via advanced oxidation. *Environmental Science & Technology* 47(13), 6799-6805.
- Kokotou, M.G., Asimakopulos, A.G. and Thomaidis, N.S. (2012) Artificial sweeteners as emerging pollutants in the environment: Analytical methodologies and environmental impact. *Analytical Methods* 4(10), 3057-3070.
- Kroger, M., Meister, K. and Kava, R. (2006). Low-calorie sweeteners and other sugar substitutes: A review of the safety issues. *Comprehensive Reviews in Food Science and Food Safety* 5(2), 35-47.
- Kwan, W.P. and Voelker, B.M. (2003). Rates of hydroxyl radical generation and organic compound oxidation in mineral-catalyzed Fenton-like systems. *Environmental Science & Technology* 37(6), 1150-1158.
- Labare, M.P. and Alexander, M. (1994) Microbial cometabolism of sucralose, a chlorinated disaccharide, in environmental samples. *Applied Microbiology and Biotechnology* 42(1), 173-178.
- Lange, F., Scheurer, M. and Brauch, H.-J. (2012) Artificial sweeteners—a recently recognized class of emerging environmental contaminants: A review. *Analytical and Bioanalytical Chemistry* 403(9), 2503-2518.
- Lei, H., Li, H., Li, Z., Li, Z., Chen, K., Zhang, X. and Wang, H. (2010) Electro-Fenton degradation of cationic red X-GRL using an activated carbon fiber cathode. *Process Safety and Environmental Protection* 88(6), 431-438.
- Li, R., Jin, X., Megharaj, M., Naidu, R. and Chen, Z. (2015) Heterogeneous Fenton oxidation of 2,4-dichlorophenol using iron-based nanoparticles and persulfate system. *Chemical Engineering Journal* 264, 587-594.
- Lin, H., Wu, J. and Zhang, H. (2013) Degradation of bisphenol A in aqueous solution by a novel electro/Fe³⁺/peroxydisulfate process. *Separation and Purification Technology* 117, 18-23.
- Lin, H., Wu, J. and Zhang, H. (2014) Degradation of clofibric acid in aqueous solution by an EC/Fe³⁺/PMS process. *Chemical Engineering Journal* 244, 514-521.

- Litter, M.I. and Blesa, M.A. (1992) Photodissolution of iron oxides. IV. A comparative study on the photodissolution of hematite, magnetite, and maghemite in EDTA media. *Canadian Journal of Chemistry* 70(9), 2502-2510.
- Long, A., Lei, Y. and Zhang, H. (2013). Degradation of toluene by a selective ferrous ion activated persulfate oxidation process. *Industrial & Engineering Chemistry Research* 53(3), 1033-1039.
- Loos, R., Gawlik, B.M., Locoro, G., Rimaviciute, E., Contini, S. and Bidoglio, G. (2009). EU-wide survey of polar organic persistent pollutants in European river waters. *Environmental Pollution* 157(2), 561-568.
- Lucas, M.S. and Peres, J.A. (2006) Decolorization of the azo dye Reactive Black 5 by Fenton and photo-Fenton oxidation. *Dyes and Pigments* 71(3), 236-244.
- Mansour, D., Fourcade, F., Soutrel, I., Hauchard, D., Bellakhal, N. and Amrane, A. (2015) Relevance of a combined process coupling electro-Fenton and biological treatment for the remediation of sulfamethazine solutions – Application to an industrial pharmaceutical effluent. *Comptes Rendus Chimie* 18(1), 39-44.
- Martínez-Huitle, C.A. and Brillas, E. (2009) Decontamination of wastewaters containing synthetic organic dyes by electrochemical methods: A general review. *Applied Catalysis B: Environmental* 87(3–4), 105-145.
- Martínez, S.S. and Bahena, C.L. (2009) Chlorbromuron urea herbicide removal by electro-Fenton reaction in aqueous effluents. *Water Research* 43(1), 33-40.
- Matta, R., Hanna, K., Kone, T. and Chiron, S. (2008) Oxidation of 2,4,6-trinitrotoluene in the presence of different iron-bearing minerals at neutral pH. *Chemical Engineering Journal* 144(3), 453-458.
- Mawhinney, D.B., Young, R.B., Vanderford, B.J., Borch, T. and Snyder, S.A. (2011). Artificial sweetener sucralose in U.S. drinking water systems. *Environmental Science & Technology* 45(20), 8716-8722.
- Mead, R.N., Morgan, J.B., Avery Jr, G.B., Kieber, R.J., Kirk, A.M., Skrabal, S.A. and Willey, J.D. (2009) Occurrence of the artificial sweetener sucralose in coastal and marine waters of the United States. *Marine Chemistry* 116(1–4), 13-17.
- Migliorini, F.L., Braga, N.A., Alves, S.A., Lanza, M.R.V., Baldan, M.R. and Ferreira,

- N.G. (2011) Anodic oxidation of wastewater containing the Reactive Orange 16 Dye using heavily boron-doped diamond electrodes. *Journal of Hazardous Materials* 192(3), 1683-1689.
- Mollah, M.Y.A., Gomes, J.A.G., Das, K.K. and Cocke, D.L. (2010) Electrochemical treatment of Orange II dye solution-Use of aluminum sacrificial electrodes and floc characterization. *Journal of Hazardous Materials* 174(1-3), 851-858.
- Moura, F.C.C., Araujo, M.H., Costa, R.C.C., Fabris, J.D., Ardisson, J.D., Macedo, W.A.A. and Lago, R.M. (2005). Efficient use of Fe metal as an electron transfer agent in a heterogeneous Fenton system based on Fe⁰/Fe₃O₄ composites. *Chemosphere* 60(8), 1118-1123.
- Munter, R. (2001) Advanced oxidation processes—current status and prospects. *Proceedings of the Estonian Academy of Science Chemistry* 50(2), 59-80.
- Muruganandham, M. and Swaminathan, M. (2004) Decolourisation of Reactive Orange 4 by Fenton and photo-Fenton oxidation technology. *Dyes and Pigments* 63(3), 315-321.
- Nidheesh, P.V. and Gandhimathi, R. (2012) Trends in electro-Fenton process for water and wastewater treatment: An overview. *Desalination* 299(0), 1-15.
- Olmez-Hanci, T., Dursun, D., Aydin, E., Arslan-Alaton, I., Girit, B., Mita, L., Diano, N., Mita, D.G. and Guida, M. (2015). S₂O₈²⁻/UV-C and H₂O₂/UV-C treatment of Bisphenol A: Assessment of toxicity, estrogenic activity, degradation products and results in real water. *Chemosphere* 119, Supplement, S115-S123.
- Olmez-Hanci, T., Imren, C., Kabdasli, I., Tunay, O. and Arslan-Alaton, I. (2011) Application of the UV-C photo-assisted peroxymonosulfate oxidation for the mineralization of dimethyl phthalate in aqueous solutions. *Photochemistry & Photobiological Sciences* 10(3), 408-413.
- Olvera-Vargas, H., Oturan, N., Aravindakumar, C.T., Paul, M.M.S., Sharma, V. and Oturan, M. (2014) Electro-oxidation of the dye azure B: kinetics, mechanism, and by-products. *Environmental Science and Pollution Research* 21(14), 8379-8386.
- Ortiz de la Plata, G.B., Alfano, O.M. and Cassano, A.E. (2008) Optical properties of goethite catalyst for heterogeneous photo-Fenton reactions: Comparison with a

- titanium dioxide catalyst. *Chemical Engineering Journal* 137(2), 396-410.
- Oturan, M.A. and Aaron, J.-J. (2014). Advanced oxidation processes in water/wastewater treatment: Principles and applications. A review. *Critical Reviews in Environmental Science and Technology* 44(23), 2577-2641.
- Özcan, A., Şahin, Y., Savaş Koparal, A. and Oturan, M.A. (2008) Carbon sponge as a new cathode material for the electro-Fenton process: Comparison with carbon felt cathode and application to degradation of synthetic dye basic blue 3 in aqueous medium. *Journal of Electroanalytical Chemistry* 616(1–2), 71-78.
- Pagano, M., Volpe, A., Mascolo, G., Lopez, A., Locaputo, V. and Ciannarella, R. (2012). Peroxymonosulfate–Co(II) oxidation system for the removal of the non-ionic surfactant Brij 35 from aqueous solution. *Chemosphere* 86(4), 329-334.
- Panizza, M. and Cerisola, G. (2009) Electro-Fenton degradation of synthetic dyes. *Water Research* 43(2), 339-344.
- Parikh, A. and Madamwar, D. (2005) Textile dye decolorization using cyanobacteria. *Biotechnology Letters* 27(5), 323-326.
- Pignatello, J.J., Oliveros, E. and MacKay, A. (2006). Advanced oxidation processes for organic contaminant destruction based on the Fenton reaction and related chemistry. *Critical Reviews in Environmental Science and Technology* 36(1), 1-84.
- Pimentel, M., Oturan, N., Dezotti, M. and Oturan, M.A. (2008). Phenol degradation by advanced electrochemical oxidation process electro-Fenton using a carbon felt cathode. *Applied Catalysis B: Environmental* 83(1–2), 140-149.
- Pozzo, A.D., Palma, L.D., Merli, C. and Petrucci, E. (2005) An experimental comparison of a graphite electrode and a gas diffusion electrode for the cathodic production of hydrogen peroxide. *Journal of Applied Electrochemistry* 35(4), 413-419.
- Rahim Pouran, S., Abdul Raman, A.A. and Wan Daud, W.M.A. (2014) Review on the application of modified iron oxides as heterogeneous catalysts in Fenton reactions. *Journal of Cleaner Production* 64, 24-35.
- Rai, H.S., Bhattacharyya, M.S., Singh, J., Bansal, T.K., Vats, P. and Banerjee, U.C. (2005). Removal of dyes from the effluent of textile and dyestuff manufacturing

- industry: A review of emerging techniques with reference to biological treatment. *Critical Reviews in Environmental Science and Technology* 35(3), 219-238.
- Rastogi, A., Al-Abed, S.R. and Dionysiou, D.D. (2009) Effect of inorganic, synthetic and naturally occurring chelating agents on Fe(II) mediated advanced oxidation of chlorophenols. *Water Research* 43(3), 684-694.
- Razo-Flores, E., Luijten, M., Donlon, B., Lettinga, G. and Field, J. (1997) Biodegradation of selected azo dyes under methanogenic conditions. *Water Science and Technology* 36(6-7), 65-72.
- Richardson, S.D. (2010) Environmental mass spectrometry: Emerging contaminants and current issues. *Analytical Chemistry* 82(12), 4742-4774.
- Richardson, S.D. (2011) Environmental mass spectrometry: Emerging contaminants and current issues. *Analytical Chemistry* 84(2), 747-778.
- Richardson, S.D. and Ternes, T.A. (2011) Water analysis: Emerging contaminants and current issues. *Analytical Chemistry* 83(12), 4614-4648.
- Robinson, T., McMullan, G., Marchant, R. and Nigam, P. (2001) Remediation of dyes in textile effluent: a critical review on current treatment technologies with a proposed alternative. *Bioresource Technology* 77(3), 247-255.
- Romero, A., Santos, A., Vicente, F. and González, C. (2010) Diuron abatement using activated persulphate: Effect of pH, Fe(II) and oxidant dosage. *Chemical Engineering Journal* 162(1), 257-265.
- Rush, J.D. and Bielski, B. (1985). Pulse radiolytic studies of the reactions of HO₂/O₂ with Fe (II)/Fe (III) ions. The reactivity of HO₂/O₂ with ferric ions and its implication on the occurrence of the Haber-Weiss reaction. *Journal of Physical Chemistry* 89(23), 5062-5066.
- Sable, S.S., Ghute, P.P., Álvarez, P., Beltrán, F.J., Medina, F. and Contreras, S. (2015). FeOOH and derived phases: Efficient heterogeneous catalysts for clofibric acid degradation by advanced oxidation processes (AOPs). *Catalysis Today* 240, Part A, 46-54.
- Salazar, R., Brillas, E. and Sirés, I. (2012) Finding the best Fe²⁺/Cu²⁺ combination for the solar photoelectro-Fenton treatment of simulated wastewater containing the

- industrial textile dye Disperse Blue 3. *Applied Catalysis B: Environmental* 115–116(0), 107-116.
- Saltmiras, D.A. and Lemley, A.T. (2002). Atrazine degradation by anodic Fenton treatment. *Water Research* 36(20), 5113-5119.
- Saratale, R.G., Saratale, G.D., Chang, J.S. and Govindwar, S.P. (2009) Decolorization and biodegradation of textile dye Navy blue HER by *Trichosporon beigeli* NCIM-3326. *Journal of Hazardous Materials* 166(2–3), 1421-1428.
- Saratale, R.G., Saratale, G.D., Chang, J.S. and Govindwar, S.P. (2011) Bacterial decolorization and degradation of azo dyes: A review. *Journal of the Taiwan Institute of Chemical Engineers* 42(1), 138-157.
- Sardesai, V.M. and Waldshan, T.H. (1991) Natural and synthetic intense sweeteners. *The Journal of Nutritional Biochemistry* 2(5), 236-244.
- Scheurer, M., Storck, F.R., Brauch, H.-J. and Lange, F.T. (2010) Performance of conventional multi-barrier drinking water treatment plants for the removal of four artificial sweeteners. *Water Research* 44(12), 3573-3584.
- Schiffman, S.S. and Gatlin, C.A. (1993) Sweeteners: State of knowledge review. *Neuroscience & Biobehavioral Reviews* 17(3), 313-345.
- Sharma, V., Oturan, M. and Kim, H. (2014) Oxidation of artificial sweetener sucralose by advanced oxidation processes: a review. *Environmental Science and Pollution Research* 21(14), 8525-8533.
- Shu, H.-Y. and Chang, M.-C. (2005) Decolorization effects of six azo dyes by O₃, UV/O₃ and UV/H₂O₂ processes. *Dyes and Pigments* 65(1), 25-31.
- Shukla, P.R., Wang, S., Ang, H.M. and Tadé M.O. (2010) Photocatalytic oxidation of phenolic compounds using zinc oxide and sulphate radicals under artificial solar light. *Separation and Purification Technology* 70(3), 338-344.
- Sirés, I., Brillas, E., Oturan, M., Rodrigo, M. and Panizza, M. (2014) Electrochemical advanced oxidation processes: today and tomorrow. A review. *Environmental Science and Pollution Research* 21(14), 8336-8367.
- Soh, L., Connors, K.A., Brooks, B.W. and Zimmerman, J. (2011). Fate of sucralose through environmental and water treatment processes and impact on plant indicator

- species. *Environmental Science & Technology* 45(4), 1363-1369.
- Soon, A.N. and Hameed, B.H. (2011) Heterogeneous catalytic treatment of synthetic dyes in aqueous media using Fenton and photo-assisted Fenton process. *Desalination* 269(1–3), 1-16.
- Staples, C.A., Dome, P.B., Klecka, G.M., Oblock, S.T. and Harris, L.R. (1998) A review of the environmental fate, effects, and exposures of bisphenol A. *Chemosphere* 36(10), 2149-2173.
- Sun, S.-P., Li, C.-J., Sun, J.-H., Shi, S.-H., Fan, M.-H. and Zhou, Q. (2009) Decolorization of an azo dye Orange G in aqueous solution by Fenton oxidation process: Effect of system parameters and kinetic study. *Journal of Hazardous Materials* 161(2–3), 1052-1057.
- Sun, S.-P., Zeng, X., Li, C. and Lemley, A.T. (2014) Enhanced heterogeneous and homogeneous Fenton-like degradation of carbamazepine by nano-Fe₃O₄/H₂O₂ with nitrilotriacetic acid. *Chemical Engineering Journal* 244, 44-49.
- Thirugnanasambandham, K., Kandasamy, S., Sivakumar, V., kumar, R.K. and Mohanavelu, R. (2015) Modeling of by-product recovery and performance evaluation of Electro-Fenton treatment technique to treat poultry wastewater. *Journal of the Taiwan Institute of Chemical Engineers* 46, 89-97.
- Torres, C.I., Ramakrishna, S., Chiu, C.-A., Nelson, K.G., Westerhoff, P. and Krajmalnik-Brown, R. (2011) Fate of sucralose during wastewater treatment. *Environmental Engineering Science* 28(5), 325-331.
- Toth, J.E., Rickman, K.A., Venter, A.R., Kiddle, J.J. and Mezyk, S.P. (2012). Reaction kinetics and efficiencies for the hydroxyl and sulfate radical based oxidation of artificial sweeteners in water. *The Journal of Physical Chemistry A* 116(40), 9819-9824.
- Trapido, M., Kulik, N., Goi, A., Veressinina, Y. and Munter, R. (2009). Fenton treatment efficacy for the purification of different kinds of wastewater. *Water Science Technology* 60(7), 1795-1801.
- Tsitonaki, A., Petri, B., Crimi, M., Mosbæk, H., Siegrist, R.L. and Bjerg, P.L. (2010). In situ chemical oxidation of contaminated soil and groundwater using persulfate: A

- review. *Critical Reviews in Environmental Science and Technology* 40(1), 55-91.
- Van Stempvoort, D.R., Roy, J.W., Brown, S.J. and Bickerton, G. (2011). Artificial sweeteners as potential tracers in groundwater in urban environments. *Journal of Hydrology* 401(1–2), 126-133.
- Vicente, F., Santos, A., Romero, A. and Rodriguez, S. (2011) Kinetic study of diuron oxidation and mineralization by persulphate: Effects of temperature, oxidant concentration and iron dosage method. *Chemical Engineering Journal* 170(1), 127-135.
- Walling, C. (1975) Fenton's reagent revisited. *Accounts of Chemical Research* 8(4), 125-131.
- Wang, A., Qu, J., Ru, J., Liu, H. and Ge, J. (2005) Mineralization of an azo dye Acid Red 14 by electro-Fenton's reagent using an activated carbon fiber cathode. *Dyes and Pigments* 65(3), 227-233.
- Wang, C.-T., Chou, W.-L., Chung, M.-H. and Kuo, Y.-M. (2010a) COD removal from real dyeing wastewater by electro-Fenton technology using an activated carbon fiber cathode. *Desalination* 253(1–3), 129-134.
- Wang, X., Wang, L., Li, J., Qiu, J., Cai, C. and Zhang, H. (2014) Degradation of Acid Orange 7 by persulfate activated with zero valent iron in the presence of ultrasonic irradiation. *Separation and Purification Technology* 122, 41-46.
- Wang, Y., Liang, J.B., Liao, X.D., Wang, L.-s., Loh, T.C., Dai, J. and Ho, Y.W. (2010b) Photodegradation of sulfadiazine by goethite–oxalate suspension under UV light irradiation. *Industrial & Engineering Chemistry Research* 49(8), 3527-3532.
- Wang, Y.R. and Chu, W. (2011a) Degradation of 2,4,5-trichlorophenoxyacetic acid by a novel Electro-Fe(II)/Oxone process using iron sheet as the sacrificial anode. *Water Research* 45(13), 3883-3889.
- Wang, Y.R. and Chu, W. (2011b) Degradation of a xanthene dye by Fe(II)-mediated activation of Oxone process. *Journal of Hazardous Materials* 186(2–3), 1455-1461.
- Wang, Y.R. and Chu, W. (2012) Photo-assisted degradation of 2,4,5-trichlorophenoxyacetic acid by Fe(II)-catalyzed activation of Oxone process: The role of UV irradiation, reaction mechanism and mineralization. *Applied*

- Catalysis B: Environmental 123–124, 151-161.
- Whitehouse, C.R., Boullata, J. and McCauley, L.A. (2008). The potential toxicity of artificial sweeteners. *AAOHN Journal* 56(6), 251.
- Wu, J., Zhang, H. and Qiu, J. (2012) Degradation of Acid Orange 7 in aqueous solution by a novel electro/ Fe^{2+} /peroxydisulfate process. *Journal of Hazardous Materials* 215–216, 138-145.
- Xie, Q.J., Lu, N., Wang, L.L. and Lu, X.H. (2005) Oxidation of hexachlorbenzene by the direct Fenton and EF-Feox method. *Fresenius Environmental Bulletin* 14(10), 894-899.
- Xie, Y.B. and Li, X.Z. (2006). Interactive oxidation of photoelectrocatalysis and electro-Fenton for azo dye degradation using TiO_2 -Ti mesh and reticulated vitreous carbon electrodes. *Materials Chemistry and Physics* 95(1), 39-50.
- Xu, P., Zeng, G.M., Huang, D.L., Feng, C.L., Hu, S., Zhao, M.H., Lai, C., Wei, Z., Huang, C., Xie, G.X. and Liu, Z.F. (2012). Use of iron oxide nanomaterials in wastewater treatment: A review. *Science of The Total Environment* 424, 1-10.
- Yan, J., Lei, M., Zhu, L., Anjum, M.N., Zou, J. and Tang, H. (2011). Degradation of sulfamonomethoxine with Fe_3O_4 magnetic nanoparticles as heterogeneous activator of persulfate. *Journal of Hazardous Materials* 186(2–3), 1398-1404.
- Yu, X., Zhou, M., Ren, G. and Ma, L. (2015) A novel dual gas diffusion electrodes system for efficient hydrogen peroxide generation used in electro-Fenton. *Chemical Engineering Journal* 263(0), 92-100.
- Yu, Z., Wang, W., Song, L., Liqin, L., Wang, Z., Jiang, X., Dong, C. and Qiu, R. (2013). Acceleration comparison between $\text{Fe}^{2+}/\text{H}_2\text{O}_2$ and $\text{Co}^{2+}/\text{oxone}$ for decolouration of azo dyes in homogeneous systems. *Chemical Engineering Journal* 234, 475-483.
- Yuan, S., Liao, P. and Alshwabkeh, A.N. (2013). Electrolytic manipulation of persulfate reactivity by iron electrodes for trichloroethylene degradation in groundwater. *Environmental Science & Technology* 48(1), 656-663.
- Yuan, S. and Lu, X. (2005) Comparison treatment of various chlorophenols by electro-Fenton method: relationship between chlorine content and degradation. *Journal of Hazardous Materials* 118(1–3), 85-92.

- Yuan, S., Tian, M., Cui, Y., Lin, L. and Lu, X. (2006) Treatment of nitrophenols by cathode reduction and electro-Fenton methods. *Journal of Hazardous Materials* 137(1), 573-580.
- Zazo, J.A., Casas, J.A., Mohedano, A.F., Gilarranz, M.A. and Rodríguez, J.J. (2005). Chemical pathway and kinetics of phenol oxidation by Fenton's reagent. *Environmental Science & Technology* 39(23), 9295-9302.
- Zhang, C., Zhou, M., Ren, G., Yu, X., Ma, L., Yang, J. and Yu, F. (2015a) Heterogeneous electro-Fenton using modified iron-carbon as catalyst for 2,4-dichlorophenol degradation: Influence factors, mechanism and degradation pathway. *Water Research* 70, 414-424.
- Zhang, H., Fei, C., Zhang, D. and Tang, F. (2007) Degradation of 4-nitrophenol in aqueous medium by electro-Fenton method. *Journal of Hazardous Materials* 145(1-2), 227-232.
- Zhang, H., Wang, Z., Liu, C., Guo, Y., Shan, N., Meng, C. and Sun, L. (2014) Removal of COD from landfill leachate by an electro/Fe²⁺/peroxydisulfate process. *Chemical Engineering Journal* 250, 76-82.
- Zhang, M., Chen, X., Zhou, H., Murugananthan, M. and Zhang, Y. (2015b) Degradation of p-nitrophenol by heat and metal ions co-activated persulfate. *Chemical Engineering Journal* 264, 39-47.
- Zhao, J., Zhang, Y., Quan, X. and Chen, S. (2010) Enhanced oxidation of 4-chlorophenol using sulfate radicals generated from zero-valent iron and peroxydisulfate at ambient temperature. *Separation and Purification Technology* 71(3), 302-307.
- Zhao, X. and Hardin, I.R. (2007) HPLC and spectrophotometric analysis of biodegradation of azo dyes by *Pleurotus ostreatus*. *Dyes and Pigments* 73(3), 322-325.
- Zhong, X., Royer, S., Zhang, H., Huang, Q., Xiang, L., Valange, S. and Barrault, J. (2011) Mesoporous silica iron-doped as stable and efficient heterogeneous catalyst for the degradation of C.I. Acid Orange 7 using sono-photo-Fenton process. *Separation and Purification Technology* 80(1), 163-171.

Zhou, G., Sun, H., Wang, S., Ming Ang, H. and Tadé, M.O. (2011) Titanate supported cobalt catalysts for photochemical oxidation of phenol under visible light irradiations. *Separation and Purification Technology* 80(3), 626-634.

**Chapter 3 Treatment of aspartame (ASP) in aqueous solution by
electro-Fenton process**

3.1 Introduction

In this study, a detailed discussion on the oxidative degradation of artificial sweetener aspartame (ASP) in acidic aqueous solution containing catalytic amount of Fe^{2+} by using electro-Fenton process was reported. The kinetics of ASP degradation by $\cdot\text{OH}$ generated during electro-Fenton process has been investigated. The absolute rate constant of the reaction between ASP and $\cdot\text{OH}$ was determined by the competition kinetic method using benzoic acid as a reference competitor (Özcan *et al.* 2009a, Özcan *et al.* 2013). The effect of the applied current and Fe^{2+} concentration on the degradation and mineralization of ASP was examined. The aliphatic short-chain carboxylic acids released during electro-Fenton process were monitored. The concentration of inorganic ions released into the solution was investigated. The variation of toxicity of ASP solution and its intermediates was assessed by Microtox method.

3.2 Materials and methods

3.2.1 Chemicals

ASP, N-L- α -aspartyl-L-phenylalanine methyl ester ($\text{C}_{14}\text{H}_{18}\text{N}_2\text{O}_5$, $\geq 98\%$), was obtained from Alfa Aesar and was used in the electrolytic experiments without further purification. Analytical grade anhydrous sodium sulfate from Sigma-Aldrich was used as supporting electrolyte. Ferrous sulfate heptahydrated of analytical grade was purchased from Acros Organics and used as catalyst source. Analytical grade benzoic acid from Prolabo (R.P. Normapur grade) was used as the competition substrate in several kinetic experiments. Analytical grade carboxylic acids and or other chemicals used for chromatographic analysis were purchased from Acros, Sigma, Riedel-de Haën and Fluka. All solutions were prepared with ultrapure water obtained from a Millipore Mill-Q system with resistivity $> 18 \text{ M}\Omega \text{ cm}$ at room temperature.

3.2.2 Procedures and equipment

Bulk experiments were carried out at room temperature in a 250 mL undivided cylindrical glass cell of 6 cm diameter containing 220 mL ASP solution. The cathode (working) electrode was a 87.5 cm² piece of carbon felt (17.5 cm × 4.5 cm, Carbon-Lorraine, France) which placed on the inner wall of the cell covering the totality of the internal perimeter. The anode (counter) electrode was a cylindrical Pt mesh (4.5 cm height, i.d. = 3.1 cm, Platecxis, France) or a 24 cm² thin-film BDD electrode (CONDIAS GmbH, Germany). The anode was centered in the cell, surrounded by the carbon felt. Electrolysis was conducted under constant current conditions using a Hameg HM8040-3 triple power supply (Germany).

Compressed air was bubbled starting 5 min before electrolysis at about 0.5 L/min through the aqueous solutions to saturate aqueous solution before starting electrolysis and it is maintained during electrolysis to ensure the continuous saturation of oxygen. H₂O₂ was supplied from the electro-reduction of O₂ dissolved in the solution in all the electrolyses. The degradation experiments were performed using 0.2 mM ASP solution with 50 mM Na₂SO₄ as supporting electrolyte. A catalytic quantity of ferrous ion was added into the solution before the beginning of electrolysis. The initial pH (pH₀) of ASP solutions was measured with a CyberScan pH 1500 pH-meter (Eutech Instrument, USA) and set at 3.0 (±0.1), adjusting by the addition of 1 M sulfuric acid.

3.2.3 High performance liquid chromatography (HPLC) analysis

The initial and residual ASP concentration was monitored by HPLC, which consists of a Merck Lachrom liquid chromatograph, equipped with a L-2130 pump and was fitted with a Purospher RP-18, 5 μm, 25 cm × 4.6 mm (i.d.) column at 40 °C, and coupled with a L-2400 UV detector at maximum absorption wavelength of 215 nm for ASP. The analysis was performed using a 70:30 (v/v) water (0.1% acetic acid)/methanol (0.1% acetic acid) isocratic solvent mixture as mobile phase at a flow rate of 0.5 mL/min. The injection volume was 20 μL.

The short-chain carboxylic acids were identified and quantified by ion-exclusion

HPLC consisting of a Merck Lachrom liquid chromatograph equipped with a L-7100 pump, a Supelcogel H column (250 mm × 4.6 mm, 9 μm (i.d.) particle size) and a L-7455 photodiode array detector at a selected wavelength of 220 nm. 0.1% H₂SO₄ solution was used as mobile phase with a flow rate of 0.2 mL/min. Calibration curves were achieved using standard solutions of related carboxylic acids. The identification of the carboxylic acids was performed by the comparison between the retention time (t_R) and internal standard addition method using standard solutions.

3.2.4 Ion chromatography (IC) analysis

Inorganic ions (NO₃⁻ and NH₄⁺) released during the treatment were monitored by ion chromatography with a Dionex ICS-1000 Basic Ion Chromatography System equipped with an IonPac AS4A-SC (anion exchange) and CS12 A (cation exchange) 250 mm × 4 mm column and fitted with a DS6 conductivity detector containing a cell heated at 35 °C under control through a Chromeleon SE software. The mobile phase was a mixture of 3.6 mM Na₂CO₃ and 3.4 mM NaHCO₃ solution for anion-exchange column with a flow rate of 2.0 mL/min and 9 mM H₂SO₄ solution for cation-exchange with a flow rate of 1.0 mL/min. The volume of injections was 25 μL.

3.2.5 Total organic carbon (TOC) analysis

The TOC of the initial and electrolyzed samples were determined by Shimadzu TOC-V_{CSH} analyser according to the combustion catalytic oxidation method at 680 °C. The carrier gas was oxygen with a flow rate of 150 mL/min. Platinum was used as catalyst to carry out the combustion at 650 °C instead of 900 °C. The injection volume was 50 μL. Calibration of the analyser was obtained with potassium hydrogen phthalate standards.

3.2.6 Toxicity measurements

The evolution of the toxicity of treated solutions during the treatment was assessed by Microtox method according to the international standard process (OIN 11348-3)

using a Microtox[®] model 500. This measurements performed with the bio-luminescence marine bacteria *V. fischeri* (Buerge *et al.* 2009; Buerge *et al.* 2010; Bokare and Choi 2014), provided by Hach Lange France SAS. Two values of the inhibition of the luminescence (%) were measured after 5 min and 15 min of exposure to samples at 15 °C.

3.3 Results and discussion

3.3.1 Effect of catalyst concentration on ASP degradation

A set of electrolysis was carried out with 0.2 mM (58.9 mg/L) ASP in aqueous solutions to determine the influence of the main operating parameters on the ASP degradation in electro-Fenton process. The results obtained show that the oxidative degradation of ASP by electro-Fenton process fits well with the first-order kinetic model and the apparent rate constant values (k_{app}) calculated accordingly under different operating conditions were given in table 3-1.

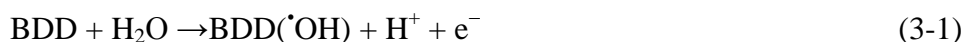
Table 3-1 Apparent rate constants (k_{app}) obtained in electro-Fenton processes for ASP degradation, assuming pseudo-first order kinetic model under different operating conditions. Operating conditions:

I and $[Fe^{2+}]$ variable, pH: 3.0 and carbon felt cathode

| Anode | $[Fe^{2+}]/mM$ | I/mA | $k_{app} (min^{-1})$ | R^2 |
|-------|----------------|--------|----------------------|-------|
| Pt | 0.05 | 200 | 0.15 ±0.01 | 0.994 |
| Pt | 0.1 | 200 | 0.24 ±0.01 | 0.992 |
| Pt | 0.2 | 200 | 0.34 ±0.01 | 0.995 |
| Pt | 0.3 | 200 | 0.26 ±0.01 | 0.996 |
| Pt | 0.5 | 200 | 0.22 ±0.02 | 0.999 |
| Pt | 0.2 | 50 | 0.14 ±0.01 | 0.997 |
| Pt | 0.2 | 100 | 0.15 ±0.01 | 0.998 |
| Pt | 0.2 | 300 | 0.34 ±0.03 | 0.968 |
| Pt | 0.2 | 500 | 0.17 ±0.01 | 0.997 |

| | | | | |
|------------|------|-----|-----------|-------|
| BDD | 0.05 | 200 | 0.30±0.02 | 0.979 |
| BDD | 0.1 | 200 | 0.34±0.01 | 0.993 |
| BDD | 0.2 | 200 | 0.51±0.05 | 0.965 |
| BDD | 0.3 | 200 | 0.32±0.01 | 0.998 |
| BDD | 0.5 | 200 | 0.28±0.02 | 0.989 |
| BDD | 0.2 | 50 | 0.15±0.01 | 0.998 |
| BDD | 0.2 | 100 | 0.25±0.01 | 0.989 |
| BDD | 0.2 | 300 | 0.40±0.01 | 0.998 |
| BDD | 0.2 | 500 | 0.25±0.01 | 0.991 |

The effect of catalyst (Fe^{2+}) concentration in ASP oxidation by electro-Fenton process was performed at current-controlled conditions and room temperature with Pt and BDD anode, respectively (Fig. 3-1). The Fe^{2+} concentration was varied in the range of 0.05–0.5 mM in 50 mM Na_2SO_4 solution, at applied current 200 mA and initial pH 3.0. As can be seen in Fig. 3-1, ASP can be totally removed in a 20 min reaction using Pt anode, while it only needs 15 min to degrade ASP completely with BDD anode. This indicated that the use of BDD did lead to the acceleration of the ASP degradation. On the one hand, due to the low adsorption ability of $\cdot\text{OH}$ on BDD, the loosely bound BDD($\cdot\text{OH}$) formed at the anode surface (Eq. (3-1)) can readily react with organic pollutant, in contrast to the chemisorbed radicals typically formed at Pt surface which limited the oxidation ability of Pt($\cdot\text{OH}$) (Özcan *et al.* 2009a; Dirany *et al.* 2012). On the other hand, reactive BDD($\cdot\text{OH}$) is generated in much higher quantities than Pt($\cdot\text{OH}$) when electrolysis is operated at the current within the water discharge region (Brillas *et al.* 2005; Panizza and Cerisola 2005; Brillas *et al.* 2009) because of the large O_2 evolution overvoltage of the former.

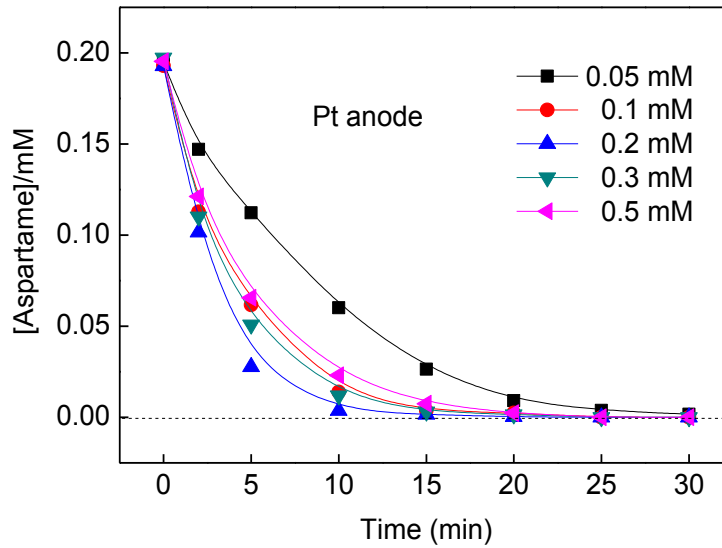


With both Pt and BDD anode, the removal efficiency and degradation rate of ASP increased significantly when Fe^{2+} concentration increased from 0.05 to 0.2 mM (Fig. 3-1 and Table 3-1). At higher Fe^{2+} concentration, a considerable amount of hydroxyl

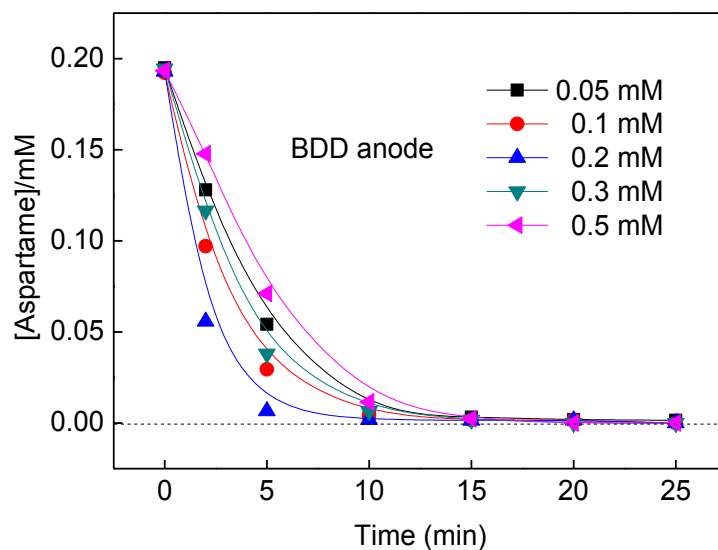
radicals would be produced via Fenton's reaction. These hydroxyl radicals react with ASP immediately, resulting in the increase of ASP degradation rate. However, further increasing the Fe^{2+} concentration to 0.5 mM, ASP removal efficiency and rate constant decreased evidently (Fig. 3-1 and Table 3-1). The negative influence of higher Fe^{2+} concentration might be attributed to the role of Fe^{2+} as scavenger of hydroxyl radicals (Eq. (3-2)) which takes place with a large rate constant ($k = 3.20 \times 10^8 \text{ M}^{-1} \text{ S}^{-1}$) (Sir és *et al.* 2007b; Oturan *et al.* 2010).



Therefore, the reaction (3-2) becomes competitive for OH consumption at higher Fe^{2+} and consequently harms the oxidation of ASP.



(a)



(b)

Fig. 3-1 Effect of Fe^{2+} (as catalyst) concentration on electro-Fenton degradation of 0.2 mM ASP with Pt (a) and BDD (b) anode versus carbon-felt cathode. Experimental conditions: $I = 200$ mA, $\text{pH}_0 = 3.0$, $[\text{Na}_2\text{SO}_4] = 50$ mM

3.3.2 Effect of applied current on ASP degradation

In electro-Fenton process, the applied current is a crucial parameter for the operational cost and process efficiency (Özcan *et al.* 2009a), because the formation rate of H_2O_2 (Eq. (3-4)), the regeneration rate of Fe^{2+} (Eq. (3-3)) and consequently the generation rate of $\bullet\text{OH}$ through Fenton's reaction (Eq. (2-1)) are governed by this parameter. The applied current governs also the formation rate (Eq. (3-1)) and the amount of heterogeneous hydroxyl radicals BDD($\bullet\text{OH}$) or Pt($\bullet\text{OH}$). Therefore the effect of applied current for the treatment of 0.2 mM ASP in electro-Fenton processes using Pt/carbon-felt (Fig. 3-2a) and BDD/carbon-felt (Fig. 3-2b) cells was examined by using the applied current of 50, 100, 200, 300 and 500 mA.

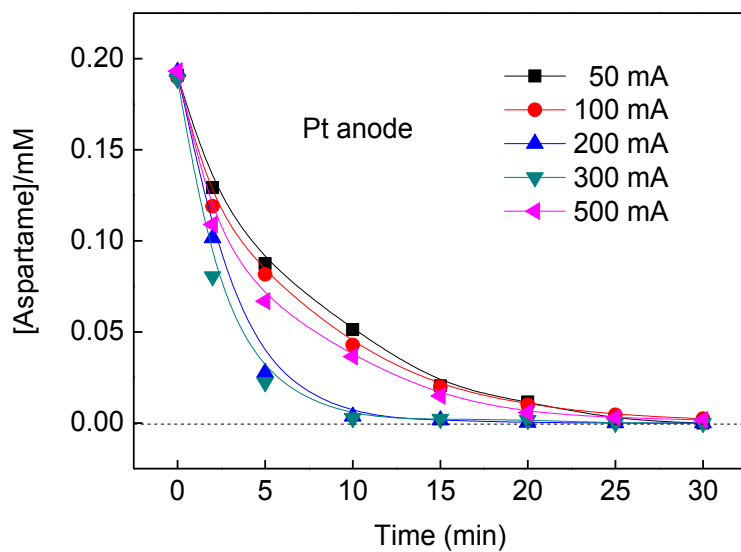
As depicted in Fig. 3-2a, the total disappearance of ASP became faster at a higher current in Pt/carbon-felt cell. The k_{app} increased from 0.14 to 0.34 min^{-1} when the applied current increased from 50 to 300 mA (Table 3-1). A higher current can promote both the Fe^{2+} regeneration (Eq. (3-3)) and the production of H_2O_2 (Eq. (3-4)) (Lin *et al.*

2014). However, further increasing the current to 500 mA resulted in the decrease of k_{app} to 0.17 min^{-1} . The decrease in ASP oxidation efficiency at higher current can be related to the increase of parasitic reactions, such as H_2 evolution reaction (Eq.(3-5)) (Dirany *et al.* 2012).

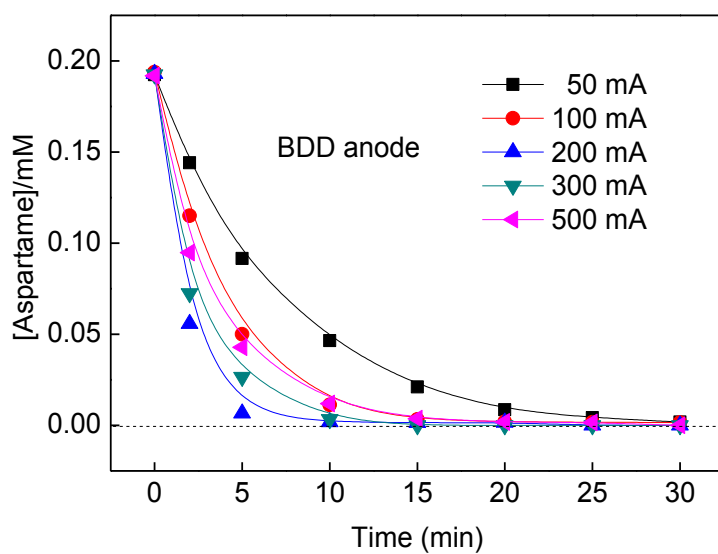


When it comes to the BDD/carbon-felt cell, the optimal current for ASP degradation was 200 mA (Fig. 3-2b). Moreover, it can be seen from Fig. 2 that the comparatively better performance of BDD was more pronounced at lower current intensities. When applied current is higher than 200 mA, the positive role of BDD favoring generation of $\cdot\text{OH}$ was insignificant (Table 3-1). This means the application of BDD anode can improve removal efficiency of ASP and reduce energy consumption by using lower current intensity. A similar behavior has been observed for the degradation of sulfachloropyridazine (Dirany *et al.* 2012). At current intensity above 200 mA, the removal efficiency decreased. This could due to the increase of side reactions: (i) H_2 evolution from H_2O reduction (Eq. (3-5)). (ii) The 4-e^{-} reduction of O_2 leading to the formation of H_2O (Eq. (3-6)) which inhibited the H_2O_2 formation reaction (Eq. (3-4)) occurring on carbon-felt cathode (Özcan *et al.* 2009b). Moreover, the O_2 evolution reaction was more dominate than $\cdot\text{OH}$ on the BDD anode at high applied current (Özcan *et al.* 2009b). (iii) The formation of weak oxidant species like $\text{HO}_2\cdot$ (Eq. (3-7)) which could react with $\cdot\text{OH}$ resulting in the formation of H_2O and O_2 (Eq.(3-8)) (Wu *et al.* 2012).





(a)



(b)

Fig. 3-2 Effect of applied current on electro-Fenton degradation of 0.2 mM ASP by Pt (a) and BDD (b) anode versus carbon-felt cathode. Experimental conditions: $[\text{Fe}^{2+}] = 0.2 \text{ mM}$, $\text{pH}_0 = 3.0$, $[\text{Na}_2\text{SO}_4] = 50 \text{ mM}$

3.3.3 Determination of absolute constants for oxidation of ASP by hydroxyl radicals

The absolute rate constant of ASP treatment by hydroxyl radicals during electro-Fenton process was determined by competition kinetics method. Benzoic acid (BA) was selected as standard competitor because the absolute rate constant ($k_{\text{abs,BA}}$) of the reaction between BA and hydroxyl radicals is well known ($k_{\text{abs,BA}} = 4.30 \times 10^9 \text{ M}^{-1} \text{ s}^{-1}$) (Özcan *et al.* 2008; Sirés *et al.* 2007c; Oturan *et al.* 2010). Experiments were performed using Pt anode with 0.1 mM ASP solution, Fe^{2+} concentration 0.2 mM, applied current 50 mA and initial pH 3.0. The absolute rate constant of the oxidation of ASP was then calculated according to the Eq. (3-9).

$$\text{Ln} \left(\frac{[\text{ASP}]_0}{[\text{ASP}]_t} \right) = \left(\frac{k_{\text{abs,ASP}}}{k_{\text{abs,BA}}} \right) \text{Ln} \left(\frac{[\text{BA}]_0}{[\text{BA}]_t} \right) \quad (3-9)$$

Based on Fig. 3-3, the absolute rate constant for the oxidation reaction of ASP and $\cdot\text{OH}$ ($k_{\text{abs,ASP}}$) was then determined as $(5.23 \pm 0.02) \times 10^9 \text{ M}^{-1} \text{ s}^{-1}$. This value is closed to that reported by Toth *et al.* 2012 $(6.06 \pm 0.05) \times 10^9 \text{ M}^{-1} \text{ s}^{-1}$) who determined the absolute rate constant by direct observation of the formation of the cyclohexadienyl radical adduct.

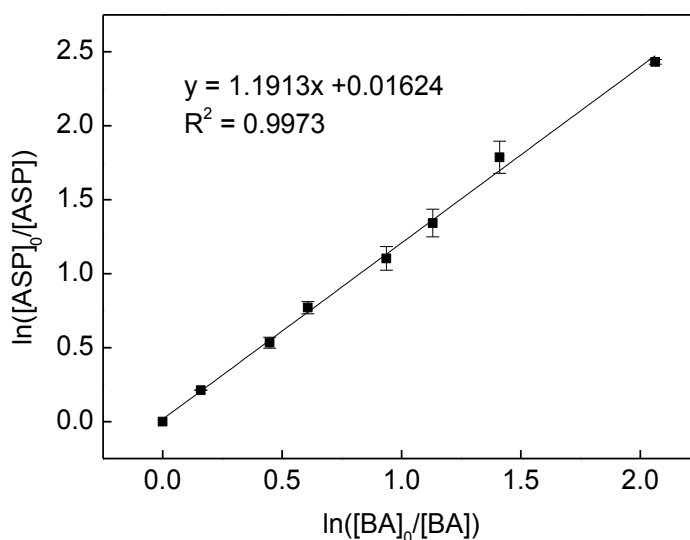


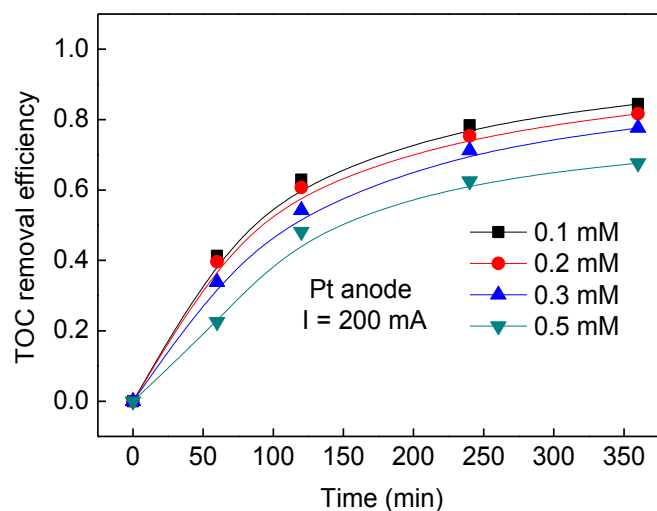
Fig. 3-3 Determination of $k_{\text{abs(ASP)}}$ by competition kinetic method according to the pseudo first-order kinetics between ASP and BA during the electro-Fenton process. Experimental conditions: $[\text{ASP}]_0 = 0.1 \text{ mM}$, $([\text{BA}]_0 = 0.1 \text{ mM}$, $[\text{Fe}^{2+}] = 0.2 \text{ mM}$, $I = 50 \text{ mA}$, $\text{pH}_0 = 3.0$, $[\text{Na}_2\text{SO}_4] = 50 \text{ mM}$

3.3.4 The effect of catalyst concentration and applied current on ASP mineralization

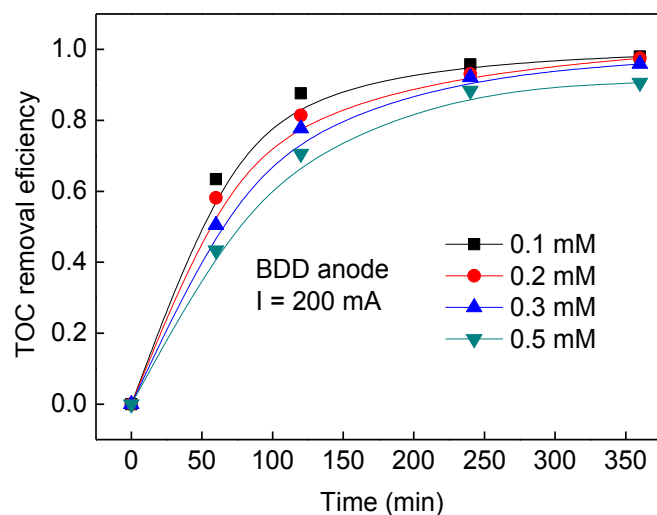
Fig. 3-4 shows the influence of Fe^{2+} concentration on the mineralization of ASP solution in terms of TOC abatement under the same conditions of Fig. 3-1.

For both Pt/carbon-felt and BDD/carbon-felt cell, the TOC removal efficiency decreased as Fe^{2+} concentration increased from 0.1 to 0.5 mM. With the increasing Fe^{2+} concentration, the percentage of scavenged hydroxyl radicals from Fe^{2+} ions increased, so the side reactions between Fe^{2+} ions and $\cdot\text{OH}$ (Eq. (3-2)) became more significant (Özcan *et al.* 2008). This reaction becomes particularly important at longer treatment time because of lower concentration of organic matter in the solution. Furthermore, as can be seen from Fig. 3-4, the TOC removal rate was fast during the first 120 min for all the Fe^{2+} concentration in both cells. After 120 min, the TOC removal values gradually decreased and reached a steady state. This is due to the quick decomposition of ASP and its aromatic derivatives which are more easily oxidizable than the ring opening products such as aliphatic acids obtained at longer treatment times (Hammami *et al.* 2008). The slower mineralization rate observed at longer electrolysis times for both Pt and BDD anodes can also be attributed to the formation of stable ferro- and/or ferri-complexes with carboxylic acids (Oturán *et al.* 2000; Brillas *et al.* 2003; Guivarch *et al.* 2003; Hammami *et al.* 2008; Haidar *et al.* 2013).

Even so, it is evident that the use of BDD anode lead to the acceleration of ASP mineralization (Fig. 3-4). For example, at the end of the 360 min electrolysis, 84.5% and 98.0% of the initial TOC value was removed, in the case of Fe^{2+} concentration of 0.1 mM, for Pt and BDD anode, respectively. Moreover, BDD/carbon-felt cell achieved > 95% mineralization in only 240 min at 0.1 mM Fe^{2+} , while 84.5% mineralization reached at 360 min for Pt/carbon-felt cell. It can be explained that BDD anode contributed to the degradation of all the byproducts, even the most refractory ones (Dirany *et al.* 2012) due to the high reactivity of BDD($\cdot\text{OH}$) largely formed at this anode.



(a)

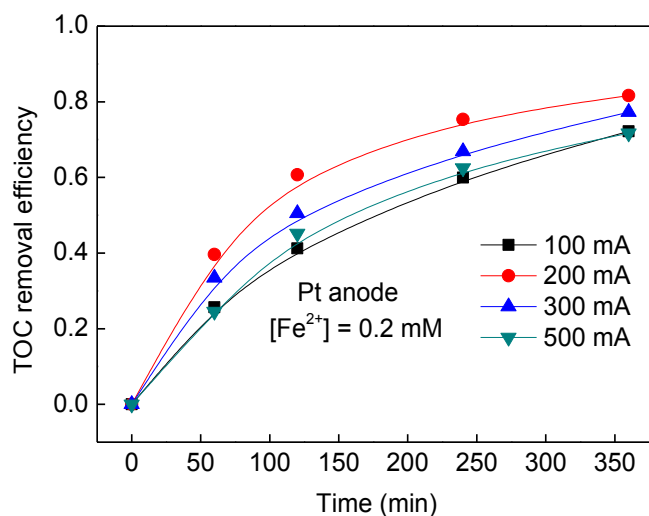


(b)

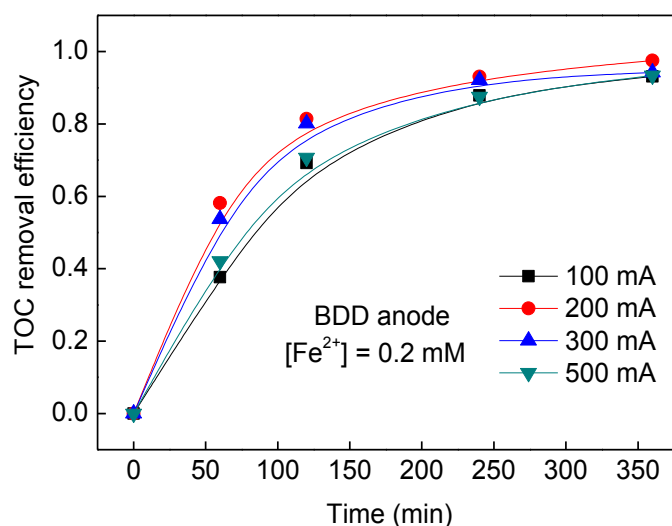
Fig. 3-4 Effect of Fe^{2+} concentration on mineralization of 0.2 mM ASP with Pt (a) and BDD (b) anode versus carbon-felt cathode. Experimental conditions: $I = 200$ mA, $\text{pH}_0 = 3.0$, $[\text{Na}_2\text{SO}_4] = 50$ mM

The effect of applied current on the mineralization of ASP solution in terms of TOC abatement under the same conditions of Fig. 3-2 was investigated and the results were shown in Fig. 3-5. With the raising applied current from 100 to 200 mA, the TOC removal efficiency was found to increase from 72.2% to 81.7% in Pt/carbon-felt cell. The TOC removal efficiency increased from 93.1% to 97.5% in BDD/carbon-felt cell at

the end of 360 min electrolysis under the same conditions. Higher applied current lead to the higher accumulation of hydroxyl radicals in the bulk, and then a greater mineralization efficiency can be achieved because of the simultaneous degradation of ASP and its byproducts (Dirany *et al.* 2012). Further increase in the applied current to 500 mA, the TOC removal efficiency declined to 71.6% and 93.4% for Pt and BDD anode, respectively. In the treatment of ASP, the application of current higher than 200 mA would increase the extent of parasitic reactions (Eq. (3-5)-(3-8)), leading to the decrease of the process efficiency (Mousset *et al.* 2014).



(a)



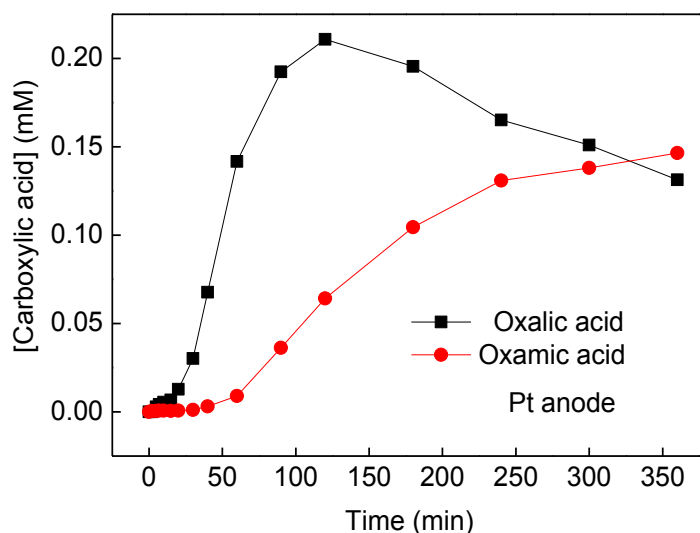
(b)

Fig. 3-5 Effect of applied current on mineralization of 0.2 mM ASP with Pt (a) and BDD (b) anode versus carbon-felt cathode. Experimental conditions: [Fe²⁺] = 0.2 mM, pH₀ 3.0, [Na₂SO₄] = 50 mM

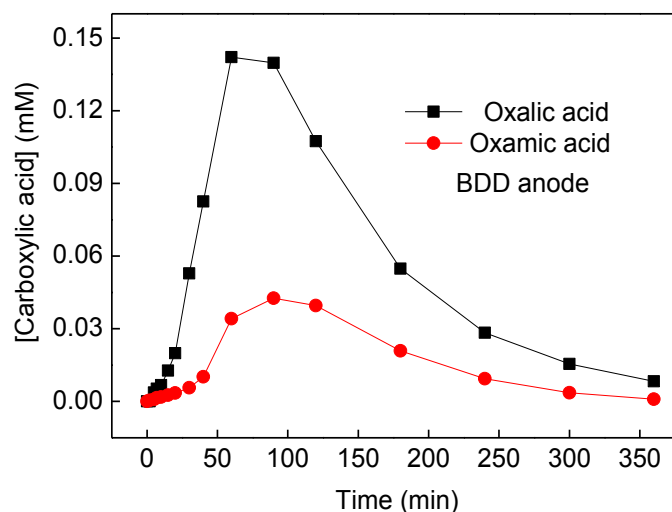
3.3.5 Identification and evolution of carboxylic acids

It is well known that the cleavage of the benzenic ring of aromatics can lead to the release of short-chain carboxylic acids in electro-Fenton process (Sirés *et al.* 2007a; Özcan *et al.* 2009b; Isarain-Chávez *et al.* 2010; Dirany *et al.* 2012; El-Ghenymy *et al.* 2013). The concentration of carboxylic acids were monitored by ion-exclusion HPLC when 0.2 mM ASP solutions were electrolyzed under the conditions of Figs. 3-4 and 3-5. In this study, oxalic, oxamic and maleic acid at retention time (t_R) of 8.90, 14.26 and 11.33 were observed, respectively, in both Pt/carbon-felt and BDD/carbon-felt cell. Among these carboxylic acids, the concentration of maleic acid was detected in trace and only exist in the first 10 min in both cells, so changes of maleic acid concentration were not shown in Fig. 3-6.

As shown in Fig. 3-6, all the carboxylic acids were generated at the beginning of the electrolysis and followed the accumulation-destruction cycles. A similar behavior has been observed for the treatment of other organic products (Özcan *et al.* 2009b; Dirany *et al.* 2012). Oxalic and oxamic acids were remained even at the end of the electrolysis indicating their lower reactivity with hydroxyl radicals and need much more time to destruction (Dirany *et al.* 2012). It also depicted by comparing Fig. 3-6a and Fig. 3-6b that all the acids were nearly disappeared at the end of electrolysis (360 min) in BDD/carbon-felt cell, in agreement with the mineralization results shown in Fig. 3-4b and Fig. 3-5b. However, oxalic and oxamic acid were still existed in Pt/carbon-felt cell in 360 min reaction, which was corresponding to the residual TOC remaining at the end of mineralization treatments (Fig. 3-4a and Fig. 3-5a).



(a)



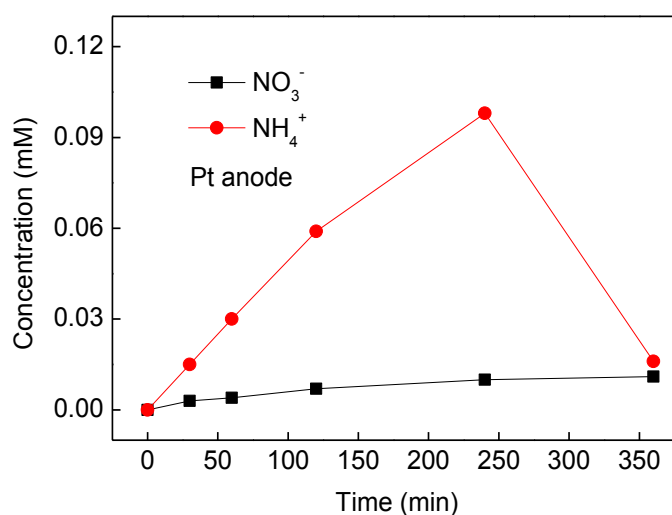
(b)

Fig. 3-6 Evolution of short-chain carboxylic acids formed during electro-Fenton processes with Pt (a) and BDD (b) anodes versus carbon-felt cathode. Experimental conditions: $[\text{ASP}]_0 = 0.2 \text{ mM}$, $[\text{Fe}^{2+}] = 0.2 \text{ mM}$, $I = 200 \text{ mA}$, $\text{pH}_0 = 3.0$, $[\text{Na}_2\text{SO}_4] = 50 \text{ mM}$

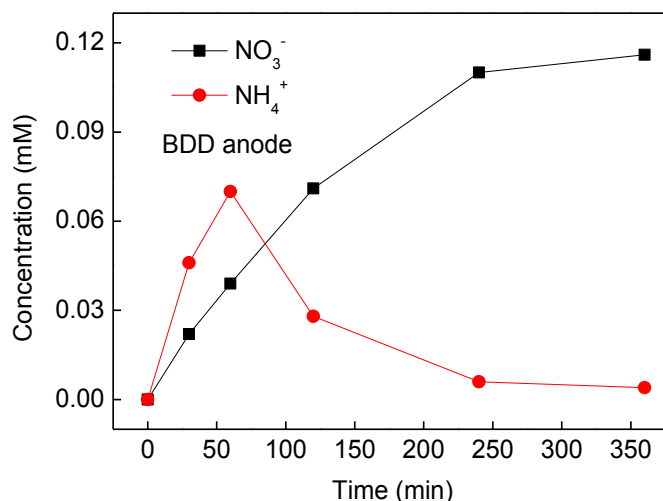
3.3.6 Identification and evolution of inorganic ions

During the mineralization of ASP, the N atoms were released as inorganic ions upon the cleavage of the ASP molecules. The qualitative and quantitative monitoring of NO_3^- and NH_4^+ was performed by the ionic chromatography analysis. The evolution of the ions concentration identified during the electro-Fenton process was shown in Fig.

3-7. The final concentration of NO_3^- was much higher with BDD anode, which agrees with the faster mineralization mentioned in Fig. 3-4. NO_3^- and NH_4^+ were formed from the beginning of the electrolysis. In Pt/carbon-felt cell, the release of ammonium ions was much larger than that of nitrate ions in 240 min reaction, but it decreased to 0.016 mM after 360 min reaction. The release of NO_3^- in Pt/carbon-felt cell increased from 0 to 0.011 mM. Moreover, Fig. 6a indicated that 0.15 mM oxamic acid was existed in Pt/carbon-felt cell at 360 min reaction. At the end of electrolysis, 43.2% of initial nitrogen of ASP as NO_3^- (6.35% of total), NH_4^+ (9.25% of total) and oxamic acid (84.4% of total) was quantified. This indicated some other refractory nitrogenated compounds are formed in the Pt/carbon-felt cell that account for the remaining TOC at 360 min. In BDD/carbon-felt cell, the concentration of NH_4^+ increased to 0.07 mM in the first 60 min, and then it decreased to 0.004 mM at 360 min. NO_3^- increased persistently from the beginning to the end of the reaction and the concentration reached 0.116 mM at 360 min. Since TOC was nearly completely removed in BDD/carbon-felt cell at 360 min reaction, the non equilibrating of the nitrogen mass balance could be attributed to the transformation of nitrogen to other nitrogen species, such as NO_2^- , gas N_2 and NH_3 (Hammami *et al.* 2008).



(a)



(b)

Fig. 3-7 Evolution of the concentration of the inorganic ions released during electro-Fenton processes with Pt (a) and BDD (b) anode versus carbon-felt cathode. Experimental conditions:

[ASP]₀ = 0.2 mM, [Fe²⁺] = 0.2 mM, *I* = 200 mA, pH₀ 3.0, [Na₂SO₄] = 50 mM

3.3.7 The evolution of solution toxicity with reaction time

In order to monitor the potential toxicity of ASP and its byproducts, 0.2 mM ASP was electrolyzed in the presence of 0.2 mM Fe²⁺ at 200 mA using Microtox method for both Pt and BDD anode. The percentage of bacteria luminescence inhibition versus the electrolysis time was recorded after 5 and 15 min exposure times of *V. fischeri* luminescent bacteria to the ASP solutions. In Fig. 3-8, only the curves obtained after a 15 min exposure time were presented, because the curves recorded after a 5 min exposure time were very similar.

For Pt/carbon-felt cell, the curves of inhibition percentage were characterized by a strong increase of the toxicity at 10 min. This indicated that the formed intermediates of ASP at the beginning of the electrolysis, which might mainly contain the cyclic compounds, were more toxic than ASP. The percentage of inhibition decreased sharply after 10 min, which showed the decrease of toxic intermediate products. The secondary peak which appeared at 120 min was much lower than the primary peak, showing the toxicity of secondary intermediates were much lower than the former byproducts, even a little lower than the untreated ASP solution. After 120 min, the inhibition percentage

decreased slowly to the end of the electrolysis.

The curves obtained for BDD anode showed an analogous behavior at the beginning of the electrolysis as Pt anode. The toxicity increased significantly and attained the maximum luminescence inhibition peak at 15 min. The secondary peak appeared at 40 min and showed the secondary intermediates still more toxic than the original ASP solution. After 40 min treatment, the percentage of inhibition decreased and became stable from 120 min. This might due to the destruction of ASP and its cyclic byproducts.

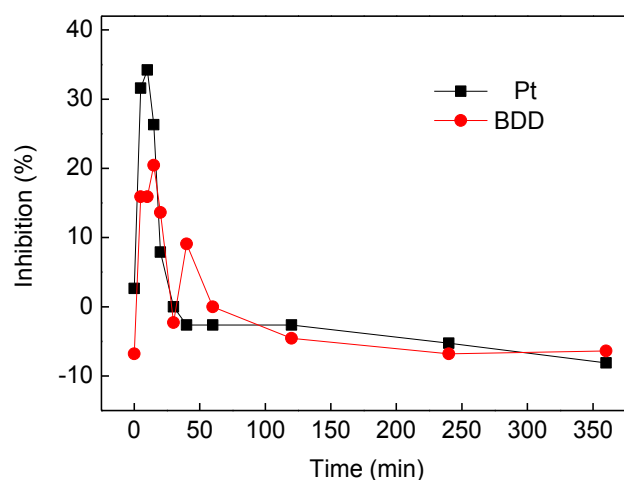


Fig. 3-8 Evolution of the inhibition of marine bacteria, *Vibrio fischeri* luminescence (Microtox method) during electro-Fenton processes. Experimental conditions: $[\text{ASP}]_0 = 0.2 \text{ mM}$, $[\text{Fe}^{2+}] = 0.2 \text{ mM}$, $I = 200 \text{ mA}$, $\text{pH}_0 = 3.0$, $[\text{Na}_2\text{SO}_4] = 50 \text{ mM}$

3.4 Conclusions

Aqueous solution of 0.2 mM ASP was degraded effectively by electro-Fenton process using a carbon-felt cathode and a Pt or BDD anode. Complete removal of ASP was attained by both anodes, due to the formation of $\cdot\text{OH}$ in the bulk from Fenton reaction and at the anode surface from water oxidation. For both anodes, ASP could be completely removed in less than 30 min and the ASP concentration decay followed pseudo-first-order kinetics. Absolute rate constant of hydroxylation reaction of ASP was determined as $(5.23 \pm 0.02) \times 10^9 \text{ M}^{-1} \text{ s}^{-1}$. The use of BDD instead of Pt anode yields a faster mineralization rate because of the higher oxidation power of BDD($\cdot\text{OH}$)

comparing with $\text{Pt}(\bullet\text{OH})$. Short-chain aliphatic carboxylic acids such as oxalic, oxamic and maleic acid were identified as aliphatic intermediates by ion-exclusion chromatography. The bacteria luminescence inhibition showed the toxicity of ASP solution increased at the beginning of electrolysis, and then it declined until lower than the untreated ASP solution at the end of the reaction.

References

- Bokare, A.D. and Choi, W. (2014) Review of iron-free Fenton-like systems for activating H_2O_2 in advanced oxidation processes. *Journal of Hazardous Materials* 275, 121-135.
- Brillas, E., Baños, M.Á. and Garrido, J.A. (2003) Mineralization of herbicide 3,6-dichloro-2-methoxybenzoic acid in aqueous medium by anodic oxidation, electro-Fenton and photoelectro-Fenton. *Electrochimica Acta* 48(12), 1697-1705.
- Brillas, E., Sirés, I., Arias, C., Cabot, P.L., Centellas, F., Rodríguez, R.M. and Garrido, J.A. (2005) Mineralization of paracetamol in aqueous medium by anodic oxidation with a boron-doped diamond electrode. *Chemosphere* 58(4), 399-406.
- Brillas, E., Sirés, I. and Oturan, M.A. (2009) Electro-Fenton process and related electrochemical technologies based on Fenton's reaction chemistry. *Chemical Reviews* 109(12), 6570-6631.
- Buerge, I.J., Buser, H.-R., Kahle, M., Müller, M.D. and Poiger, T. (2009). Ubiquitous occurrence of the artificial sweetener acesulfame in the aquatic environment: An ideal chemical marker of domestic wastewater in groundwater. *Environmental Science & Technology* 43(12), 4381-4385.
- Buerge, I.J., Keller, M., Buser, H.-R., Müller, M.D. and Poiger, T. (2010). Saccharin and other artificial sweeteners in soils: Estimated inputs from agriculture and households, degradation, and leaching to groundwater. *Environmental Science & Technology* 45(2), 615-621..
- Dirany, A., Sirés, I., Oturan, N., Özcan, A. and Oturan, M.A. (2012) Electrochemical treatment of the antibiotic sulfachloropyridazine: Kinetics, reaction pathways, and toxicity Evolution. *Environmental Science & Technology* 46(7), 4074-4082.

- El-Ghenymy, A., Oturan, N., Oturan, M.A., Garrido, J.A., Cabot, P.L., Centellas, F., Rodríguez, R.M. and Brillas, E. (2013) Comparative electro-Fenton and UVA photoelectro-Fenton degradation of the antibiotic sulfanilamide using a stirred BDD/air-diffusion tank reactor. *Chemical Engineering Journal* 234, 115-123.
- Guivarch, E., Trevin, S., Lahitte, C. and Oturan, M. (2003) Degradation of azo dyes in water by Electro-Fenton process. *Environmental Chemistry Letters* 1(1), 38-44.
- Haidar, M., Dirany, A., Sirés, I., Oturan, N. and Oturan, M.A. (2013) Electrochemical degradation of the antibiotic sulfachloropyridazine by hydroxyl radicals generated at a BDD anode. *Chemosphere* 91(9), 1304-1309.
- Hammami, S., Bellakhal, N., Oturan, N., Oturan, M.A. and Dachraoui, M. (2008) Degradation of Acid Orange 7 by electrochemically generated $\cdot\text{OH}$ radicals in acidic aqueous medium using a boron-doped diamond or platinum anode: A mechanistic study. *Chemosphere* 73(5), 678-684.
- Isarain-Chávez, E., Arias, C., Cabot, P.L., Centellas, F., Rodríguez, R.M., Garrido, J.A. and Brillas, E. (2010) Mineralization of the drug β -blocker atenolol by electro-Fenton and photoelectro-Fenton using an air-diffusion cathode for H_2O_2 electrogeneration combined with a carbon-felt cathode for Fe^{2+} regeneration. *Applied Catalysis B: Environmental* 96(3-4), 361-369.
- Lin, H., Zhang, H., Wang, X., Wang, L. and Wu, J. (2014) Electro-Fenton removal of Orange II in a divided cell: Reaction mechanism, degradation pathway and toxicity evolution. *Separation and Purification Technology* 122, 533-540.
- Mousset, E., Oturan, N., van Hullebusch, E.D., Guibaud, G., Esposito, G. and Oturan, M.A. (2014) Influence of solubilizing agents (cyclodextrin or surfactant) on phenanthrene degradation by electro-Fenton process – Study of soil washing recycling possibilities and environmental impact. *Water Research* 48, 306-316.
- Oturan, M.A., Edelahi, M.C., Oturan, N., El kacemi, K. and Aaron, J.-J. (2010) Kinetics of oxidative degradation/mineralization pathways of the phenylurea herbicides diuron, monuron and fenuron in water during application of the electro-Fenton process. *Applied Catalysis B: Environmental* 97(1-2), 82-89.
- Oturan, M.A., Peirotten, J., Chartrin, P. and Acher, A.J. (2000). Complete destruction of

- p-Nitrophenol in aqueous medium by electro-Fenton method. *Environmental Science & Technology* 34(16), 3474-3479.
- Özcan, A., Oturan, M.A., Oturan, N. and Şahin, Y. (2009a) Removal of Acid Orange 7 from water by electrochemically generated Fenton's reagent. *Journal of Hazardous Materials* 163(2–3), 1213-1220.
- Özcan, A., Şahin, Y., Koparal, A.S. and Oturan, M.A. (2008) Degradation of picloram by the electro-Fenton process. *Journal of Hazardous Materials* 153(1–2), 718-727.
- Özcan, A., Şahin, Y., Koparal, A.S. and Oturan, M.A. (2009b) A comparative study on the efficiency of electro-Fenton process in the removal of prothionamide from water. *Applied Catalysis B: Environmental* 89(3–4), 620-626.
- Özcan, A., Şahin, Y. and Oturan, M.A. (2013) Complete removal of the insecticide azinphos-methyl from water by the electro-Fenton method – A kinetic and mechanistic study. *Water Research* 47(3), 1470-1479.
- Panizza, M. and Cerisola, G. (2005) Application of diamond electrodes to electrochemical processes. *Electrochimica Acta* 51(2), 191-199.
- Sirés, I., Centellas, F., Garrido, J.A., Rodríguez, R.M., Arias, C., Cabot, P.-L. and Brillas, E. (2007a) Mineralization of clofibric acid by electrochemical advanced oxidation processes using a boron-doped diamond anode and Fe^{2+} and UVA light as catalysts. *Applied Catalysis B: Environmental* 72(3–4), 373-381.
- Sirés, I., Garrido, J.A., Rodríguez, R.M., Brillas, E., Oturan, N. and Oturan, M.A. (2007b) Catalytic behavior of the $\text{Fe}^{3+}/\text{Fe}^{2+}$ system in the electro-Fenton degradation of the antimicrobial chlorophene. *Applied Catalysis B: Environmental* 72(3–4), 382-394.
- Sirés, I., Oturan, N., Oturan, M.A., Rodríguez, R.M., Garrido, J.A. and Brillas, E. (2007c) Electro-Fenton degradation of antimicrobials triclosan and triclocarban. *Electrochimica Acta* 52(17), 5493-5503.
- Toth, J.E., Rickman, K.A., Venter, A.R., Kiddle, J.J. and Mezyk, S.P. (2012). Reaction kinetics and efficiencies for the hydroxyl and sulfate radical based oxidation of artificial sweeteners in water. *The Journal of Physical Chemistry A* 116(40), 9819-9824.

Wu, J., Zhang, H., Oturan, N., Wang, Y., Chen, L. and Oturan, M.A. (2012) Application of response surface methodology to the removal of the antibiotic tetracycline by electrochemical process using carbon-felt cathode and DSA (Ti/RuO₂-IrO₂) anode. *Chemosphere* 87(6), 614-620.

**Chapter 4 Treatment of saccharin (SAC) in aqueous solution by
electro-Fenton process**

4.1 Introduction

In this part, the effect of different anode materials and different supporting electrolyte on the removal of sweetener saccharine (SAC) was investigated by electro-Fenton process. The absolute rate constant of the reaction between SAC and $\cdot\text{OH}$ was determined by the competition kinetic method. The effect of the Fe^{2+} concentration and applied current on the degradation and mineralization of SAC was examined. The aliphatic short-chain carboxylic acids released during electro-Fenton process were monitored. The variation of toxicity of SAC solution and its intermediates was determined by Microtox method.

4.2 Materials and methods

4.2.1 Chemicals

Saccharin (1,1-dioxo-1,2-benzothiazol-3-one (or o-benzoic sulfimide), $\text{C}_7\text{H}_5\text{CNO}_3\text{S}$) was purchased from Sigma-Aldrich. Analytical grade anhydrous sodium sulfate and ferrous sulfate heptahydrated were obtained from Sigma-Aldrich and Acros Organics, respectively. Regent grade benzoic acid was purchased from Problabo (France) used as the competition substrate in several kinetic experiments. Analytical grade carboxylic acids and other chemicals used for chromatographic analysis were purchased from Acros, Merck, Sigma, Riedel-de Haën and Fluka. Ultrapure water used for the preparation of the working solutions and HPLC eluting solutions was obtained from a Millipore Milli-Q (simplicity 185) system with resistivity $> 18 \text{ M}\Omega \text{ cm}$ at room temperature.

4.2.2 Electrochemical apparatus and procedures

Electrolyses were performed at constant current and room temperature using a Hameg HM8040-3 triple power supply (Germany) in an open, cylindrical undivided glass cell of 6 cm diameter and 250 mL capacity containing 220 mL SAC solution.

Electro-Fenton oxidation was conducted using three anodes: a cylindrical Pt mesh (4.5 cm height, i.d. = 3.1 cm, Platecxis, France), a 25 cm² thin-film BDD (CONDIAS GmbH, Germany) and a commercial DSA (mixed metal oxide Ti/RuO₂-IrO₂, Baoji Xinyu GuangJiDian Limited Liability Company, China). A 87.5 cm² piece of carbon felt (17.5 × 5 cm, Carbon-Lorraine, France) was used as cathode.

In all cases, the anode was centered in the electrolytic cell and was surrounded by the cathode that covered the inner wall of the cell. H₂O₂ was produced from reduction of O₂ dissolved in the solution. Continuous saturation of O₂ at atmospheric pressure was ensured by bubbling compressed air passing through a frit at about 0.5 L/min, starting 5 min before the beginning of the electrolysis. Prior to the electrolysis, a catalytic quantity of ferrous ion and 50 mM Na₂SO₄ (supporting electrolyte) were added to the SAC solutions with constant stirring by using a magnetic stirrer (IKA, Germany).

The pH of initial solutions (pH₀) was set at 3.0 by the addition of 1 M sulfuric acid because this value was reported as the optimal pH value for the electro-Fenton processes (Özcan *et al.* 2008a). The pH of SAC solutions was measured with a CyberScan pH 1500 pH-meter (Eutech Instrument, USA).

4.2.3 Analytical methods and procedures

The concentration of residual SAC was monitored by high performance liquid chromatography (HPLC), which consist of a Merck Lachrom liquid chromatograph, equipped with a L-2130 pump and fitted with a Purospher RP-18, 5 μm, 25 × 4.6 mm (i.d.) column at 40 °C, and coupled with a L-2400 UV detector at maximum absorption wavelength of 218 nm for SAC. The analyses were performed using a phosphoric acid (pH 3.0)/methanol (80:20, v/v) as mobile phase in isocratic mode at a flow rate of 1.0 mL/min. The injection volume was 20 μL.

The short-chain carboxylic acids were identified and quantified by ion-exclusion HPLC using a L-7100 pump, a Merck Lachrom liquid chromatograph equipped with a Supelcogel H column (250 × 4.6 mm, 9 μm) and a L-7455 photodiode array detector at the wavelength of 220 nm. The mobile phase was 0.1% H₂SO₄ solution and flow rate

was fixed to 0.2 mL/min. Calibration curves were achieved using standard solutions of related carboxylic acids. The identification of the carboxylic acids was performed by the retention time (t_R) comparison and standard addition methods using standard substances.

The TOC of the samples withdrawn from the treated solution at different electrolysis times was determined by Shimadzu TOC-V_{CSH} analyser consisting of a non dispersive infra-red absorption detector (NDIR) according to the 680 °C combustion catalytic oxidation method. Platinum based catalyst was used to facilitate the combustion at 650 °C. The carrier gas was oxygen with a flow rate of 150 mL/min. The injection volume was 50 µL.

4.2.4 Toxicity measurements

The toxicity of SAC and its intermediates generated in electro-Fenton processes was investigated on samples collected from solutions at different electrolysis times. Experiments were performed with the bio-luminescence marine bacteria *V. fischeri* (Hach Lange France SAS) by Microtox method according to the international standard process (OIN 11348-3). Two values of the inhibition of the luminescence (%) were measured after 5 min and 15 min of exposure to samples at 15 °C using a Microtox model 500 system.

4.3 Results and discussion

4.3.1 Effect of supporting electrolyte on the degradation of SAC

In order to investigate the effect of the supporting electrolyte on the degradation kinetics of SAC aqueous solutions, experiments were performed in acidic medium (pH 3.0) containing different supporting electrolytes as 50 mM Na₂SO₄, 100 mM NaNO₃ and 100 mM NaCl with three anodes (Fig. 4-1). The removal of SAC followed the first-order kinetic model and the apparent rate constant values (k_{app}) were determined

accordingly and given in table 4-1.

Table 4-1 Apparent rate constants (k_{app}) obtained in electro-Fenton processes for SAC degradation, assuming pseudo-first order kinetic model under different operating conditions.

| Electrode | [Fe ²⁺]/mM | I/mA | supporting electrolyte | k_{app} (min ⁻¹) | R ² |
|------------|------------------------|------|---|-----------------------------------|----------------|
| DSA | 0.2 | 200 | Na ₂ SO ₄ (50 mM) | 0.181±0.004 | 0.997 |
| DSA | 0.2 | 200 | NaNO ₃ (100 mM) | 0.170±0.030 | 0.998 |
| DSA | 0.2 | 200 | NaCl (100 mM) | 0.019±0.001 | 0.994 |
| Pt | 0.2 | 200 | Na ₂ SO ₄ (50 mM) | 0.211±0.008 | 0.990 |
| Pt | 0.2 | 200 | NaNO ₃ (100 mM) | 0.125±0.007 | 0.977 |
| Pt | 0.2 | 200 | NaCl (100 mM) | 0.038±0.001 | 0.999 |
| BDD | 0.2 | 200 | Na ₂ SO ₄ (50 mM) | 0.194±0.008 | 0.988 |
| BDD | 0.2 | 200 | NaNO ₃ (100 mM) | 0.143±0.002 | 0.998 |
| BDD | 0.2 | 200 | NaCl (100 mM) | 0.023±0.001 | 0.999 |
| Pt | 0.05 | 200 | Na ₂ SO ₄ (50 mM) | 0.047±0.004 | 0.945 |
| Pt | 0.1 | 200 | Na ₂ SO ₄ (50 mM) | 0.108±0.003 | 0.995 |
| Pt | 0.3 | 200 | Na ₂ SO ₄ (50 mM) | 0.147±0.012 | 0.953 |
| Pt | 0.5 | 200 | Na ₂ SO ₄ (50 mM) | 0.063±0.004 | 0.972 |
| BDD | 0.05 | 200 | Na ₂ SO ₄ (50 mM) | 0.077±0.002 | 0.994 |
| BDD | 0.1 | 200 | Na ₂ SO ₄ (50 mM) | 0.106±0.003 | 0.995 |
| BDD | 0.3 | 200 | Na ₂ SO ₄ (50 mM) | 0.117±0.001 | 0.999 |
| BDD | 0.5 | 200 | Na ₂ SO ₄ (50 mM) | 0.095±0.002 | 0.996 |
| Pt | 0.2 | 50 | Na ₂ SO ₄ (50 mM) | 0.070±0.001 | 0.999 |
| Pt | 0.2 | 100 | Na ₂ SO ₄ (50 mM) | 0.176±0.005 | 0.994 |
| Pt | 0.2 | 300 | Na ₂ SO ₄ (50 mM) | 0.256±0.005 | 0.998 |
| Pt | 0.2 | 500 | Na ₂ SO ₄ (50 mM) | 0.259±0.005 | 0.999 |
| BDD | 0.2 | 50 | Na ₂ SO ₄ (50 mM) | 0.089±0.001 | 0.998 |
| BDD | 0.2 | 100 | Na ₂ SO ₄ (50 mM) | 0.137±0.005 | 0.991 |
| BDD | 0.2 | 300 | Na ₂ SO ₄ (50 mM) | 0.187±0.006 | 0.993 |
| BDD | 0.2 | 500 | Na ₂ SO ₄ (50 mM) | 0.156±0.002 | 0.998 |

For all the anodes, the complete removal of SAC almost finished in a 30 min electrolysis period in the presence of Na₂SO₄ and NaNO₃. However, it was removed

only about 50% in 30 min in the case of NaCl. The main reason of this low degradation is related to the formation of active chlorine generated by the oxidation of chloride ions at the surface of DSA, Pt and BDD anode when NaCl used as supporting electrolyte (Eq. (4-1)) (Özcan *et al.* 2008b; Loaiza-Ambuludi *et al.* 2013; De Moura *et al.* 2014). Therefore, part of electrical energy provided is lost in this reaction.



The electrogenerated active chlorine can acts as oxidation mediator in the bulk of the solution, which can accelerate the removal rate of organic pollutants through the production of HClO (Eq. (4-2)) according to some researches (Özcan *et al.* 2008b; Loaiza-Ambuludi *et al.* 2013).



However, in electro-Fenton process, the electrogenerated chlorine can also react with Fe^{2+} (Eq. (4-3)) or decompose hydrogen peroxide (Eq. (4-4)) (Loaiza-Ambuludi *et al.* 2013), and then reducing the production rate of strong oxidant $\cdot\text{OH}$ by Fenton's reaction.

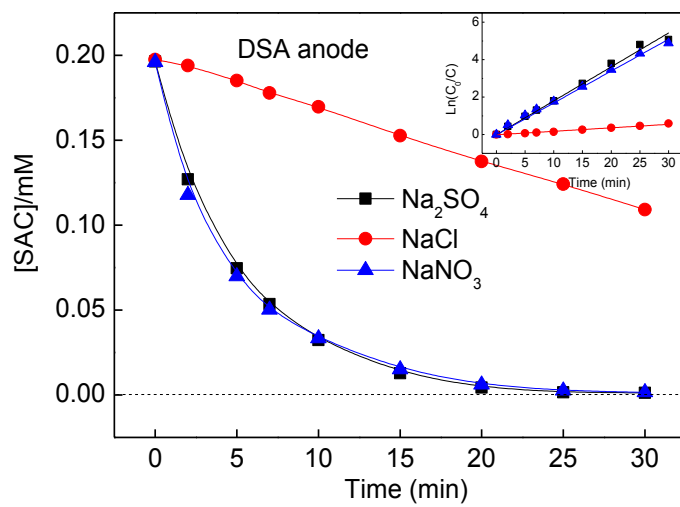


Moreover, Cl^- could consume $\cdot\text{OH}$ and lead to the formation of $\text{ClOH}^{\cdot-}$ through Eq. (4-5) (Nidheesh *et al.* 2014). Oxidative capacity of $\text{ClOH}^{\cdot-}$ towards organic compounds is much lower than that of $\cdot\text{OH}$ formed during the EF process.

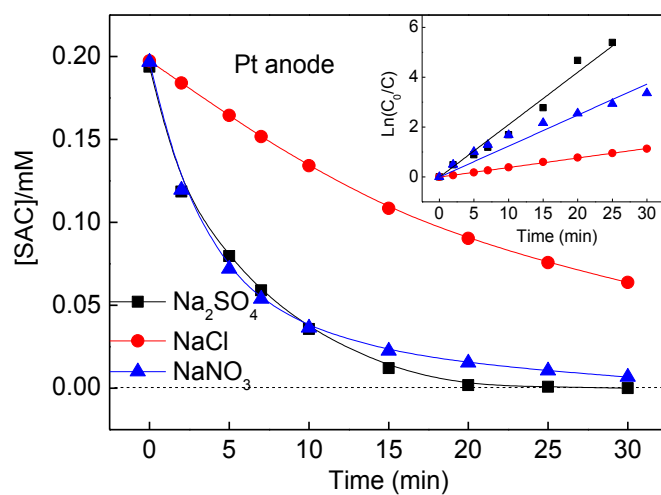


Therefore, the removal efficiency of SAC was much lower when NaCl used as background electrolyte.

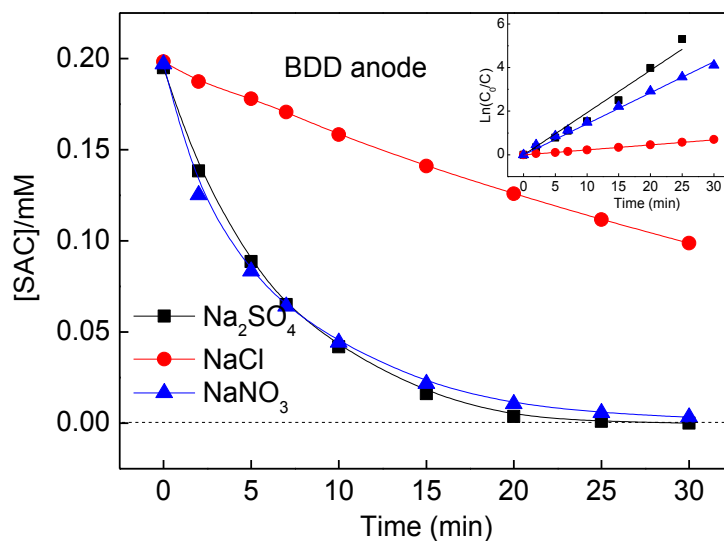
It can also be seen from Fig. 4-1 and Table 4-1 that the removal rate of SAC for Na_2SO_4 was a little higher than that obtained for NaNO_3 in three electrolysis cells. For example, when DSA was used as anode and at 200 mA applied current, the k_{app} for Na_2SO_4 was 0.181 min^{-1} , while it was 0.170 min^{-1} for NaNO_3 . Therefore, Na_2SO_4 was chosen to be the supporting electrolyte in the following experiments.



(a)



(b)



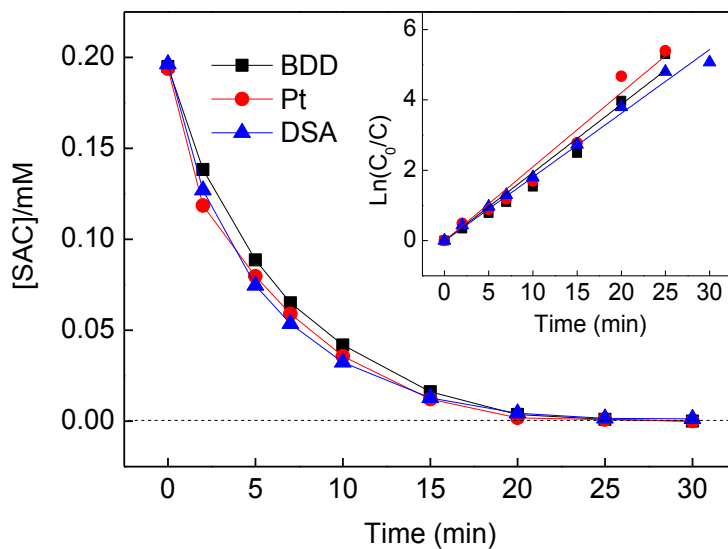
(c)

Fig. 4-1 Effect of the nature of supporting electrolyte on the oxidative degradation of SAC with DSA (a), Pt (b) and BDD (c) anodes ($[SAC]_0 = 0.2 \text{ mM}$, $[Fe^{2+}] = 0.2 \text{ mM}$, $I = 200 \text{ mA}$, $pH_0 3.0$)

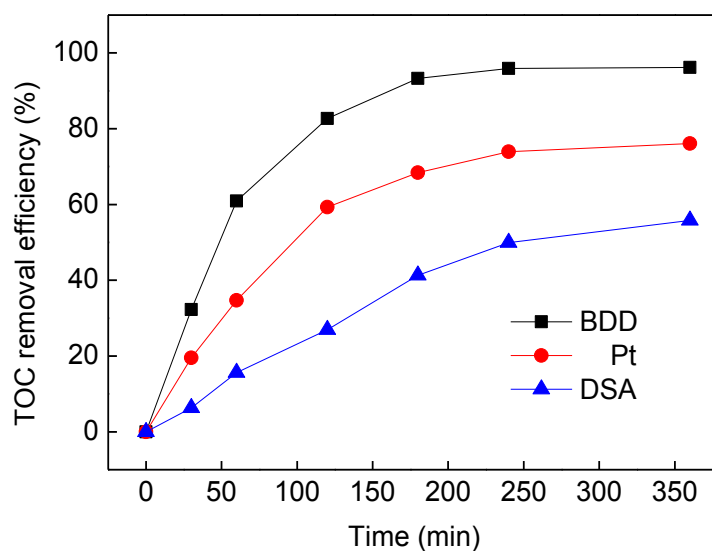
4.3.2 Effect of anode materials on the removal and mineralization of SAC

The removal of SAC by electro-Fenton process using DSA, Pt and BDD as anodes was investigated by keeping the same cathode as carbon-felt. Experiments were performed at Fe^{2+} concentration 0.2 mM, Na_2SO_4 concentration 50 mM, applied current 200 mA and $pH_0 3.0$. 0.2 mM SAC could be completely removed in a 30 min reaction for all the anode materials (Fig. 4-2a). The k_{app} values for SAC removal using DSA, Pt and BDD anodes were very similar (0.181, 0.194 and 0.211 min^{-1} , respectively). However, when it comes to mineralization, BDD anode showed its great superiority. In a 360 min reaction, the TOC removal efficiencies for SAC were 55.8%, 76.1% and 96.2% for DSA, Pt and BDD anodes, respectively (Fig. 4-2b). On the one hand, the BDD($\cdot OH$) radicals can effectively mineralize short chain carboxylic acids generated in the electro-Fenton process, which are relatively recalcitrant to mineralization (Oturán *et al.* 2013). On the other hand, Fe(III)–carboxylic acid complexes formed in electro-Fenton process were difficultly oxidizable with $\cdot OH$ produced in the medium from Fenton's reaction and at the DSA and Pt anode surface from Eq. (4-6) (Boye *et al.* 2002; Sirés *et*

al. 2007). These complexes are completely destroyed using a BDD anode due to the great amount of $\cdot\text{OH}$ generated on its surface (Sirés *et al.* 2007) because of its large O_2 evolution overpotential. Since poor TOC removal efficiency was obtained using DSA anode, only Pt and BDD anodes were applied in the following experiments.



(a)



(b)

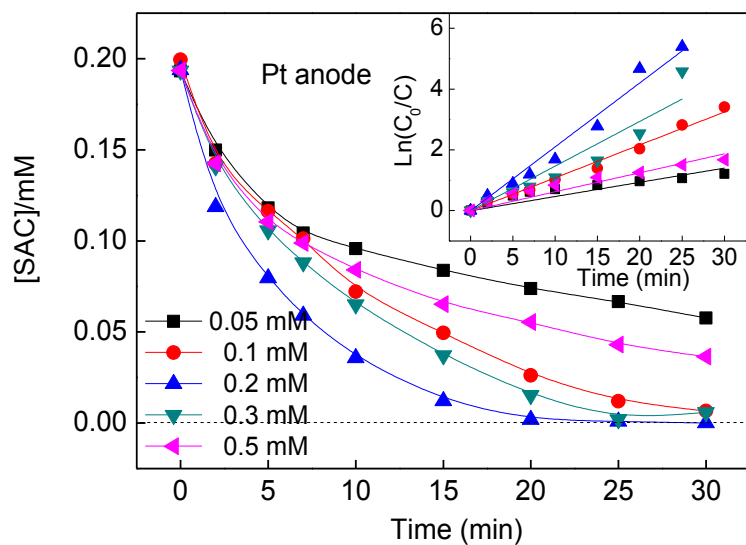
Fig. 4-2 Comparison of the performance of different anode in the degradation (a) and mineralization (b) of SAC ($[\text{SAC}]_0 = 0.2 \text{ mM}$, $[\text{Fe}^{2+}] = 0.2 \text{ mM}$, $[\text{Na}_2\text{SO}_4] = 50 \text{ mM}$, $I = 200 \text{ mA}$, $\text{pH}_0 = 3.0$)

4.3.3 Effect of Fe²⁺ concentration on the removal of SAC

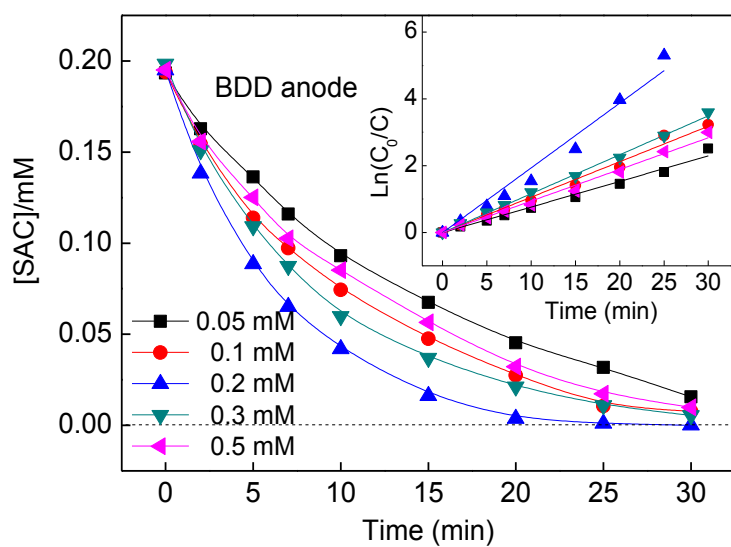
The effect of Fe²⁺ (catalyst) concentration on the removal of SAC was examined by using the Fe²⁺ concentration of 0.05, 0.1, 0.2, 0.3 and 0.5 mM. The time-course of SAC concentration decay was determined by HPLC, where SAC displayed a well-defined peak at the retention time (t_R) 14.2 min under the operating conditions of Fig. 4-3.

As can be observed in Fig.4-3 and Table 4-1, the removal rate for SAC was enhanced by increasing the Fe²⁺ concentration from 0.05 to 0.2 mM for both Pt and BDD anode. Moreover, the kinetics of SAC removal increases more rapidly (1.8 times) in the case of Pt/carbon-felt cell when the Fe²⁺ increased from 0.05 to 0.2 mM, compared to BDD/carbon-felt cell. Since the applied current was kept constant at 200 mA, it can be assumed that the production rate of H₂O₂ via the oxygen reduction would be identical for all the Fe²⁺ concentrations under this study (Oturán *et al.* 2010). Then increasing the Fe²⁺ concentration could lead to the increase of hydroxyl radicals generated via Fenton's reaction. These hydroxyl radicals reacted with SAC immediately, resulting in the increase of SAC degradation. On the contrary, further increasing the Fe²⁺ concentration to 0.5 mM, the removal rate declined. The observed decrease in SAC degradation rate upon increasing the Fe²⁺ concentration might due to the role of Fe²⁺ as scavenger of hydroxyl radicals (Eq. (4-7)) which takes place with a large rate constant ($k = 3.20 \times 10^8 \text{ M}^{-1} \text{ s}^{-1}$) (Oturán *et al.* 2010). Therefore, the optimal Fe²⁺ concentration for the removal of SAC was 0.2 mM.





(a)



(b)

Fig. 4-3 Effect of Fe^{2+} (as catalyst) concentration on the removal of SAC with Pt (a) and BDD (b) anode ($[\text{SAC}]_0 = 0.2 \text{ mM}$, $[\text{Na}_2\text{SO}_4] = 50 \text{ mM}$, $I = 200 \text{ mA}$, $\text{pH}_0 = 3.0$)

4.3.4 Effect of applied current on the removal of SAC

The applied current is another important parameter for the effectiveness of the electro-Fenton process. In order to investigate the effect of current intensity on the

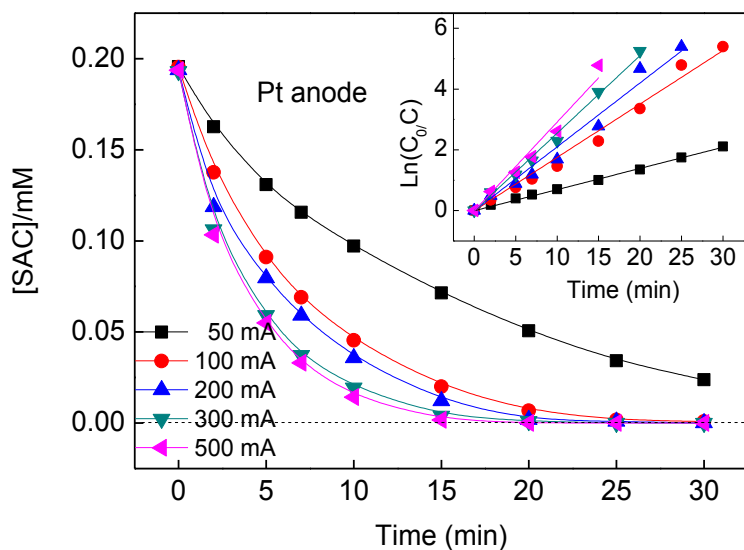
oxidative degradation of SAC, several experiments were performed by varying applied current in the range of 50–500 mA at the optimal Fe^{2+} concentration of 0.2 mM as assessed above. The results were shown in Fig. 4-4 and Table 4-1. When Pt was used as anode, the removal rate of SAC increased as the applied current increasing. The electrolysis time for complete disappearance of SAC has been changed from $\gg 30$ min for 50 mA to 30, 25, 20 and 15 min for 100, 200, 300 and 500 mA current intensity, respectively (Fig. 4-4a). The k_{app} was increased from 0.07 to 0.26 min^{-1} when applied current increased from 50 to 500 mA. The oxidation of SAC was accelerated by increasing the applied current because of progressively large production of $\cdot\text{OH}$ (Loaiza-Ambuludi *et al.* 2013).

As in the case of BDD anode, the removal rate of SAC increased significantly from 0.09 to 0.19 min^{-1} when applied current increased from 50 to 200 mA. However, it decreased slightly to 0.16 min^{-1} as applied current increased to 500 mA. At higher applied current than 200 mA, the $4e^-$ reduction of O_2 leading to the formation of H_2O (Eq. (4-8)) would compete with the formation of H_2O_2 (Eq. (4-9)) (Özcan *et al.* 2008a).

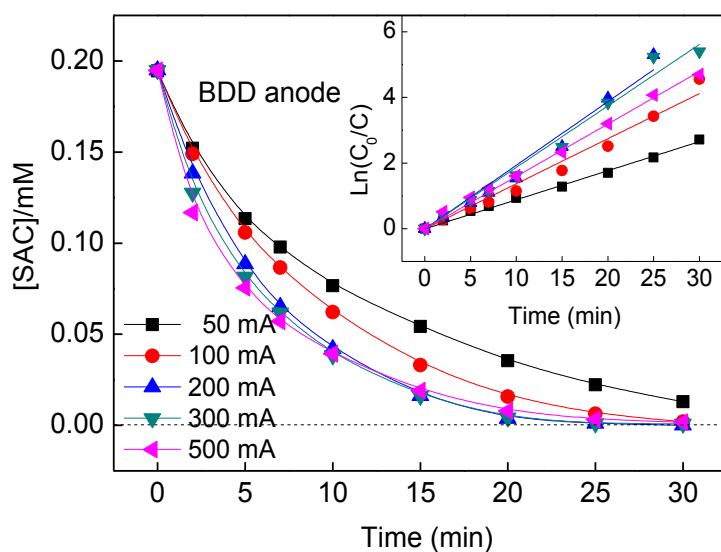


In addition, the progressive enhancement of other parasitic reactions at higher current, such as hydrogen evolution (Eq. (4-10)) at the cathode and oxygen evolution (Eq. (4-11)) at the anode (Yahya *et al.* 2014), also contributed to the lower SAC removal rate. It could be concluded that the comparatively better performance of BDD was more pronounced at lower current intensities.





(a)



(b)

Fig. 4-4 Effect of applied current on the destruction kinetics of SAC with Pt (a) and BDD (b) anode

($[SAC]_0 = 0.2 \text{ mM}$, $[Fe^{2+}] = 0.2 \text{ mM}$, $[Na_2SO_4] = 50 \text{ mM}$, $pH_0 = 3.0$)

4.3.5 Determination of the rate constant of reaction between SAC and $\cdot OH$

The absolute rate constant for the second order kinetics of the reaction between SAC and $\cdot OH$ ($k_{abs,SAC}$) was determined by using the competitive kinetics method

(Mhemdi *et al.* 2013). Benzoic acid (BA) was employed as the standard competitor because the absolute rate constant of the reaction between BA and $\cdot\text{OH}$ ($k_{\text{abs,BA}}$) is known as $4.30 \times 10^9 \text{ M}^{-1} \text{ s}^{-1}$ (Özcan *et al.* 2008a; Oturan *et al.* 2010). Experiments of competitive kinetics were carried out in the presence of equal concentrations of SAC and BA (0.1 mM). The hydroxylation rate constant of SAC can be calculated according to Eq. (4-12) and determined from Fig. 4-5 to be $k_{\text{abs,SAC}} = (1.85 \pm 0.01) \times 10^9 \text{ M}^{-1} \text{ s}^{-1}$.

$$\text{Ln} \left(\frac{[\text{SAC}]_0}{[\text{SAC}]_t} \right) = \left(\frac{k_{\text{abs,SAC}}}{k_{\text{abs,BA}}} \right) \text{Ln} \left(\frac{[\text{BA}]_0}{[\text{BA}]_t} \right) \quad (4-12)$$

Interestingly, this rate constant value is the same as that reported by Toth *et al.* (Toth *et al.* 2012).

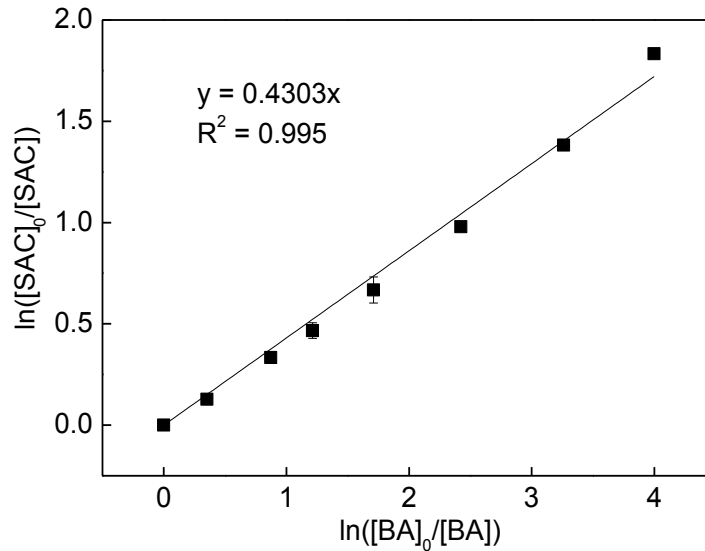


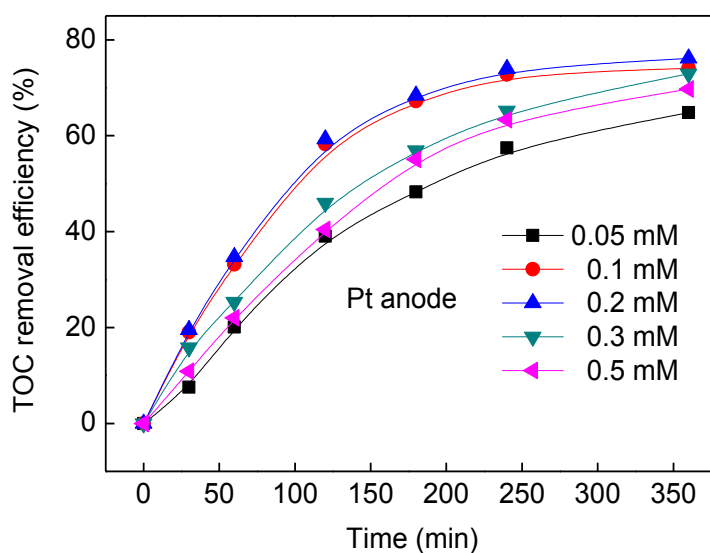
Fig. 4-5 Determination of the absolute constant of reaction between SAC and $\cdot\text{OH}$ using competition kinetics method by taking BA as standard competitors ($[\text{SAC}]_0 = 0.1 \text{ mM}$, $[\text{BA}]_0 = 0.1 \text{ mM}$, $[\text{Fe}^{2+}] = 0.2 \text{ mM}$, $I = 50 \text{ mA}$, $\text{pH}_0 = 3.0$, $[\text{Na}_2\text{SO}_4] = 50 \text{ mM}$)

4.3.6 The effect of Fe^{2+} concentration and applied current on SAC mineralization

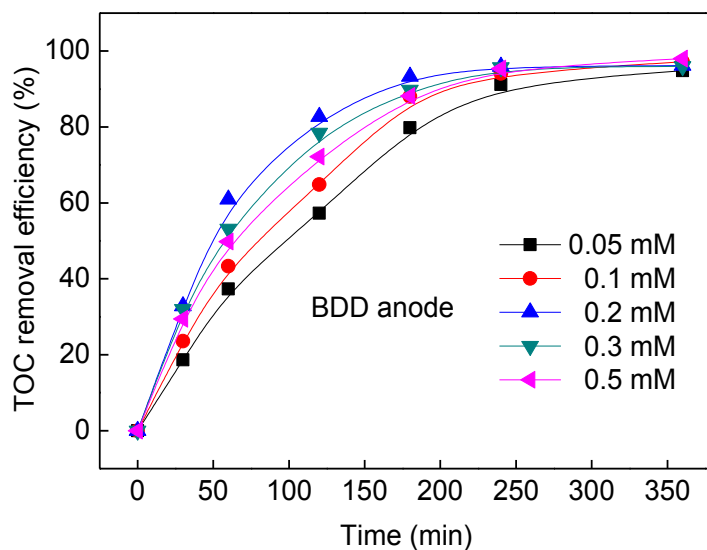
The mineralization ability of SAC by electro-Fenton process was assessed from the TOC abatement over electrolysis time. The influence of the Fe^{2+} concentration in the Pt/carbon-felt and BDD/carbon-felt cells under the same condition of Fig. 4-3 was shown in Fig. 4-6.

Figure 4-6 indicated the optimal Fe^{2+} concentration for both Pt/carbon-felt and BDD/carbon-felt cells was 0.2 mM. When the Fe^{2+} concentration was higher than 0.2 mM, the percentage of scavenged hydroxyl radicals from Fe^{2+} ions increased, thus the side reactions between Fe^{2+} ions and $\cdot\text{OH}$ (Eq. (4-7)) became more significant (Özcan *et al.* 2008a).

It can be seen by comparing Fig. 4-6a and Fig.4-6b that the mineralization of SAC was accelerated by the employ of BDD anode. At optimal conditions, BDD/carbon-felt cell achieved 93.3% mineralization in only 180 min, while this rate was about 70% for or Pt/carbon-felt cell at same time. A mineralization rate of 76.1% was reached by this cell at 360 min. BDD anode has the much higher O_2 evolution overpotential (1.27 V) than Pt (0.27 V) (Oturán *et al.* 2011). So the oxidative action of BDD($\cdot\text{OH}$) is much more efficient than Pt($\cdot\text{OH}$) (Martínez-Huitle and Brillas 2009). Moreover, the loosely bound BDD($\cdot\text{OH}$) formed at the anode surface (Eq. (4-6)) can readily react with organic pollutant due to the low adsorption ability of $\cdot\text{OH}$ on BDD, in contrast to the chemisorbed radicals Pt($\cdot\text{OH}$) which relatively strongly attached to the surface and less reactive (Oturán *et al.* 2011; Dirany *et al.* 2012).



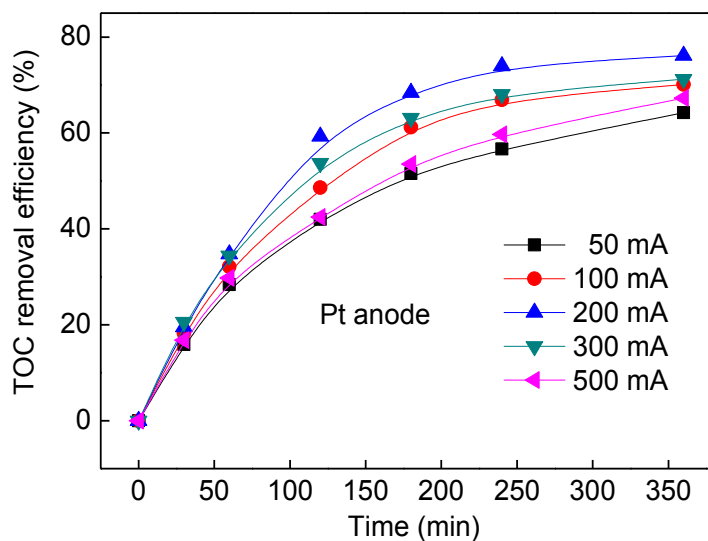
(a)



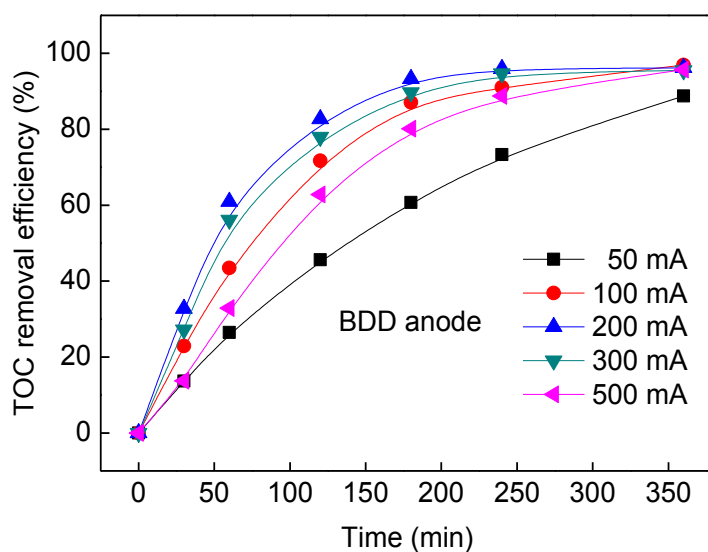
(b)

Fig. 4-6 Effect of Fe^{2+} concentration on mineralization of SAC by electro-Fenton process with Pt (a) and BDD (b) anode ($[\text{SAC}]_0 = 0.2 \text{ mM}$, $[\text{Na}_2\text{SO}_4] = 50 \text{ mM}$, $I = 200 \text{ mA}$, $\text{pH}_0 = 3.0$)

The effect of applied current on the mineralization of 0.2 mM SAC solution was investigated under the same condition as Fig. 4-4 and the results were shown in Fig. 4-7. When applied current raised from 50 to 200 mA, the TOC removal efficiency was increased from 64.2% to 76.1% in Pt/carbon-felt cell and from 88.9% to 96.2% in BDD/carbon-felt cell. However, the TOC removal efficiency decreased slightly for both anodes when current intensity further increased to 500 mA. As applied current increased, the higher electrogenerated H_2O_2 concentration was obtained and larger amounts of $\cdot\text{OH}$ was yielded from Fenton's reaction, and then a greater mineralization efficiency can be achieved due to the simultaneous degradation of SAC and its byproducts (Dirany *et al.* 2012). But a current intensity higher than 200 mA would increase the extent of parasitic reactions (Eqs. (4-8), (4-10) and (4-11)) and decrease the mineralization efficiency of SAC (Mousset *et al.* 2014).



(a)



(b)

Fig. 4-7 Effect of applied current on mineralization of SAC by electro-Fenton process with Pt (a) and BDD (b) anode ($[\text{SAC}]_0 = 0.2 \text{ mM}$, $[\text{Fe}^{2+}] = 0.2 \text{ mM}$, $[\text{Na}_2\text{SO}_4] = 50 \text{ mM}$, $\text{pH}_0 = 3.0$)

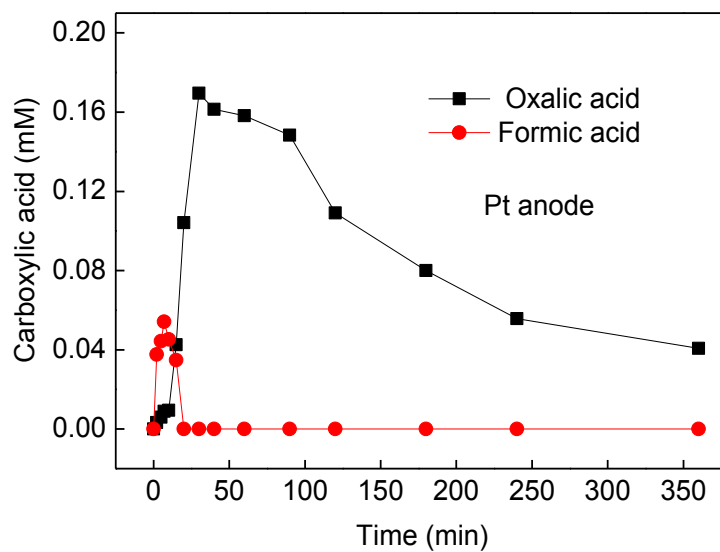
4.3.7 Identification and evolution of short-chain carboxylic acids

Generation of short chain carboxylic acids is expected from the oxidative breaking of aryl moieties of organic/cyclic oxidation intermediates. Experiments were performed

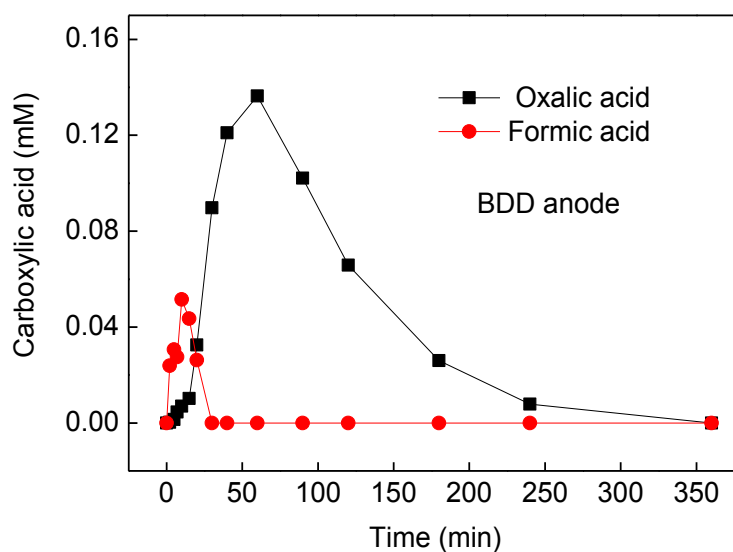
when initial SAC concentration was 0.2 mM, Fe^{2+} concentration was 0.2 mM, Na_2SO_4 concentration was 50 mM, applied current was 200 mA and pH_0 was 3.0.

Oxalic, formic, and maleic acid at retention time (t_R) of 8.90, 16.03 and 11.33, respectively, were observed during electro-Fenton process. Since the concentration of maleic acid was detected in trace level, the changes of maleic acid concentration were not shown in Fig. 4-8. In Pt/carbon-felt cells, formic acid presented only in the first 20 min and then it undergo to the mineralization (Fig. 4-8a) (Özcan *et al.* 2008a). Oxalic acid showed the largest accumulation and the higher persistence due to its lower reactivity with $\cdot\text{OH}$, which suggested that it can be generated from different ways as ultimate reaction intermediate (Dirany *et al.* 2010). In addition, oxalic acid was still existed with a concentration of 0.04 mM after a 360 min reaction. This relatively weak degradation of oxalic acid can be attributed to its high stability in the presence of ferric ions and its weaker reactivity toward $\cdot\text{OH}$ radicals ($k_2 = 2.8 \times 10^7 \text{ M}^{-1} \text{ s}^{-1}$) (Oturán *et al.* 2008). This was also corresponding to the residual TOC remaining at the end of mineralization treatments in Pt/carbon-felt cells.

On the other hand, oxalic acid showed high persistence, but it disappeared at the end of the reaction in BDD/carbon-felt cell (Fig. 4-8b). This phenomenon was in agreement with the faster TOC removal in BDD/carbon-felt cells as described in section 4.3.6.



(a)



(b)

Fig. 4-8 Evolution of short-chain carboxylic acids formed during electro-Fenton processes using Pt (a) and BDD (b) anodes ($[SAC]_0 = 0.2 \text{ mM}$, $[Fe^{2+}] = 0.2 \text{ mM}$, $[Na_2SO_4] = 50 \text{ mM}$, $I = 200 \text{ mA}$, $pH_0 = 3.0$)

4.3.8 Evolution of SAC solution toxicity during electro-Fenton process

In order to determine the potential toxicity of SAC and its intermediates,

mineralization of a 0.2 mM SAC solution was examined at 200 mA constant current. The evolution of the luminescence inhibition as function of the electrolysis time for exposition time of 5 and 15 min are tested. Only the curves obtained at both Pt and BDD anodes after a 15-min exposure time were presented in Fig. 4-9, because the curves recorded after a 5-min exposure time were very similar. For both Pt and BDD anode, the toxicity increased significantly and reached the maximum luminescence inhibition peak at 30 min, indicating the formation of significantly more toxic by-products at the beginning of the treatment. The inhibition ratio decreased after 30 min, in relation to the destruction of aromatics and the increase of the less toxic by-products. These less toxic byproducts mainly included the carboxylic acids, which present a very low toxicity toward *V. fischeri* bacteria (Dirany *et al.* 2012).

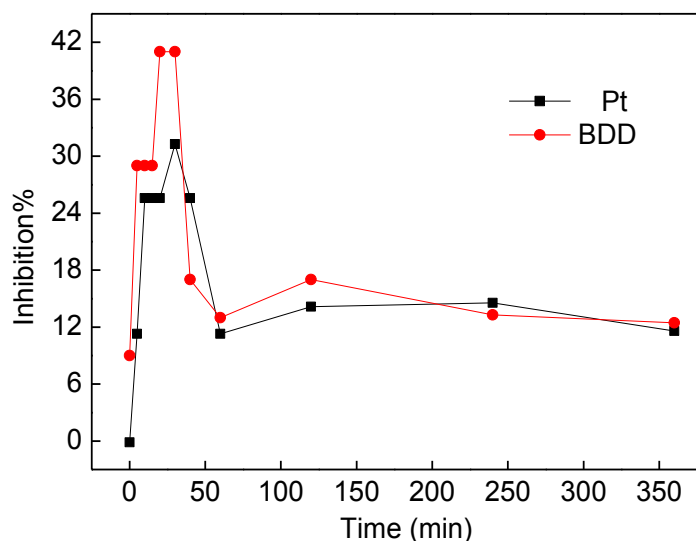


Fig. 4-9 Inhibition of luminescence of *V. fischeri* bacteria during electro-Fenton processes with Pt and BDD anode ($[SAC]_0 = 0.2$ mM, $[Fe^{2+}] = 0.2$ mM, $I = 200$ mA, $pH_0 = 3.0$, $[Na_2SO_4] = 50$ mM)

4.4 Conclusions

It was demonstrated that electro-Fenton process with a Pt or BDD anode and a carbon felt cathode was a very effective method for the degradation of SAC in water.

The effect of Fe^{2+} concentration and applied current on the removal and mineralization of SAC was investigated. For both anodes, SAC could be completely degraded in less than 30 min. The oxidative degradation of SAC followed pseudo-first-order kinetics. Absolute rate constant of hydroxylation reaction of SAC was determined as $(1.85 \pm 0.01) \times 10^9 \text{ M}^{-1} \text{ s}^{-1}$ using competition kinetics method. The optimal conditions for SAC removal were SAC concentration 0.2 mM, Fe^{2+} concentration 0.2 mM, Na_2SO_4 concentration 50 mM, applied current 200 mA and initial pH 3.0. The use of BDD anode yields a faster mineralization rate because of the higher oxidation power of BDD comparing with Pt. Short-chain aliphatic carboxylic acids such as oxalic, formic and maleic acids are identified as aliphatic by-products. The bacteria luminescence inhibition showed the toxicity of SAC solution increased at the first 30 min of electrolysis, and then it decreased after a 60 min reaction for both Pt and BDD anodes.

References

- Boye, B., Dieng, M.M. and Brillas, E. (2002). Degradation of herbicide 4-chlorophenoxyacetic acid by advanced electrochemical oxidation methods. *Environmental Science & Technology* 36(13), 3030-3035.
- De Moura, D.C., de Araújo, C.K.C., Zanta, C.L.P.S., Salazar, R. and Martínez-Huitle, C.A. (2014). Active chlorine species electrogenerated on $\text{Ti/Ru}_{0.3}\text{Ti}_{0.7}\text{O}_2$ surface: Electrochemical behavior, concentration determination and their application. *Journal of Electroanalytical Chemistry* 731, 145-152.
- Dirany, A., Sirés, I., Oturan, N. and Oturan, M.A. (2010). Electrochemical abatement of the antibiotic sulfamethoxazole from water. *Chemosphere* 81(5), 594-602.
- Dirany, A., Sirés, I., Oturan, N., Özcan, A. and Oturan, M.A. (2012). Electrochemical treatment of the antibiotic sulfachloropyridazine: Kinetics, reaction pathways, and toxicity evolution. *Environmental Science & Technology* 46(7), 4074-4082.
- Loaiza-Ambuludi, S., Panizza, M., Oturan, N., Özcan, A. and Oturan, M.A. (2013). Electro-Fenton degradation of anti-inflammatory drug ibuprofen in hydroorganic medium. *Journal of Electroanalytical Chemistry* 702, 31-36.
- Martínez-Huitle, C.A. and Brillas, E. (2009) Decontamination of wastewaters

- containing synthetic organic dyes by electrochemical methods: A general review. *Applied Catalysis B: Environmental* 87(3–4), 105-145.
- Mhemdi, A., Oturan, M.A., Oturan, N., Abdelhédi, R. and Ammar, S. (2013) Electrochemical advanced oxidation of 2-chlorobenzoic acid using BDD or Pt anode and carbon felt cathode. *Journal of Electroanalytical Chemistry* 709, 111-117.
- Mousset, E., Oturan, N., van Hullebusch, E.D., Guibaud, G., Esposito, G. and Oturan, M.A. (2014) Influence of solubilizing agents (cyclodextrin or surfactant) on phenanthrene degradation by electro-Fenton process – Study of soil washing recycling possibilities and environmental impact. *Water Research* 48, 306-316.
- Nidheesh, P.V., Gandhimathi, R. and Sanjini, N.S. (2014) NaHCO₃ enhanced Rhodamine B removal from aqueous solution by graphite–graphite electro Fenton system. *Separation and Purification Technology* 132, 568-576.
- Oturan, M.A., Edelahi, M.C., Oturan, N., El kacemi, K. and Aaron, J.-J. (2010) Kinetics of oxidative degradation/mineralization pathways of the phenylurea herbicides diuron, monuron and fenuron in water during application of the electro-Fenton process. *Applied Catalysis B: Environmental* 97(1–2), 82-89.
- Oturan, M.A., Pimentel, M., Oturan, N. and Sirés, I. (2008) Reaction sequence for the mineralization of the short-chain carboxylic acids usually formed upon cleavage of aromatics during electrochemical Fenton treatment. *Electrochimica Acta* 54(2), 173-182.
- Oturan, N., Hamza, M., Ammar, S., Abdelhédi, R. and Oturan, M.A. (2011) Oxidation/mineralization of 2-Nitrophenol in aqueous medium by electrochemical advanced oxidation processes using Pt/carbon-felt and BDD/carbon-felt cells. *Journal of Electroanalytical Chemistry* 661(1), 66-71.
- Oturan, N., Wu, J., Zhang, H., Sharma, V.K. and Oturan, M.A. (2013) Electrocatalytic destruction of the antibiotic tetracycline in aqueous medium by electrochemical advanced oxidation processes: Effect of electrode materials. *Applied Catalysis B: Environmental* 140–141(0), 92-97.
- Özcan, A., Şahin, Y., Koparal, A.S. and Oturan, M.A. (2008a) Degradation of picloram by the electro-Fenton process. *Journal of Hazardous Materials* 153(1–2), 718-727.

- Özcan, A., Şahin, Y., Koparal, A.S. and Oturan, M.A. (2008b) Protham mineralization in aqueous medium by anodic oxidation using boron-doped diamond anode: Influence of experimental parameters on degradation kinetics and mineralization efficiency. *Water Research* 42(12), 2889-2898.
- Sirés, I., Garrido, J.A., Rodríguez, R.M., Brillas, E., Oturan, N. and Oturan, M.A. (2007) Catalytic behavior of the $\text{Fe}^{3+}/\text{Fe}^{2+}$ system in the electro-Fenton degradation of the antimicrobial chlorophene. *Applied Catalysis B: Environmental* 72(3–4), 382-394.
- Toth, J.E., Rickman, K.A., Venter, A.R., Kiddle, J.J. and Mezyk, S.P. (2012). Reaction kinetics and efficiencies for the hydroxyl and sulfate radical based oxidation of artificial sweeteners in water. *The Journal of Physical Chemistry A* 116(40), 9819-9824.
- Yahya, M.S., Oturan, N., El Kacemi, K., El Karbane, M., Aravindakumar, C.T. and Oturan, M.A. (2014) Oxidative degradation study on antimicrobial agent ciprofloxacin by electro-fenton process: Kinetics and oxidation products. *Chemosphere* 117, 447-454.

**Chapter 5 Electrochemical mineralization of sucralose in aqueous
medium at ambient temperature by electro-Fenton process**

5.1 Introduction

In this part, the effect of the Fe^{2+} concentration and applied current on the mineralization of sucralose (SUC) was examined. The effect of applied current on the mineralization efficiency was assessed. The aliphatic short-chain carboxylic acids and inorganic ions released during electro-Fenton process were monitored by ion-exclusion chromatography and ion chromatography (IC). The variation of toxicity of SUC solution and its intermediates was determined by Microtox method.

5.2 Materials and methods

5.2.1 Chemicals

Sucralose(1,6-dichloro-1,6-dideoxy- β -D-fructofuranosyl-4-chloro-4-deoxy- α -D-galactopyranoside, $\text{C}_{12}\text{H}_{19}\text{Cl}_3\text{O}_8$) was purchased from Sigma-Aldrich. The chemical structure and main characteristics of SUC were presented in Table 2-1. Analytical grade anhydrous sodium sulfate (supporting electrolyte) and ferrous sulfate heptahydrated (catalyst source) were obtained from Sigma-Aldrich and Acros Organics, respectively. Analytical grade carboxylic acids and other chemicals used for chromatographic analysis were purchased from Acros, Merck, Sigma, Riedel-de Haën and Fluka. Ultrapure water used for the preparation of the working solutions and HPLC eluting solutions was obtained from a Millipore Milli-Q (simplicity 185) system with resistivity $> 18 \text{ M}\Omega \text{ cm}$ at room temperature.

5.2.2 Electrochemical apparatus and procedures

Bulk experiments were conducted in an open, undivided and cylindrical glass cell of 250 mL capacity containing 220 mL SUC solution. Either a cylindrical Pt mesh (4.5 cm height, i.d. = 3.1 cm, Platecxis, France) or a 24 cm^2 thin-film BDD electrode (CONDIAS GmbH, Germany) was used as anode, and a 87.5 cm^2 piece of carbon felt ($17.5 \times 5 \text{ cm}$, Carbon-Lorraine, France) was used as cathode. In all electrolyses, the

anode was centered in the cell, surrounded by the carbon felt which placed on the inner wall of the cell covering the totality of the internal perimeter. H_2O_2 was generated from the reduction of O_2 dissolved in the solution. The continuous saturation of oxygen at atmospheric pressure was assured by bubbling compressed air through a frit at about 0.5 L/min, starting 5 min before electrolysis. All the electrolytic trials were conducted under constant current conditions by a Hameg HM8040-3 triple power supply (Germany).

The degradation experiments were performed using 0.2 mM SUC solution with constant stirring by using a magnetic stirrer. 50 mM Na_2SO_4 was added into the SUC solution as supporting electrolyte. A catalytic quantity of ferrous ion was added into the solution before the beginning of electrolysis. The initial pH (pH_0) of SUC solutions was measured with a CyberScan pH 1500 pH-meter (Eutech Instrument, USA) and set at 3.0 (± 0.1), adjusting by the addition of 1 M sulfuric acid.

5.2.3 Analytical methods and procedures

The TOC of the samples withdrawn from treated solutions at different electrolysis times were determined by Shimadzu TOC-V_{CSH} analyser consisting of a non-dispersive infra-red absorption detector (NDIR) according to the 680 °C combustion catalytic oxidation method. Platinum was applied as catalyst to facilitate the combustion at 650 °C. The carrier gas was oxygen with a flow rate of 150 mL/min. The injection volume was 50 μL .

The short-chain carboxylic acids were identified and quantified by ion-exclusion HPLC using a L-7100 pump, a Merck Lachrom liquid chromatograph equipped with a Supelcogel H column (250 \times 4.6 mm, 9 μm) and a L-7455 photodiode array detector at the wavelength of 220 nm. The mobile phase was 0.1% H_2SO_4 solution and flow rate was fixed to 0.2 mL/min. Calibration curves were achieved using standard solutions of related carboxylic acids. The identification of the carboxylic acids was performed by the retention time (t_R) comparison and standard addition methods using standard substances.

Inorganic ions (Cl^-) released in the electro-Fenton process were monitored by ion

chromatography with a Dionex ICS-1000 Basic Ion Chromatography (IC) System equipped with an IonPac AS4A-SC (anion exchange) 250 × 4 mm column and fitted to a DS6 conductivity detector containing a cell heated at 35 °C under control through a Chromeleon SE software. The mobile phase was a mixture of 3.6 mM Na₂CO₃ and 3.4 mM NaHCO₃ solution with a flow rate of 2.0 mL/min. The volume of injections was 25 µL.

5.2.4 Toxicity measurements

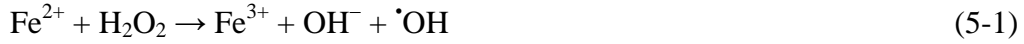
The toxicity of SUC and its intermediates generated during the electrolyses were investigated via samples collected from treated solutions at different times. Experiments were performed with the bio-luminescence marine bacteria *V. fischeri* (Hach Lange France SAS) by Microtox method according to the international standard process (OIN 11348-3). Two values of the inhibition of the luminescence (%) were calculated after 5 and 15 min of exposure to samples at 15 °C.

5.3 Results and discussion

5.3.1 Effect of Fe²⁺ concentration on the mineralization of sucralose

Mineralization efficiency in both Pt/carbon-felt and BDD/carbon-felt cells was assessed by solution TOC (as equivalent of dissolved organic carbon) measurements during electrolysis of SUC solutions. The effect of Fe²⁺ concentration on the mineralization of SUC solution was monitored by using the Fe²⁺ concentration of 0.05, 0.1, 0.2, 0.3 and 0.5 mM. The SUC concentration was fixed at 0.2 mM, applied current was 200 mA and initial pH was 3.0. As can be observed in Fig. 5-1, the mineralization for SUC was enhanced by increasing the Fe²⁺ concentration from 0.05 to 0.2 mM for both Pt and BDD anode. Since the applied current was kept constant at 200 mA, it can be assumed that the production rate of H₂O₂ via the oxygen reduction would be identical for all the Fe²⁺ concentrations under this study (Oturán *et al.* 2010). On the basis of the same H₂O₂ production rate, a higher Fe²⁺ concentration could lead to the increase of

hydroxyl radicals generated in bulk of solution via Fenton's reaction (Eq. (5-1)). These hydroxyl radicals would react with SUC immediately, resulting in the increase of SUC mineralization.



However, further increasing the Fe^{2+} concentration to 0.5 mM, the mineralization efficiency of SUC declined evidently in both Pt/carbon-felt and BDD/carbon-felt cells. The negative influence of higher Fe^{2+} concentration might due to the role of Fe^{2+} as scavenger of hydroxyl radicals (Eq. (5-2)) which takes place with a large rate constant ($k = 3.20 \times 10^8 \text{ M}^{-1} \text{ s}^{-1}$) (Sir  et al. 2007b; Oturan et al. 2010). Therefore, the value of 0.2 mM was chosen as the optimal Fe^{2+} concentration under these conditions and used in the following experiments.

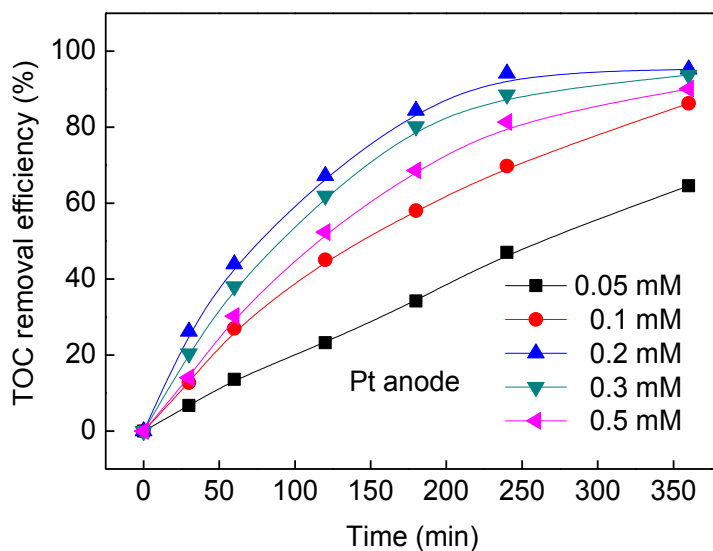


By comparing Fig. 5-1a and Fig. 5-1b, it can be seen that the use of BDD anode lead to the acceleration of SUC mineralization. At optimal condition (Fe^{2+} concentration 0.2 mM), 96.1% of the initial TOC value was removed in BDD/carbon-felt cell after only 180 min reaction, while it takes 240 min for Pt/carbon-felt cell to achieve 94.2% of mineralization efficiency. This fact can be explained by following reasons: Firstly, a much higher quantities of BDD($\cdot\text{OH}$) than Pt($\cdot\text{OH}$) is provided when electrolysis is operated at the current within the water discharge region (Eq. (5-3) and (5-4)) (Brillas et al. 2005; Panizza and Cerisola 2005; Brillas et al. 2009).

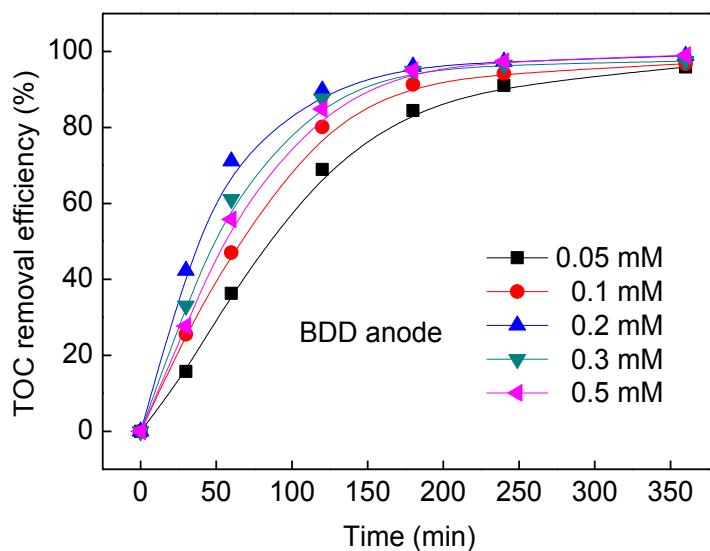


Secondly, since BDD anode presents the highest O_2 -overvoltage (1.27 V), which is much higher than Pt anode (0.27 V) (Mart nez-Huitle and Brillas 2009; Oturan *et al.* 2011), the oxidative action of BDD($\cdot\text{OH}$) is rather effective than Pt($\cdot\text{OH}$) (Oturan *et al.* 2011). Thirdly, due to the low adsorption ability of $\cdot\text{OH}$ on BDD, the physisorbed and labile BDD($\cdot\text{OH}$) formed at the anode surface (Eq. (5-3)) can readily react with organic pollutant, in contrast to the chemisorbed radicals typically formed at Pt surface (Eq. (5-4)) which limited the oxidation ability of Pt($\cdot\text{OH}$) (Oturan *et al.* 2011; Dirany *et al.*

2012.). Finally, BDD anode contributed to the degradation of all the byproducts, even the most refractory ones (Dirany *et al.* 2012).



(a)

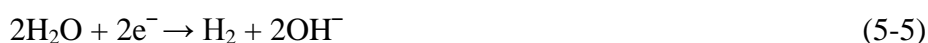


(b)

Fig. 5-1 Effect of Fe²⁺ concentration on mineralization of SAC during electro-Fenton process using Pt (a) and BDD (b) anode ([SUC]₀ = 0.2 mM, [Na₂SO₄] = 50 mM, I = 200 mA, pH₀ 3.0)

5.3.2 Effect of current intensity on the mineralization of SUC aqueous solutions

In order to investigate the effect of current intensity on the mineralization of SUC, several experiments were carried out by varying applied current in the range of 100–500 mA at the optimal Fe^{2+} concentration of 0.2 mM as assessed above. The results were shown in Fig. 5-2. In both Pt/carbon-felt and BDD/carbon-felt cells, the mineralization efficiency of SUC solution increased significantly as the applied current increased from 100 to 200 mA. Taking Pt/carbon-felt cell as an example, when current intensity was 100 mA, the TOC removal efficiency was 69.7% in a 360 min treatment. Increasing the current to 200 mA resulted in 94.1% of mineralization efficiency in a 240 min reaction. The mineralization of SUC aqueous solution was accelerated by increasing the applied current because both Fe^{2+} regeneration and H_2O_2 production would be promoted, and then large amount of $\cdot\text{OH}$ would be produced (Boye *et al.* 2002; Lin *et al.* 2014). When the applied current increased from 200 to 500 mA, the mineralization efficiency of sucralose in both cells changed slightly. On the one hand, a higher current leads to the increase of parasitic reactions, such as hydrogen evolution (Eq.(5-5)) and oxygen evolution (Eq. (5-6)) reactions (Dirany *et al.* 2010; Dirany *et al.* 2012).

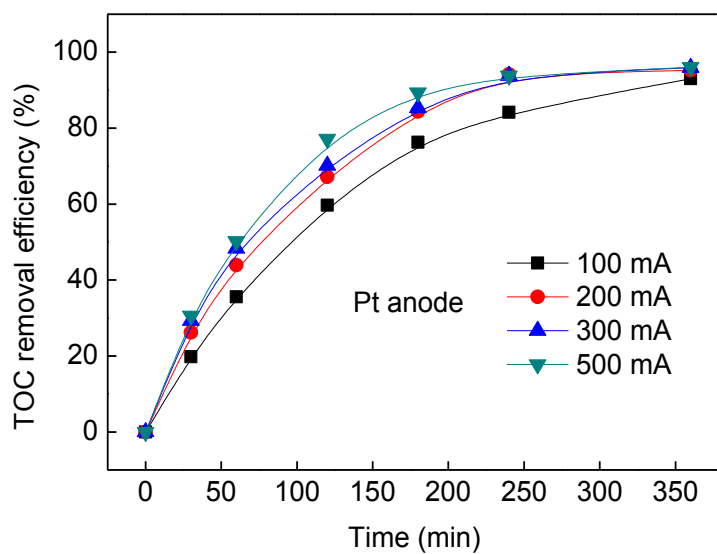


On the other hand, when the current density was further increased, excessive hydroxyl radicals would be consumed via the following side reactions (Eqs. (5-7) and (5-8)) (Wu *et al.* 2012; Lin *et al.* 2014). As a result, 200 mA was selected as the optimal current value and used in the remaining experiments.

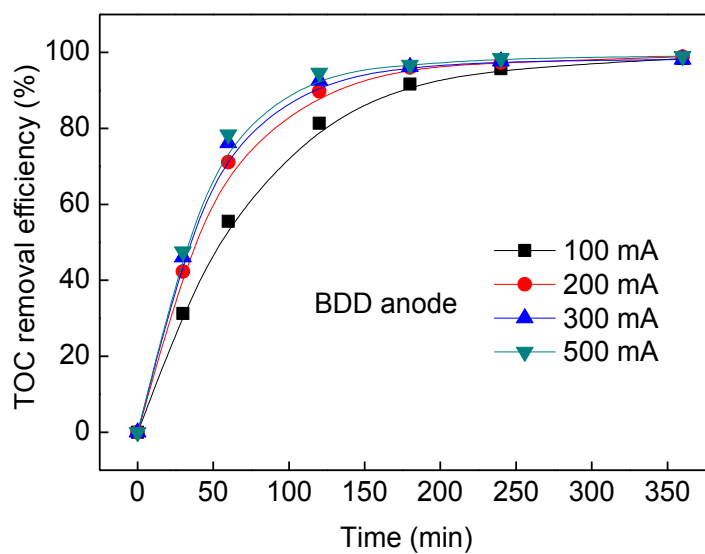


It also be observed from Fig. 5-2 that SUC solutions could be almost totally mineralized after 240 min of electrolysis at optimal conditions (Fe^{2+} concentration 0.2 mM and applied current 200 mA) in both Pt/carbon-felt and BDD/carbon-felt cells, indicating that electro-Fenton process with the use of Pt or BDD anode and a piece of carbon-felt cathode was quite effective for the mineralization of SUC in aqueous

medium.



(a)



(b)

Fig. 5-2 Effect of applied current on mineralization of SAC by electro-Fenton process with Pt (a) and BDD (b) anode ($[SUC]_0 = 0.2$ mM, $[Fe^{2+}] = 0.2$ mM, $[Na_2SO_4] = 50$ mM, $pH_0 = 3.0$)

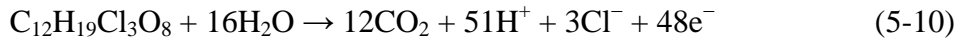
5.3.3 Mineralization current efficiency (MCE)

The mineralization capacity of the process can be expressed by MCE which can be

determined from the following equation (Eq. (5-9)) (Skoumal *et al.* 2008; Brillas *et al.* 2009; Oturan *et al.* 2011):

$$MCE = \frac{n F V_s \Delta(\text{TOC})_{\text{exp}}}{4.32 \times 10^7 m I t} \quad (5-9)$$

where n is the number of electrons consumed per SUC molecule according to Eq. (5-10) ($= 48$), F is the Faraday constant ($= 96,487 \text{ C/mol}$), V_s is the solution volume (L), $\Delta(\text{TOC})_{\text{exp}}$ is the experimental TOC decay (mg/L), 4.32×10^7 is the conversion factor to homogenize units ($= 3600 \text{ s/h} \times 12,000 \text{ mg of C/mol}$), m is the number of carbon atoms of sucralose ($= 12$), I is the applied current (A) and t is the given treatment time (h).



By comparing Fig. 5-3(a) and Fig. 5-3(b), it can be seen that the MCE in Pt/carbon-felt cell was lower at all the chosen time than that in BDD/carbon-felt cell. This was attributed to the low oxidation power of Pt anode (Oturan *et al.* 2011).

Figure 5-3 indicated that the MCE values decreased with rising applied current from 100 to 500 mA in both Pt/carbon-felt and BDD/carbon-felt cells. For example, the MCE values after 60 min of electrolysis in BDD/carbon-felt cell for 100, 200, 300 and 500 mA were 31.49%, 20.17%, 14.40% and 8.90%, respectively. This was related to the involvement of some parasitic reactions and particularly the hydrogen gas evolution reaction (Eq. (5-5)), which competed with the formation of H_2O_2 (Eq.(5-11)) (Özcan *et al.* 2008).

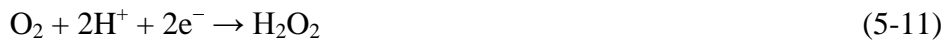
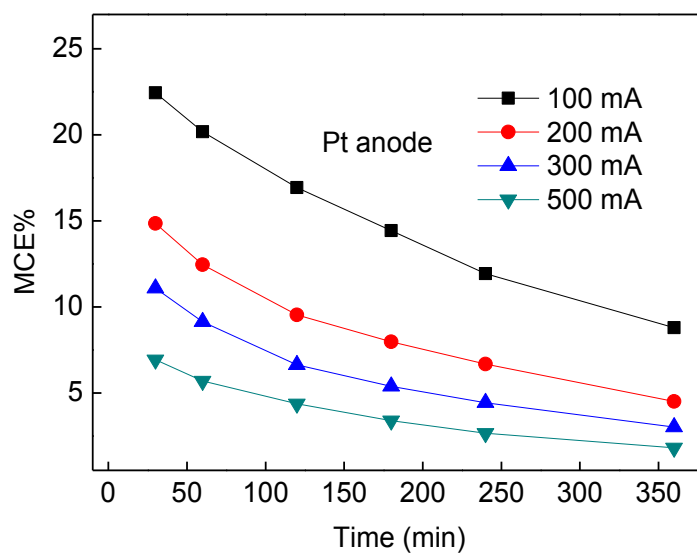
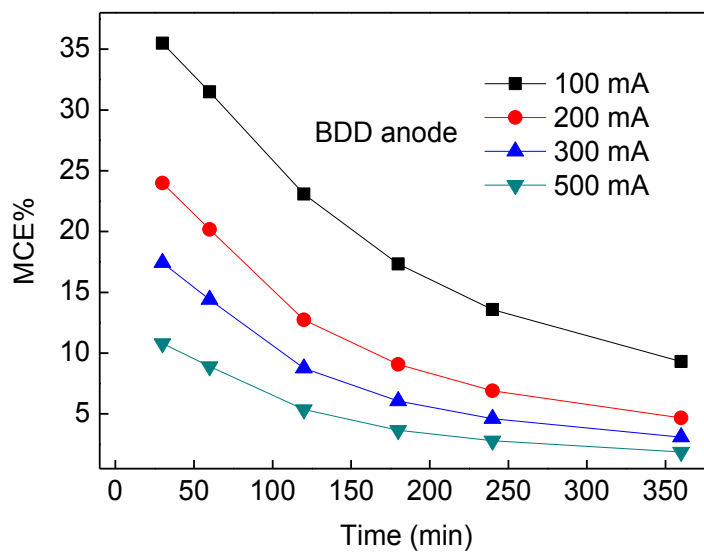


Figure 5-3 also showed that the MCE values decreased continuously from the beginning to the end of the electrolysis for every trial in both cells. This was due to the gradual formation of intermediates such as carboxylic acids that are more difficult to destroy by BDD($\cdot\text{OH}$) and also due to mass transport limitations because of the presence of small concentration of organic matter (Sir  s *et al.* 2007a;  zcan *et al.* 2008).



(a)



(b)

Fig. 5-3 Dependence of mineralization current efficiency calculated from Eq. (5-10) on the electrolysis time for the experiments reported in: (a) Fig. 5-2a and (b) Fig. 5-2b

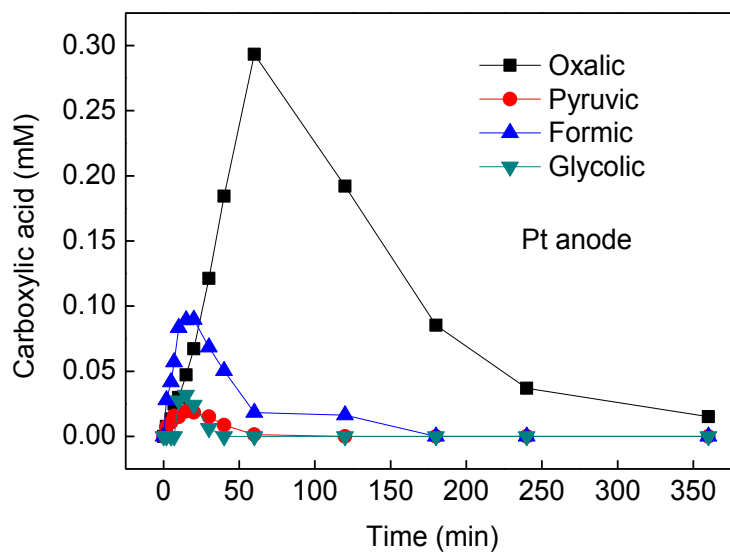
5.3.4 Identification and evolution of short-chain carboxylic acids

To identify the generated carboxylic acids released in the electro-Fenton process,

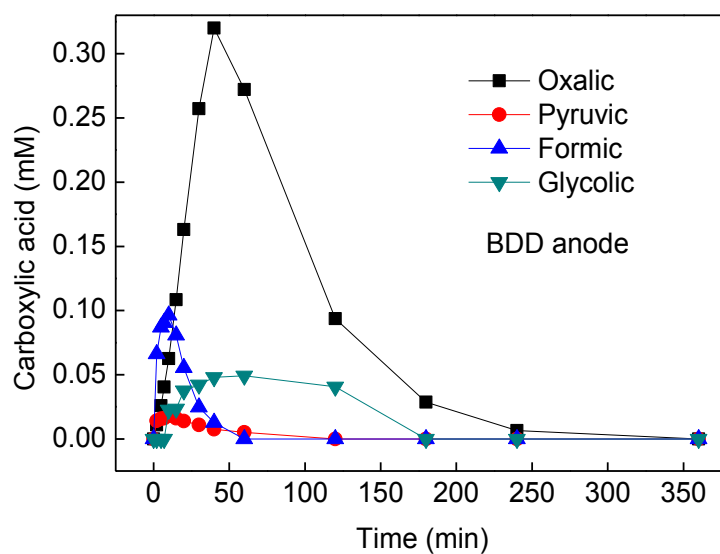
0.2 mM SUC solution aqueous solution was treated when Fe^{2+} concentration was 0.2 mM, Na_2SO_4 concentration was 50 mM, applied current was 200 mA and pH_0 was 3.0.

The concentration of carboxylic acids was monitored by ion-exclusion HPLC and the results were shown in Fig. 5-4. In both Pt/carbon-felt and BDD/carbon-felt cells, oxalic, pyruvic, formic and glycolic acid at retention time (t_R) 8.90, 11.57, 16.03 and 14.53, respectively, were observed. As shown in Fig. 5-4, formic acid was observed as soon as the electrolysis started in both cells. Its concentration reaches the maximum value of 0.090 mM after a 20 min reaction in Pt/carbon-felt cell and 0.096 mM after only 10 min in BDD/carbon-felt cell. Then it decreased gradually to be completely mineralized after 180 min and 60 min in Pt/carbon-felt and BDD/carbon-felt cells, respectively. Pyruvic acid was also generated at the beginning of the electrolysis and followed the accumulation-destruction cycles in two cells. It disappeared after 120 min electrolysis in both cells. The accumulation of glycolic acid was a little slower and appeared after 7 min of electrolysis. Oxalic acid showed the largest accumulation and the higher persistence in both cells due to its high stability in the presence of ferric ions and its weaker reactivity toward $\cdot\text{OH}$ radicals ($k_2 = 2.8 \times 10^7 \text{ M}^{-1} \text{ s}^{-1}$) (Oturán *et al.* 2008). This suggested that oxalic acid would be generated from different ways as ultimate reaction intermediates.

Moreover, all the carboxylic acids were vanished after a 360 min electrolysis in Pt/carbon-felt cell and a 240 min electrolysis in BDD/carbon-felt cell, which was corresponding to the residual TOC remaining at the end of mineralization treatments (Fig. 5-2a and Fig. 5-2b).



(a)



(b)

Fig. 5-4 Evolution of short-chain carboxylic acids formed during electro-Fenton processes with Pt v(a) and BDD (b) anodes ($[SUC]_0 = 0.2 \text{ mM}$, $[Fe^{2+}] = 0.2 \text{ mM}$, $[Na_2SO_4] = 50 \text{ mM}$, $I = 200 \text{ mA}$, $pH_0 = 3.0$)

5.3.5 Identification and evolution of chloride ions

Upon bond cleavage of the sucralose molecules, the Cl atoms are released into the

solution as inorganic ions and the concentration of Cl^- was shown in Figure 5-5. When Pt was used as anode, a progressive accumulation of Cl^- was observed, until reaching the expected maximum value of 0.6 mM. In contrast, the release of Cl^- was increased significantly and reached a maximum concentration of 0.544 mM after 30 min, whereupon it decreased until a final value of 0.063 mM at 360 min. This phenomenon could be explained by the oxidation of Cl^- to Cl_2 and/or ClO^-/HClO , ClO_3^- , and ClO_4^- by BDD($\cdot\text{OH}$) and/or $\cdot\text{OH}$ in the bulk (Randazzo *et al.* 2011; Dirany *et al.* 2012).

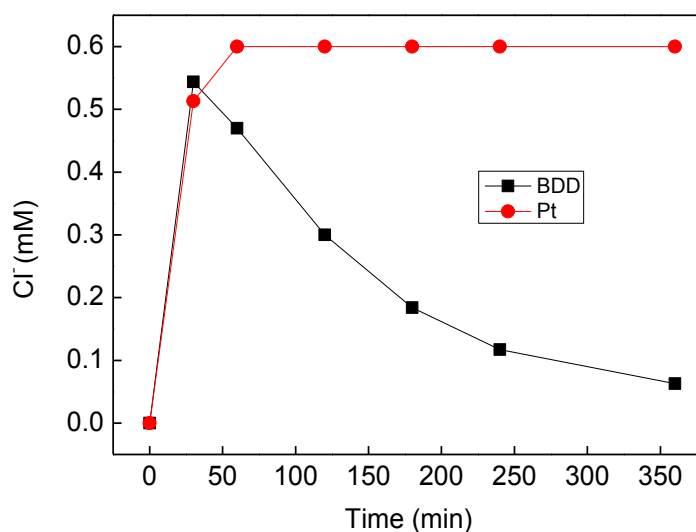


Fig. 5-5 Evolution of chloride ions released during electro-Fenton processes with Pt (a) and BDD (b) anode ($[\text{sucralose}]_0 = 0.2 \text{ mM}$, $[\text{Fe}^{2+}] = 0.2 \text{ mM}$, $[\text{Na}_2\text{SO}_4] = 50 \text{ mM}$, $I = 200 \text{ mA}$, $\text{pH}_0 = 3.0$)

5.3.6 The evolution of toxicity with reaction time

In order to monitor the potential toxicity of sucralose and its intermediates, 0.2 mM sucralose was electrolyzed in the existence of 0.2 mM Fe^{2+} at 200 mA using Microtox method for both Pt/carbon-felt and BDD/carbon-felt cells. The percentage of bacteria luminescence inhibition versus the electrolysis time after 15 min exposure times of *V. fischeri* luminescent bacteria to the sucralose solutions was shown in Fig. 5-6.

When Pt was used as anode, there were several peaks due to the degradation primary intermediates and formation to secondary/tertiary intermediates that were more

toxic than the previous sucralose solution in the first 60 min electrolysis (Feng *et al.* 2014). The other peak appeared at 120 min, indicating the generation of other toxic byproducts. From 120 to 240 min, the inhibition percentage decreased sharply. The toxicity was much lower than the untreated sucralose solution at 240 min, in relation to the increase of the less toxic byproducts, such as carboxylic acids, which present a very low toxicity toward *V. fischeri* bacteria (Dirany *et al.* 2012). Consequently, the toxicity kept stable from 240 min to the end of the electrolysis.

The curves obtained for BDD anode showed a similar behavior at the beginning of the electrolysis as Pt anode. Several peaks were obtained, indicating the formation of some intermediates that were more toxic than the previous sucralose solution in a 60 min reaction. The secondary peak appeared at 40 min and showed the secondary intermediates still more toxic than the original sucralose solution. The secondary peak which appeared at 240 min was much lower than the primary peak, showing the toxicity of secondary intermediates were much lower than the primary byproducts. After 240 min, the inhibition percentage decreased significantly and was much lower than the untreated sucralose solution at the end of the electrolysis, showing the disappearance of toxic intermediate products.

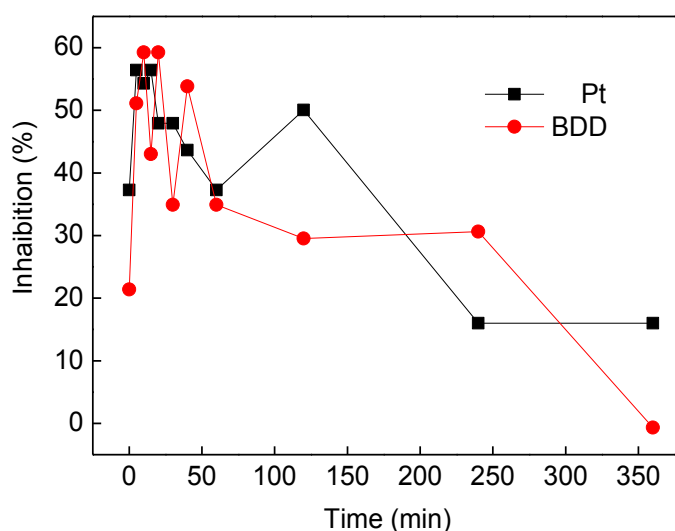


Fig. 5-6 Evolution of the inhibition of marine bacteria, *Vibrio fischeri* luminescence (Microtox method) during electro-Fenton processes with Pt (a) and BDD (b) anode ($[\text{sucralose}]_0 = 0.2 \text{ mM}$, $[\text{Fe}^{2+}] = 0.2 \text{ mM}$, $[\text{Na}_2\text{SO}_4] = 50 \text{ mM}$, $I = 200 \text{ mA}$, $\text{pH}_0 3.0$)

5.4 Conclusions

Electro-Fenton process using a carbon-felt cathode and a Pt or BDD anode was successfully applied to the mineralization of sucralose in aqueous solutions in this study. The optimal conditions for the mineralization of 0.2 mM sucralose solution were Fe^{2+} concentration 0.2 mM, Na_2SO_4 concentration 50 mM, applied current 200 mA and initial pH 3.0. At optimal conditions, sucralose could be totally mineralized in 240 min for BDD anode and 360 min for Pt anode. Short-chain aliphatic carboxylic acids such as oxalic, pyruvic, formic and glycolic are identified as aliphatic byproducts during the electro-Fenton process. Cl atoms were found in the structure of sucralose and were converted to Cl^- . The bacteria luminescence inhibition showed the toxicity of sucralose solution increased at the beginning of electrolysis, and then it declined until much lower than the original sucralose solution at the end of the reaction.

References

- Boye, B., Dieng, M.M. and Brillas, E. (2002) Degradation of herbicide 4-Chlorophenoxyacetic acid by advanced electrochemical oxidation methods. *Environmental Science & Technology* 36(13), 3030-3035.
- Brillas, E., Sirés, I., Arias, C., Cabot, P.L., Centellas, F., Rodríguez, R.M. and Garrido, J.A. (2005) Mineralization of paracetamol in aqueous medium by anodic oxidation with a boron-doped diamond electrode. *Chemosphere* 58(4), 399-406.
- Brillas, E., Sirés, I. and Oturan, M.A. (2009) Electro-Fenton process and related electrochemical technologies based on Fenton's reaction chemistry. *Chemical Reviews* 109(12), 6570-6631.
- Dirany, A., Sirés, I., Oturan, N. and Oturan, M.A. (2010) Electrochemical abatement of the antibiotic sulfamethoxazole from water. *Chemosphere* 81(5), 594-602.
- Dirany, A., Sirés, I., Oturan, N., Özcan, A. and Oturan, M.A. (2012) Electrochemical treatment of the antibiotic sulfachloropyridazine: Kinetics, reaction pathways, and toxicity evolution. *Environmental Science & Technology* 46(7), 4074-4082.
- Feng, L., Oturan, N., van Hullebusch, E., Esposito, G. and Oturan, M. (2014) Degradation of anti-inflammatory drug ketoprofen by electro-oxidation: comparison of electro-Fenton and anodic oxidation processes. *Environmental Science and Pollution Research* 21(14), 8406-8416.
- Lin, H., Zhang, H., Wang, X., Wang, L. and Wu, J. (2014) Electro-Fenton removal of Orange II in a divided cell: Reaction mechanism, degradation pathway and toxicity evolution. *Separation and Purification Technology* 122, 533-540.
- Martínez-Huitle, C.A. and Brillas, E. (2009) Decontamination of wastewaters containing synthetic organic dyes by electrochemical methods: A general review. *Applied Catalysis B: Environmental* 87(3-4), 105-145.
- Oturan, M.A., Edelahe, M.C., Oturan, N., El kacemi, K. and Aaron, J.-J. (2010) Kinetics of oxidative degradation/mineralization pathways of the phenylurea herbicides diuron, monuron and fenuron in water during application of the electro-Fenton process. *Applied Catalysis B: Environmental* 97(1-2), 82-89.
- Oturan, M.A., Pimentel, M., Oturan, N. and Sirés, I. (2008) Reaction sequence for the

- mineralization of the short-chain carboxylic acids usually formed upon cleavage of aromatics during electrochemical Fenton treatment. *Electrochimica Acta* 54(2), 173-182.
- Oturan, N., Hamza, M., Ammar, S., Abdelhédi, R. and Oturan, M.A. (2011) Oxidation/mineralization of 2-Nitrophenol in aqueous medium by electrochemical advanced oxidation processes using Pt/carbon-felt and BDD/carbon-felt cells. *Journal of Electroanalytical Chemistry* 661(1), 66-71.
- Özcan, A., Şahin, Y. and Oturan, M.A. (2008) Removal of prothionamide from water by using electro-Fenton technology: Kinetics and mechanism. *Chemosphere* 73(5), 737-744.
- Panizza, M. and Cerisola, G. (2005) Application of diamond electrodes to electrochemical processes. *Electrochimica Acta* 51(2), 191-199.
- Randazzo, S., Scialdone, O., Brillas, E. and Sirés, I. (2011) Comparative electrochemical treatments of two chlorinated aliphatic hydrocarbons. Time course of the main reaction by-products. *Journal of Hazardous Materials* 192(3), 1555-1564.
- Sirés, I., Arias, C., Cabot, P.L., Centellas, F., Garrido, J.A., Rodríguez, R.M. and Brillas, E. (2007a) Degradation of clofibric acid in acidic aqueous medium by electro-Fenton and photoelectro-Fenton. *Chemosphere* 66(9), 1660-1669.
- Sirés, I., Garrido, J.A., Rodríguez, R.M., Brillas, E., Oturan, N. and Oturan, M.A. (2007b) Catalytic behavior of the $\text{Fe}^{3+}/\text{Fe}^{2+}$ system in the electro-Fenton degradation of the antimicrobial chlorophene. *Applied Catalysis B: Environmental* 72(3-4), 382-394.
- Skoumal, M., Arias, C., Cabot, P.L., Centellas, F., Garrido, J.A., Rodríguez, R.M. and Brillas, E. (2008) Mineralization of the biocide chloroxylenol by electrochemical advanced oxidation processes. *Chemosphere* 71(9), 1718-1729.
- Wu, J., Zhang, H., Oturan, N., Wang, Y., Chen, L. and Oturan, M.A. (2012) Application of response surface methodology to the removal of the antibiotic tetracycline by electrochemical process using carbon-felt cathode and DSA ($\text{Ti}/\text{RuO}_2\text{-IrO}_2$) anode. *Chemosphere* 87(6), 614-620.

**Chapter 6 Decolorization of Orange II in water by
electro/ α -FeOOH/PDS process**

6.1 Introduction

In this part, peroxydisulfate (PDS), which has the similar structure of O-O bond contained in H₂O₂(Hou *et al.* 2012), was activated by goethite to generate sulfate radicals and remove Orange II from water in a electrochemical (EC) reactor (electro/ α -FeOOH/peroxydisulfate process).

The traditional one-factor-at-a-time approach has been widely used to study the effects of various factors in most experiments. Experimental factors are varied one at a time, with the remaining factors being held constantly (Zhang *et al.* 2011). This method fails to investigate the interactive influences of different variables. When a combination of several independent variables and their interactions affect decolorization efficiency, response surface methodology (RSM) is effective for optimizing the operating parameters in multivariable systems (Gong *et al.* 2010; Zhang *et al.* 2011). As one of the RSM designs, Box-Behnken design (BBD) is known as a modified central composite experimental design (Ay *et al.* 2009; Zhang *et al.* 2011). BBD is an independent, rotatable quadratic design with no embedded factorial or fractional factorial points where the variable combinations are at the midpoints of the edges of the variable space and at the center. In addition, BBD requires fewer runs than other RSM designs with the same number of variables. For example, only 15 runs are needed for a three-parameter experimental design. As a result, BBD was applied in this study to investigate the effect of electric current, α -FeOOH concentration and PDS concentration on the results of the pseudo-first-order decolorization rate constant of Orange II (a kind of widely used zao dyes) in electro/ α -FeOOH/peroxydisulfate process.

6.2 Materials and methods

6.2.1 Chemicals

Orange II (4-(2-hydroxynaphthylazo) benzenesulfonic acid sodium salt) was purchased from Sinopharm Chemical Reagent Co., Ltd. (China) and used without further purification. The Chemical structure and main characteristics of Orange II were

presented in Table 6-1. α -FeOOH was obtained from Sigma-Aldrich. Stock solution was prepared by dissolving a selected amount of Orange II in deionized water and the initial concentration (C_0) was fixed at 50 mg/L. 50 mM Sodium sulfate was added as a supporting electrolyte.

Table 6-1 Chemical structure and main characteristics of Orange II

| | |
|------------------------|-------------------------|
| Name | Orange II |
| Chemical structure | |
| Molecular formula | $C_{16}H_{11}N_2NaO_4S$ |
| CAS number | 633-96-5 |
| Molecular weight | 350.32 |
| λ_{max} (nm) | 485 |
| Water solubility (g/L) | 116 |

6.2.2 Electrochemical apparatus and procedures

Batch experiments were conducted in an undivided electrolytic reactor (glass beaker) containing 400 mL of Orange II solution. Electrolyses were performed at constant current controlled by a direct current (DC) power supply (Model WYK-305) from Yangzhou Jintong Source, Co., Ltd. (China). One 5×11.9 cm plate anode (Ti/RuO₂-IrO₂) and one plate cathode (stainless steel) of the same dimensions were arranged parallel to each other at a distance of 4.0 cm. Prior to the electrolysis, the initial pH (pH₀) of Orange II solutions were measured with a Mettler-Toledo FE20 pH-meter (Mettler-Toledo Instruments Co., Ltd., Shanghai) and adjusted by sulfuric acid and sodium hydroxide. A magnetic stirrer (model 78-1, Hangzhou Instrument Motors Factory, China) was applied to achieve the transport of electroactive matter toward the electrode and ensure homogeneity throughout the reaction. The DC power supply was initiated when PDS solutions and α -FeOOH were added to the electrolytic cell. Samples were taken from electrolytic reactor at each predetermined time interval.

These samples were filtered through 0.22 μm membranes (Millipore Co.) before analysis and then mixed with the same volume of methanol to quench the reaction before analysis.

6.2.3 Analytical methods and procedures

The absorbance of Orange II was measured at maximum absorption wavelength of 485 nm using a Rayleigh UV-9100 spectrophotometer (Rayleigh Co., China). The UV-visible spectrum from 200 to 800 nm was achieved by a spectrophotometer (Shimadzu, UV-1700). The concentration of residual PDS was measured by an iodometric titration method (Wahba *et al.* 1959). Total organic carbon (TOC) analyses were carried out with non dispersive infra red absorption detector (NDIR) using an Analytikjena multi N/C 3100 analyzer. The carrier gas was oxygen with a flow rate of 150 mL/min. The structure of α -FeOOH was characterized by X-ray diffraction (XRD). XRD patterns are collected on a X'Pert Pro Xray diffractometer (PANalytical B.V., Holland), using a Cu $K\alpha$ radiation ($\lambda = 1.5406 \text{ \AA}$). The X-ray photoelectron spectroscopy (XPS) was operated on a ESCALAB 250Xi spectrometer (Thermo fisher, USA) which equipped with Al $K\alpha$ X-ray source. The XPS data analysis was performed using the XPSPeak4.1 program with a symmetric Gaussian–Lorentzian sum function and Shirley background subtraction.

6.2.4 Box-Behnken design (BBD)

Box-Behnken statistical experiment design and response surface methodology were employed to investigate the effects of the three independent variables on the response functions. The independent variables were electric current (X_1), α -FeOOH dosage (X_2) and PDS concentration (X_3). The low, center and high levels for each variable are designed as -1, 0 and +1, respectively as illustrated in Table 6-2. The experimental levels for each variable were determined based results from preliminary experiments of operating parameters. The dependent variable or objective function was the pseudo-first-order decolorization rate constant (Y).

Table 6-2 Experimental range and levels of the independent variables

| Variables | Symbol | -1 | 0 | +1 |
|-------------------------|----------------|-----|-----|-----|
| Electric current (A) | X ₁ | 0.2 | 0.5 | 0.8 |
| α-FeOOH dosage (g/L) | X ₂ | 0.2 | 0.5 | 0.8 |
| PDS concentration (g/L) | X ₃ | 1 | 2 | 3 |

Each independent variable was coded as X_i and determined by the following equation:

$$X_i = \frac{x_i - x_0}{\Delta x_i} \quad (6-1)$$

where X_i is dimensionless code value of the ith independent variable, x_i is the uncoded value of the ith independent variable, x₀ is the uncoded ith independent variable at the center point and Δx_i is the step change value between low level (−1) and high level (+1). As can be seen in Table 6-3, the total number of experiments in this study was 15 based on 3 levels and a 3 factor experimental design, with three replicates at the center of the design for estimation of a pure error sum of squares. Experimental data from the BBD could be analyzed and fitted to a second-order polynomial model using Design Expert 8.0 software:

$$Y = \beta_0 + \sum \beta_i X_i + \sum \beta_{ii} X_i^2 + \sum \beta_{ij} X_i X_j \quad (6-2)$$

where Y is the response and X_i and X_j are the independent variables, square effects and interaction effects; β_i, β_{ij} and β_{ii} are the linear coefficients, interaction coefficients and squared coefficients; β₀ is the intercept parameter.

Table 6-3 Design matrix in coded units and the experiments

| Stand no. | X ₁ | X ₂ | X ₃ | k (min ⁻¹) | |
|-----------|----------------|----------------|----------------|------------------------|-----------|
| | | | | Observed | Predicted |
| 1 | -1 | -1 | 0 | 0.0079 | 0.0093 |
| 2 | 1 | -1 | 0 | 0.021 | 0.020 |
| 3 | -1 | 1 | 0 | 0.011 | 0.011 |
| 4 | 1 | 1 | 0 | 0.022 | 0.020 |
| 5 | -1 | 0 | -1 | 0.011 | 0.0092 |
| 6 | 1 | 0 | -1 | 0.017 | 0.017 |
| 7 | -1 | 0 | 1 | 0.011 | 0.011 |
| 8 | 1 | 0 | 1 | 0.021 | 0.023 |

| | | | | | |
|----|---|----|----|-------|-------|
| 9 | 0 | -1 | -1 | 0.017 | 0.018 |
| 10 | 0 | 1 | -1 | 0.012 | 0.014 |
| 11 | 0 | -1 | 1 | 0.018 | 0.016 |
| 12 | 0 | 1 | 1 | 0.023 | 0.022 |
| 13 | 0 | 0 | 0 | 0.020 | 0.021 |
| 14 | 0 | 0 | 0 | 0.021 | 0.021 |
| 15 | 0 | 0 | 0 | 0.021 | 0.021 |

6.3 Results and discussion

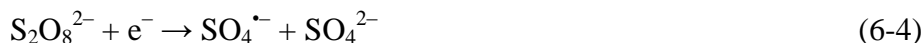
6.3.1 Decolorization of Orange II under different systems

In order to investigate the decolorization efficiency of Orange II under different oxidation systems, 50 mg/L Orange II solution was treated for 120 min by PDS alone, α -FeOOH alone, α -FeOOH/PDS process, EC alone, EC/ α -FeOOH process, EC/PDS process and EC/ α -FeOOH/PDS process. The results were shown in Fig. 6-1. It can be seen from Fig. 6-1a that little decolorization occurred when Orange II was treated by PDS alone, because PDS is stable at ambient temperature and its oxidation power is limited ($E^0 = 2.01$ V) (Zhao *et al.* 2010; Wu *et al.* 2012b), which could hardly degrade Orange II. What's more, the remaining percentage of PDS after 120 min reaction in the PDS alone process was 98.2% (Fig. 6-1b), indicating almost no PDS decomposed in this case. Negligible color removed was also observed when α -FeOOH alone was applied, indicating the effect of adsorption of Orange II decolorization was not obvious under the condition investigated. Orange II was hardly removed in α -FeOOH/PDS process and the remaining percentage of PDS was 95.7%, because PDS can not be activated by Fe(III) on the surface of α -FeOOH. When treated by EC alone, 51.8% of 50 mg/L Orange II was decolorized because a certain amount of hydroxyl radicals ($M(\cdot OH)$) was formed as intermediate of water discharge on DSA anode (M) (Eq. (9)) (Özcan *et al.* 2009).

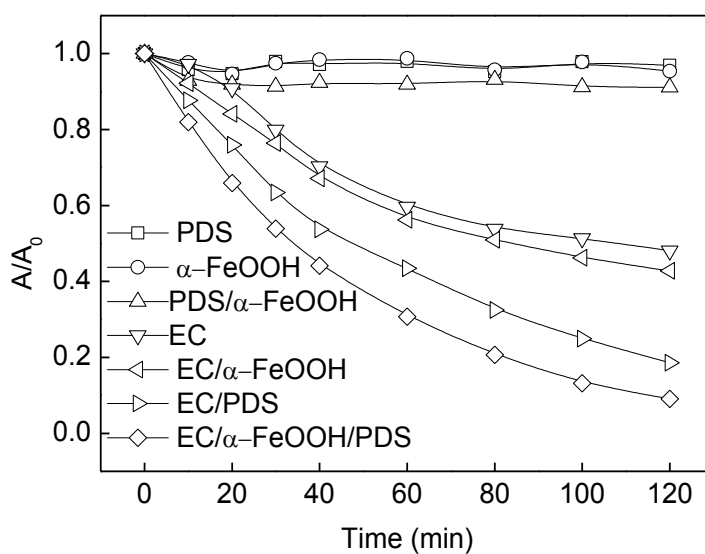
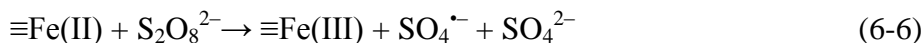


Adding 0.5 g/L α -FeOOH to the electrolytic reactor (EC/ α -FeOOH process) could

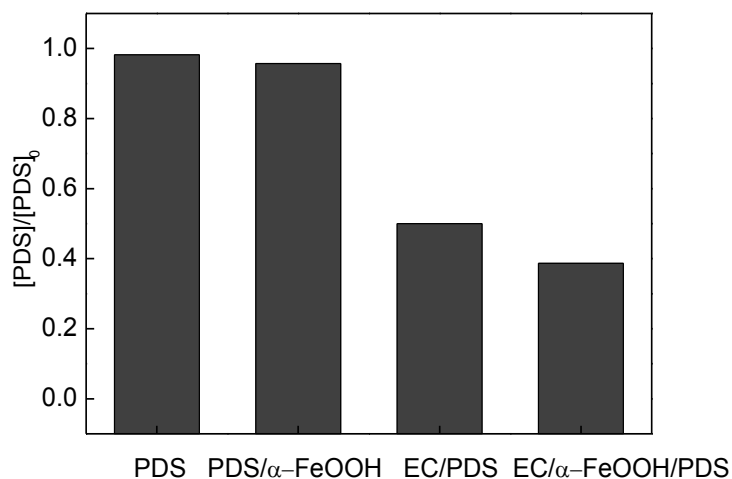
not improve the decolorization efficiency of Orange II. The decolorization efficiency was 57.2% after 120 min reaction in EC/ α -FeOOH process. The decolorization efficiency improved significantly to 81.4% in EC/PDS process, which might be attributed to sulfate radicals produced via Eq. (6-4). 50.0% of PDS was decomposed in this case (Fig. 6-1b).



The decolorization efficiency of Orange II was 90.9% and the remaining percentage of PDS was 38.7% in the process of EC/ α -FeOOH /PDS, indicating Fe(II) can be generated by the cathodic reduction of Fe(III) (Eq. (6-5)), and then more sulfate radicals can formed by Fe(II) activating PDS reaction (Eq. (6-6)).



(a)



(b)

Fig. 6-1 Decolorization of Orange II (a) and remaining percentage of PDS (b) after 120 min of reaction under different systems ($C_0 = 50$ mg/L, $[\alpha\text{-FeOOH}] = 0.5$ g/L, $[\text{PDS}] = 2$ g/L, $I = 0.5$ A, $\text{pH}_0 = 3.0$, $[\text{Na}_2\text{SO}_4] = 50$ mM)

In order to investigate the mechanism of Orange II decolorization in EC/ α -FeOOH/PDS process, the catalyst α -FeOOH was characterized by XRD and XPS. The XRD analysis was applied to define the structure of fresh α -FeOOH and the obtained patterns were shown on Fig. 6-2. The peaks at the angle of 2θ 21.223°, 33.241°, 34.700°, 36.649°, 39.984°, 41.186°, 50.613°, 53.237° and 59.023° are specific of α -FeOOH (Jaiswal *et al.* 2013).

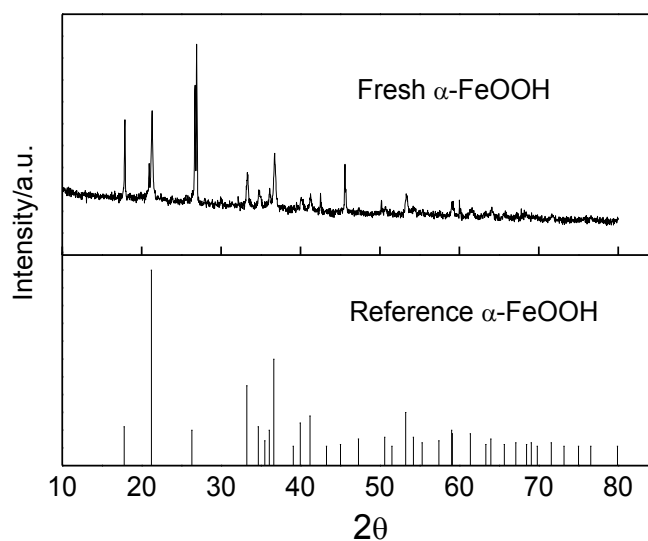
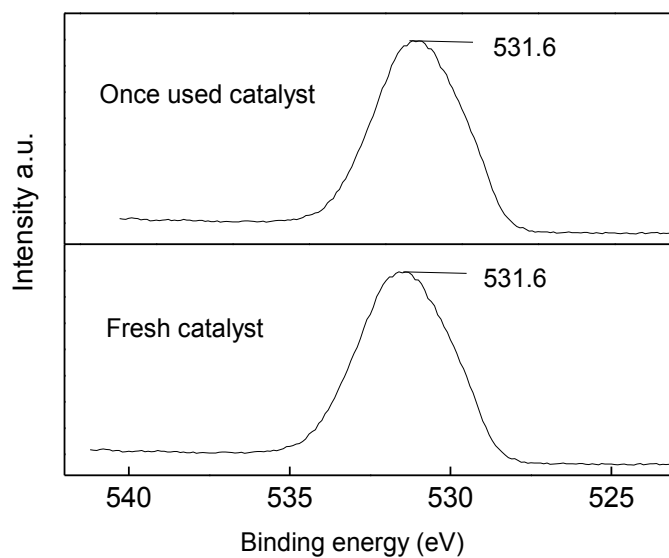
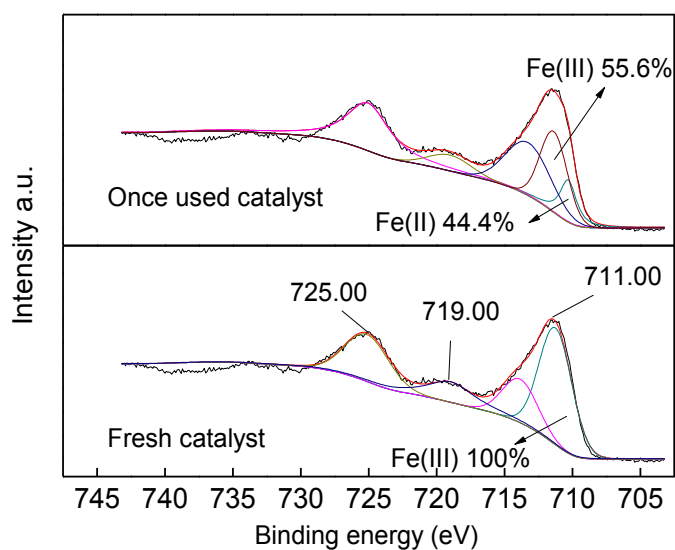


Fig. 6-2 XRD pattern of α -FeOOH (Reference X-ray lines belonging to α -FeOOH (JCPDS card n^o 29-0713) are given at the bottom of the figure)

XPS was used to applied to observe the surface properties of α -FeOOH before and after reaction. The results were showed in Fig. 6-3. The domain peak for O 1s was at 531.6 eV. The O 1s peak of α -FeOOH is shifted significantly higher (0.4 eV) than that of α -Fe₂O₃ (531.2 eV)(Guo *et al.* 2010), indicating the proton on the hydroxyl oxygen has some interaction with the O₂⁻ oxygen (McIntyre and Zetaruk 1977). Fig. 6-3a showed the O 1s peak of α -FeOOH did not change obviously after the reaction. So the properties of oxygen on the surface of α -FeOOH did not change during the EC/ α -FeOOH/PDS process. The peaks of Fe 2p spectrum at 711, 719, and 725 eV represented the binding energies of Fe 2p_{3/2}, shake-upsatellite Fe 2p_{3/2}, and Fe 2p_{1/2}, respectively (Nie *et al.* 2009). As can be seen from Fig. 6-3b, there was no Fe (II) on the surface of α -FeOOH before the reaction. However, The ratio of Fe(II)/Fe(III) on the surface of α -FeOOH adsorbent increased to 0.80 after 120 min reaction. This implied more Fe(II) was generated on the surface of α -FeOOH particles during EC/ α -FeOOH/PDS process (Eq. (6-5)).



(a)



(b)

Fig. 6-3 O 1s (a) and Fe2p (b) XPS spectra of fresh and used α -FeOOH after the reaction

Based on the results and the previous studies, (Liang *et al.* 2007; Özcan *et al.* 2009; Lin *et al.* 2013), the mechanism of EC/ α -FeOOH/PDS process was shown in Fig. 6-4. Fe(II) was generated by the reduction and transformation of Fe(III) on the surface of α -FeOOH due to the direct electron transfer (Eq. (6-5)), and then Fe(II) activated PDS

to generate sulfate radicals (Eq. (6-6)). Meanwhile, hydroxyl radicals were generated both by water discharge on DSA anode (Eq. (6-3)) and the reaction between sulfate radicals and H₂O or OH⁻ (Eqs. (6-7) and (6-8)) (Liang *et al.* 2007; Saien *et al.* 2011). Orange II was degraded by both sulfate radicals and hydroxyl radicals.

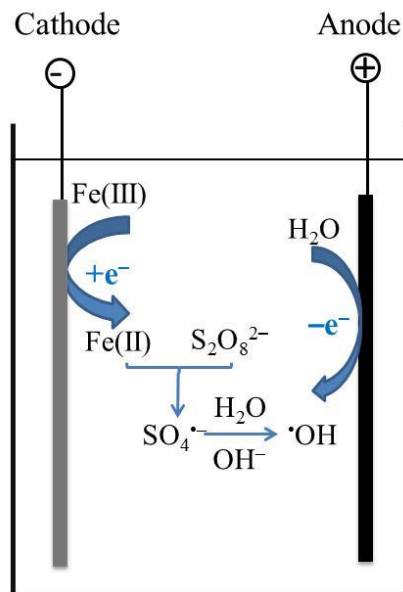
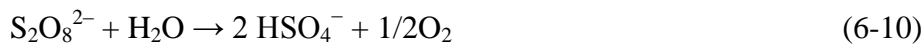


Fig. 6-4 Proposed mechanism of EC/ α -FeOOH/PDS process

6.3.2 Effect of initial pH

The effect of pH on degradation of Orange II was investigated when initial Orange II concentration was 50 mg/L, α -FeOOH dosage was 0.5 g/L, PDS concentration was 2 g/L, Na₂SO₄ solution concentration was 50 mM and the electrical current was 0.5 A. The initial pH values investigated were 3, 7 and 10. As it indicated in Fig. 6-5, no significant effect of pH on the decolorization efficiency was observed. The final efficiency was 90.9%, 92.1% and 89.1% at initial pH 3.0, 7.0 and 10.0, respectively. It is reported that sulfate radicals could react with H₂O or OH⁻ to produce hydroxyl radicals (Eqs. (6-7) and (6-8)) (Liang *et al.* 2007; Saien *et al.* 2011). Either H⁺ could be generated or OH⁻ could be consumed, which led to the reduction of solution pH in EC/FeOOH/PDS process. Moreover, the reaction of hydroxyl radical and sulfate radical

(Eq. (6-9)) as well as the decomposition of PDS in water (Eq. (6-10)) would generate HSO_4^- . The dissociation of HSO_4^- (Eq. (6-11)) would further release H^+ and decrease the solution pH (Kusic *et al.* 2011; Wu *et al.* 2012b).



Therefore, the final pH was almost the same value (about 2.5) and the decolorization of Orange II tended to be operated under similar conditions as the reaction proceeded. This indicated that the EC/ α -FeOOH/PDS process could be successfully applied at a wide range of initial pH. Since pH of most actual textile effluent was neutral, pH 7.0 was chosen as the optimal initial value used in the following experiments.

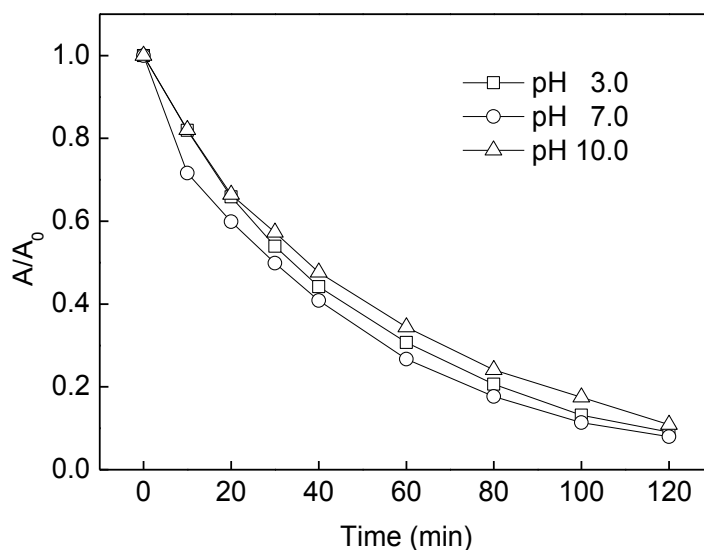


Fig. 6-5 The effect of initial pH value on the degradation of Orange II ($C_0 = 50 \text{ mg/L}$, $[\alpha\text{-FeOOH}] = 0.5 \text{ g/L}$, $[\text{PDS}] = 2 \text{ g/L}$, $I = 0.5 \text{ A}$, $[\text{Na}_2\text{SO}_4] = 50 \text{ mM}$)

6.3.3 Response surface analysis

6.3.3.1 Main variables

The full factorial BBD with three factors in three levels as well as results of Orange II decolorization rate constant for each run are listed in Table 6-3. Based on Table 6-3, the main effects plot and the interaction plots for Orange II decolorization rate constant at 120 min were developed. The main effects plot illustrated that the effects of electrical current, α -FeOOH dosage and PDS concentration on Orange II decolorization rate constant were positive (Fig. 6-6). This means that the greater removal efficiency could be achieved at high level (+1) of each factor than that at low level (-1) of the factor. Among the variables, the influence of electrical current was the greatest, and the second one was the PDS concentration. The influence of α -FeOOH dosage was softer than the other two variables at 120 min.

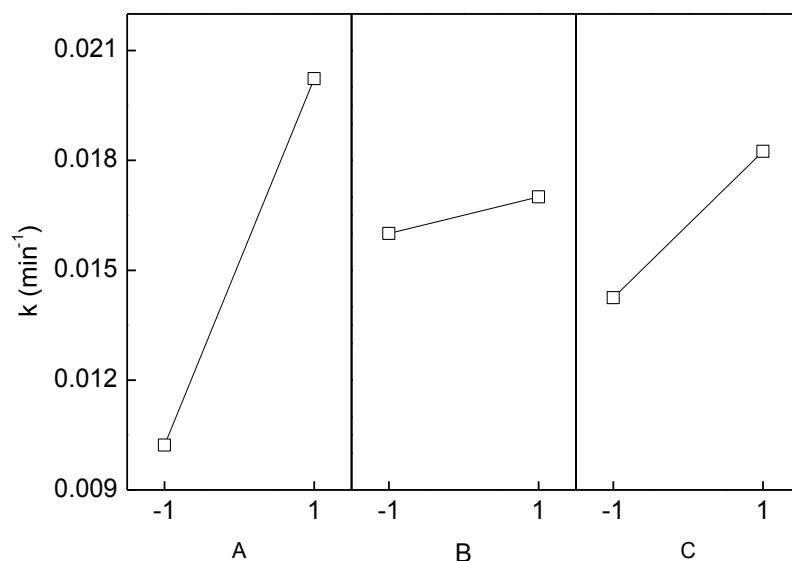


Fig. 6-6 Main effects plot for Orange II decolorization rate constant: Applied current (A); α -FeOOH dosage (B); PDS concentration (C)

6.3.3.2 Interaction between variables

Fig. 6-7 illustrated interaction plots showing the existence or not of interaction

among the factors. One factor was fixed at its high (+1) or low (-1) level while the other was investigated (Domínguez *et al.* 2010). As can be seen in Fig. 6-4, the curves of interaction between α -FeOOH dosage and PDS concentration are across, indicating the interaction between two variables is significant. The curves of interaction between electrical current and PDS concentration are tending to cross. It may assume that the interaction between two variables is significant. The interaction effect between electrical current and α -FeOOH dosage are less significant than that between α -FeOOH dosage and PDS concentration. This was also confirmed by the high probability value ((Prob > F) > 0.1) through analysis of variance (ANOVA).

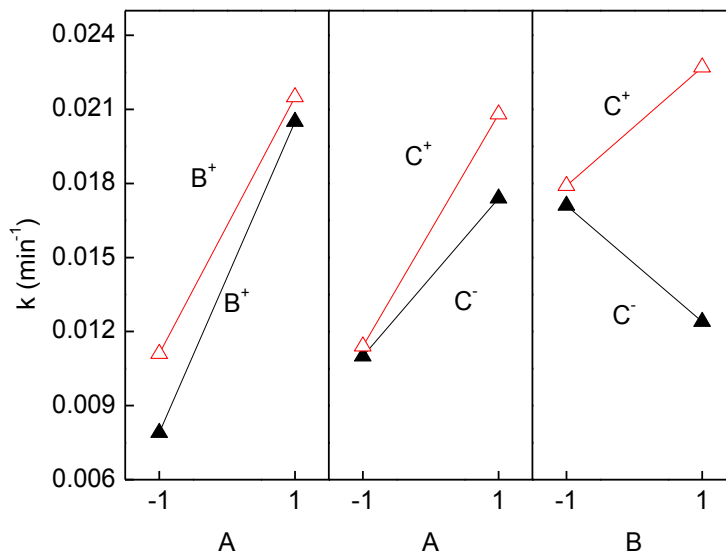


Fig. 6-7 Interaction plots for Orange II decolorization rate constant: Applied current (A); α -FeOOH dosage (B); PDS concentration (C)

6.3.3.3 Fitting model and analysis of variance

In order to justify the significance and adequacy of the model, the ANOVA analysis is required. The value of (Prob > F) was used as a tool to check the significant of each model terms. The smaller the value of (Prob > F) means the more significant of the corresponding model term. Generally, the value of (Prob > F) over 0.1 implies that the model term is insignificant (Zhang *et al.* 2010). Based on the results shown in Table 6-4, RSM model of second order polynomial equations was determined as follows,

$$Y = 0.021 + 4.85 \times 10^{-3} X_1 + 5.38 \times 10^{-4} X_2 + 1.86 \times 10^{-3} X_3 - 5.50 \times 10^{-4} X_1 X_2 + 7.50 \times 10^{-4} X_1 X_3 + 2.38 \times 10^{-3} X_2 X_3 - 3.93 \times 10^{-3} X_1^2 - 1.55 \times 10^{-3} X_2^2 - 1.65 \times 10^{-3} X_3^2$$

(6-12)

The coefficients of determination R^2 gave the proportion of the total variation in the response variable explained. The R^2 obtained in this work (0.9507) ensured a satisfactory adjustment of the quadratic model to the experimental data. The coefficient of variation (CV) is a measure expressing standard deviation as a percentage of the mean. It illustrates the extent to which the data were dispersed. The lower values of CV give better reproducibility (Ahmad *et al.* 2005; Zinatizadeh *et al.* 2006). In this work, the CV value (10.6%) was within the acceptable range (0.5–13.5%) (Zinatizadeh *et al.* 2006; Wu *et al.* 2012a). In addition, adequate precision was used to assess the signal to noise ratio. The value of adequate precision greater than 4 is considered to give accurate prediction (Körbahti 2007). Therefore, the adequate precision value of 9.126 indicated adequate signals for the models to be used to navigate the design space.

Table 6-4 ANOVA for response surface quadratic model

| Source of variation | Sum of squares | Degree of freedom | Mean square | F-value | p-value |
|---------------------|-----------------------|-------------------|-----------------------|---------|---------|
| Model | 3.13×10^{-4} | 9 | 3.48×10^{-4} | 10.72 | 0.0089 |
| X_1 | 1.88×10^{-4} | 1 | 1.88×10^{-4} | 57.98 | 0.0006 |
| X_3 | 2.78×10^{-5} | 1 | 2.78×10^{-5} | 8.55 | 0.0329 |
| $X_2 X_3$ | 2.26×10^{-5} | 1 | 2.26×10^{-5} | 6.95 | 0.0462 |
| X_1^2 | 5.70×10^{-5} | 1 | 5.70×10^{-5} | 17.56 | 0.0086 |
| Residue | 1.62×10^{-5} | 5 | 3.25×10^{-6} | | |
| Lack of fit | 1.52×10^{-5} | 3 | 5.08×10^{-6} | 10.30 | 0.0898 |
| Pure error | 9.87×10^{-7} | 2 | 4.93×10^{-7} | | |
| Cor. Total | 3.29×10^{-4} | 14 | | | |

6.3.3.4 Adequacy check of the model

The examination of residuals was employed to investigate the model adequacy. It

would give poor or misleading results if the model was not adequate fit (Wu *et al.* 2012a). The normal probability and studentized residuals plots illustrate whether the studentized residuals follow a normal distribution. Normal plot presented at Fig. 6-8 is normally distributed and resemble a straight line, indicating that there is no apparent problem with normality and no need for transformation of response (Khataee *et al.* 2010). Fig. 6-9 shows the studentized residual versus predicted value, and the residuals appear to be a random scatter. It suggests that the equality of variance does not seem to be violated (Grčić *et al.* 2009). Furthermore, the similarity between predicted and actual values of the response which was illustrated in Fig. 6-10 indicated that there was no significant violation of the models and the models were satisfactory and accurate.

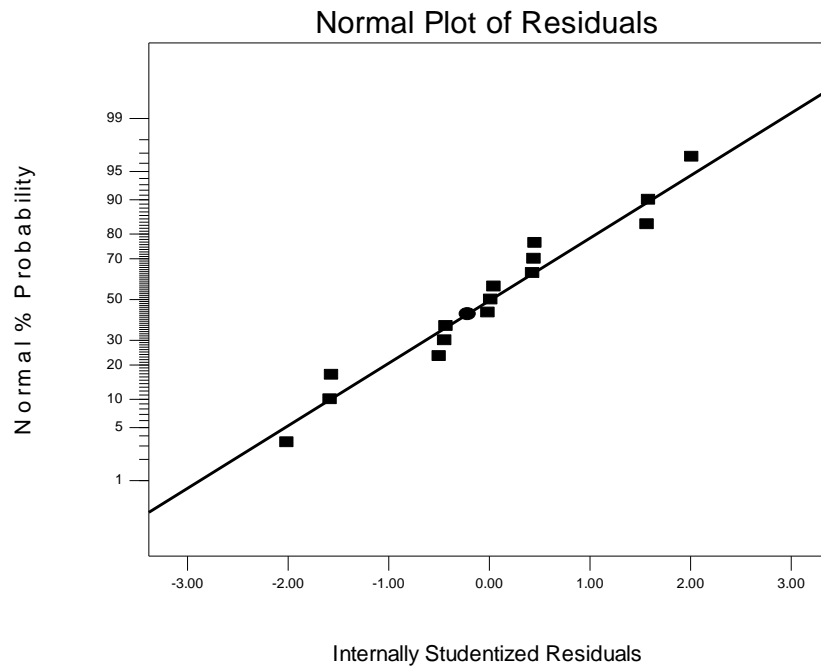


Fig. 6-8 The internally studentized residuals and normal % probability plot for Orange II decolorization rate constant

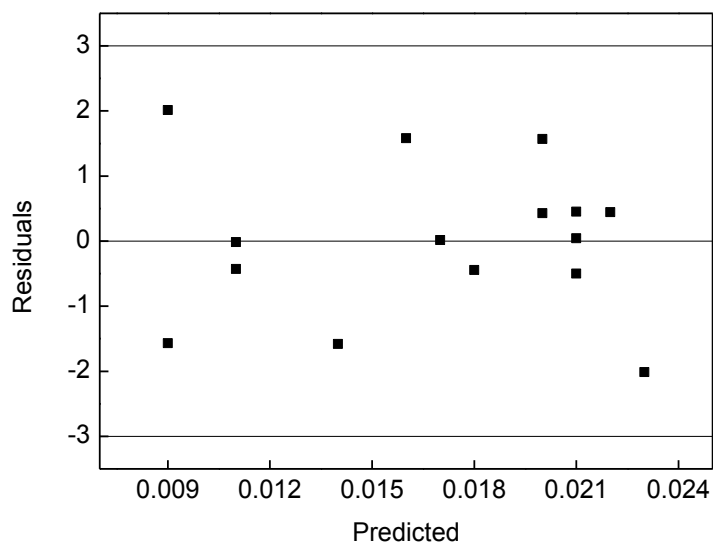


Fig. 6-9 Residuals vs. predicted plot for Orange II decolorization rate constant

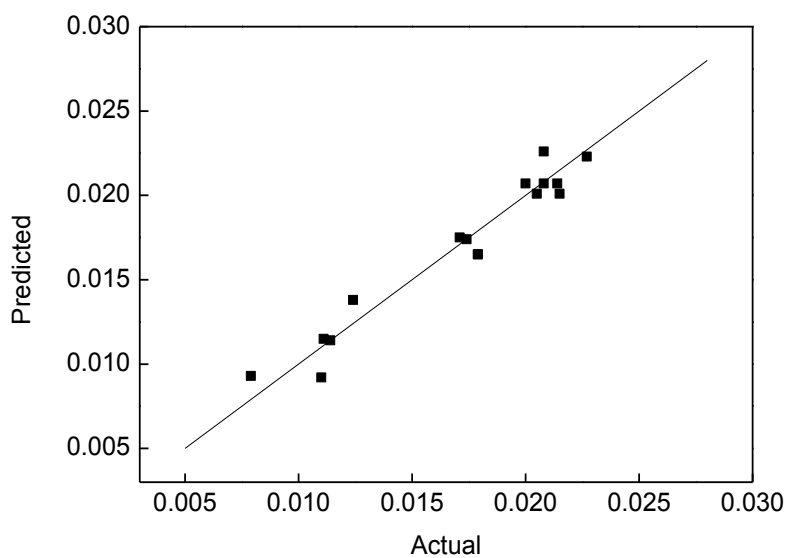


Fig. 6-10 Predicted vs. actual plot for Orange II decolorization rate constant

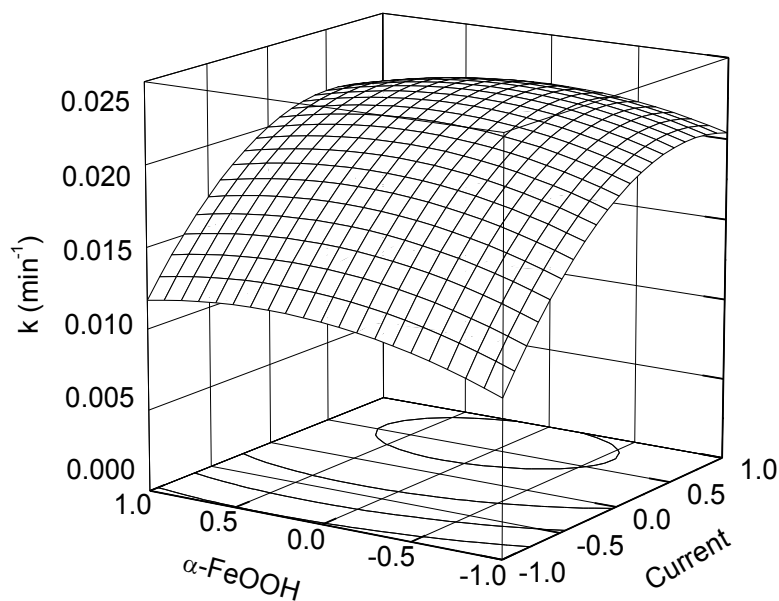
6.3.3.5 Response surface analysis

The 3D response surfaces plots were developed based on the RSM equation and showed in Fig. 6-11. There is an optimum current value for Orange II decolorization rate. In other word, increasing electrical current to certain extent could increase Orange II decolorization rate, while further increasing electrical current would decrease the

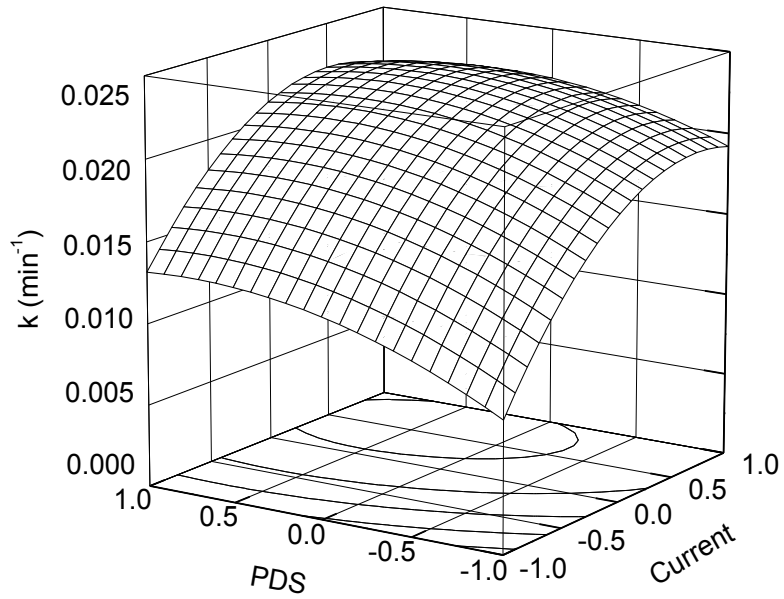
decolorization rate. On the one hand, increase of applied current could promote the conversion of Fe(III) to Fe(II) on the surface of the catalyst (Eq. (6-5)) which resulted in more sulfate radicals generated on α -FeOOH surface. On the other hand, higher electrical current improves the generation of sulfate radicals and hydroxyl radicals via electron transfer reaction (Eq. (6-4)) and water discharge on DSA anode (M) (Eq. (6-3)) (Lin *et al.* 2014; Nidheesh and Gandhimathi 2014), respectively. However, further increasing the electrical current might lead to the side reactions and particularly the hydrogen gas evolution (Eq. (6-12)) which lead to the decline of the decolorization rate (Wu *et al.* 2012a).



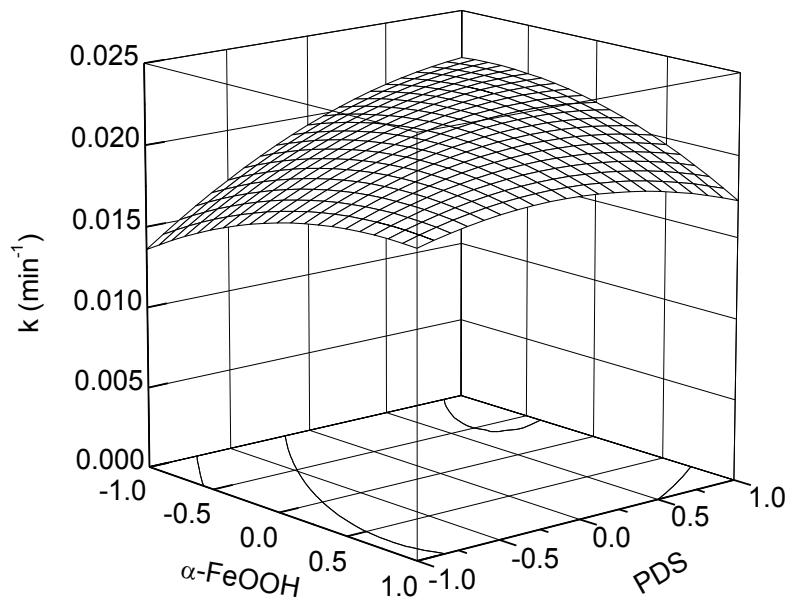
Fig. 6-11 also showed that the decolorization rate of Orange II increased slightly with the increase of α -FeOOH dosage and PDS concentration, because higher concentration of catalyst and PDS favored the generation of sulfate radicals.



(a)



(b)



(c)

Fig. 6-11 Response surface showing removal efficiency as a function of two independent variables:
 (a) electrical current (A) and α -FeOOH dosage (B), (b) electrical current (A) and PDS concentration
 (C), (c) α -FeOOH dosage (B) and and PDS concentration (C)

6.3.4 Stability of α -FeOOH

The recycle experiments were performed to investigate the stability of α -FeOOH. The solid was easily removed from the electrochemical reactor after each repetitive oxidation process, then washed by deionised water, dried in the vacuum oven and stored at ambient temperature. The initial concentration of Orange II solution was fixed at 50 mg/L, PDS concentration was 2 g/L, α -FeOOH dosage was 0.8 g/L, Na_2SO_4 solution concentration was 50 mM, initial pH was 7.0 and the applied current was 0.5 A. As shown in Fig. 6-12, the decolorization efficiencies of Orange II during three reaction cycles ranged from 86.5% to 92.1%, indicating α -FeOOH is stable and can be reused.

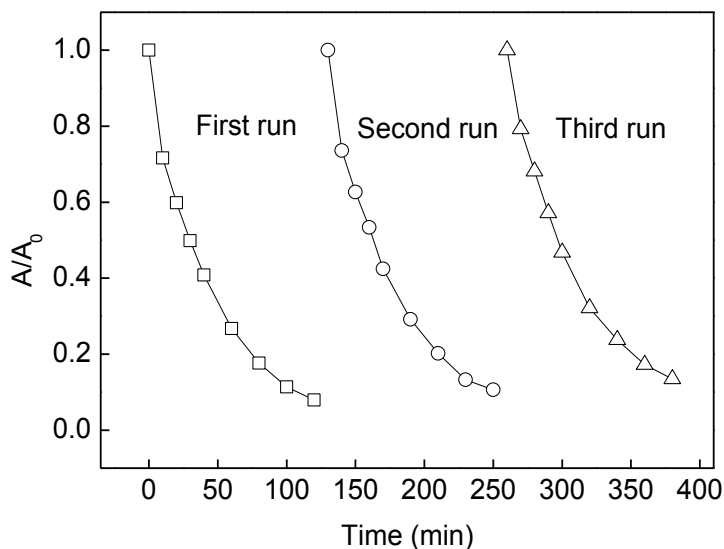


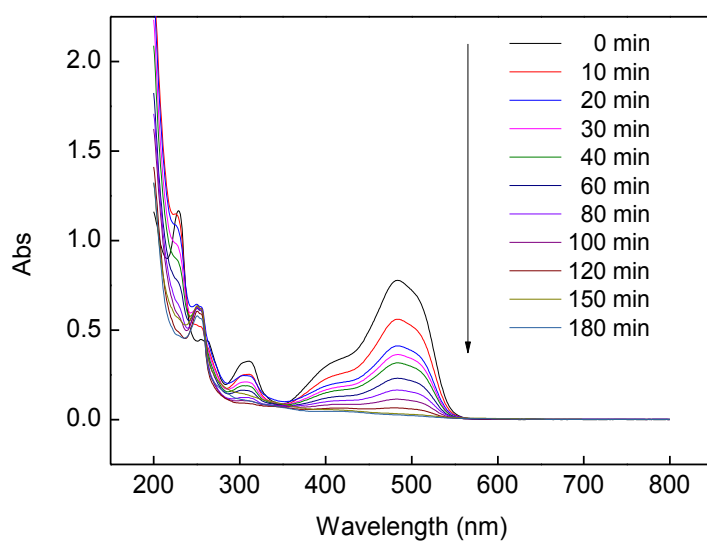
Fig. 6-12 Recycling study of α -FeOOH during Orange II degradation ($C_0 = 50$ mg/L, $[\alpha\text{-FeOOH}] = 0.5$ g/L, $[\text{PDS}] = 2$ g/L, $I = 0.5$ A, $\text{pH}_0 = 7$, $[\text{Na}_2\text{SO}_4] = 50$ mM)

6.3.5 Changes in the UV-visible spectrum and mineralization efficiency of Orange II

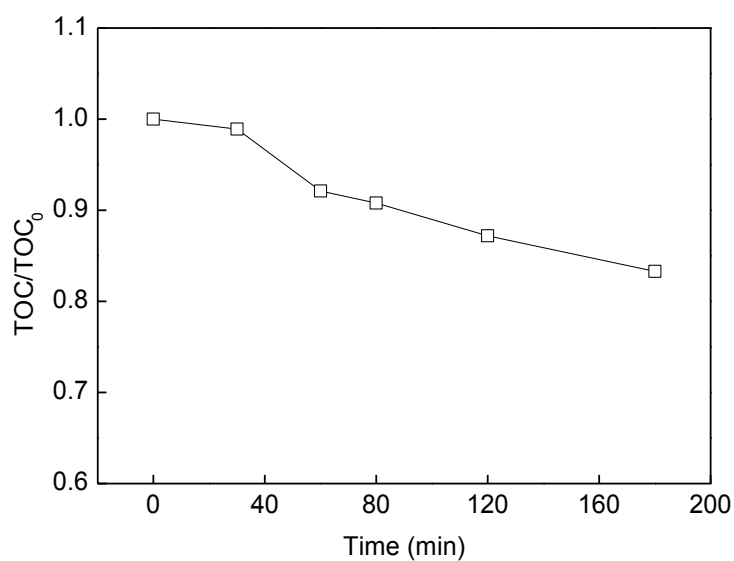
To clarify the changes in molecular and structural characteristics of Orange II as a result of oxidation in the electro/ α -FeOOH/PDS process, representative UV-visible spectra changes in the dye solution as a function of reaction time were depicted and the

corresponding spectra are indicated in Fig. 6-13. As can be seen from these spectra, there was one main band located at 485 nm in the visible region, which was originated from the azo-band chromophore ($-N=N-$) (Wu *et al.* 2012b). Meanwhile, the absorption at 310 nm and 228 nm in the ultraviolet region were corresponded to naphthalene ring and benzene ring structures in the dye molecule (Zhang *et al.* 2009). As shown in Fig. 6-13(a), the visible band disappeared as the reaction proceeded, due to the fragmentation of the azo links by the reaction. The decay of the absorbance at 310 nm was considered as evidence of aromatic fragment degradation in the dye molecule and its intermediates. However, the absorbance at 228 nm increased, indicating that the azo structure was destroyed and some aromatic fragment such as benzene rings were formed.

In order to investigate the mineralization efficiency of Orange II electro/ α -FeOOH/peroxydisulfate process, the changes of TOC were observed with initial Orange II concentration 50 mg/L, α -FeOOH dosage 0.5 g/L, PDS concentration 2 g/L, Na_2SO_4 solution concentration 50 mM, initial pH 7.0 and the electrical current 0.5A. As can be seen in Fig. 6-13(b), the TOC removal efficiency was only 12.8% after 120 min compared with 92.1% of Orange II degradation efficiency. Interestingly, by extending the reaction time to 180 min the TOC removal efficiency slightly increased to 16.7%, indicating most Orange II were converted to more simple intermediate products in electro/ α -FeOOH/peroxydisulfate process.



(a)



(b)

Fig. 6-13 UV-visible spectra changes with reaction time in EC/ α -FeOOH/PDS process (a) and the changes of TOC removal efficiency with reaction time (b) ($C_0 = 50$ mg/L, $[\alpha\text{-FeOOH}] = 0.5$ g/L, $I = 0.5$ A, $\text{pH}_0 = 7$, $[\text{Na}_2\text{SO}_4] = 50$ mM)

6.4 Conclusion

Aqueous solutions of Orange II were effectively degraded by a novel

electro/ α -FeOOH/peroxydisulfate process. Orange II decolorization efficiency first increased with the increase of electrical current, α -FeOOH dosage and PDS concentration, then it decreased when electric current, α -FeOOH dosage and PDS concentration were further increased. Initial pH value has insignificant influence on the decolorization of Orange II. ANOVA indicated both the interaction effect and the quadratic effect were significant on Orange II decolorization rate. The models were significant and could fit the experimental data well.

References

- Ahmad, A.L., Ismail, S. and Bhatia, S. (2005). Optimization of coagulation–flocculation process for palm oil mill effluent using response surface methodology. *Environmental Science & Technology* 39(8), 2828-2834.
- Ay, F., Catalkaya, E.C. and Kargi, F. (2009) A statistical experiment design approach for advanced oxidation of Direct Red azo-dye by photo-Fenton treatment. *Journal of Hazardous Materials* 162(1), 230-236.
- Domínguez, J.n.R., González, T., Palo, P. and Sánchez-Martín, J. (2010). Electrochemical advanced oxidation of carbamazepine on Boron-doped diamond anodes. Influence of Operating Variables. *Industrial & Engineering Chemistry Research* 49(18), 8353-8359.
- Gong, Y.H., Zhang, H., Li, Y.L., Xiang, L.J., Royer, S., Valange, S. and Barrault, J. (2010). Evaluation of heterogeneous photo-Fenton oxidation of Orange II using response surface methodology. *Water Science Technology* 62(6), 1320-1326.
- Grčić, I., Vujević, D., Šepčić, J. and Koprivanac, N. (2009) Minimization of organic content in simulated industrial wastewater by Fenton type processes: A case study. *Journal of Hazardous Materials* 170(2–3), 954-961.
- Guo, L., Chen, F., Fan, X., Cai, W. and Zhang, J. (2010) S-doped α -Fe₂O₃ as a highly active heterogeneous Fenton-like catalyst towards the degradation of acid orange 7 and phenol. *Applied Catalysis B: Environmental* 96(1–2), 162-168.
- Hou, L., Zhang, H. and Xue, X. (2012) Ultrasound enhanced heterogeneous activation of peroxydisulfate by magnetite catalyst for the degradation of tetracycline in water. *Separation and Purification Technology* 84, 147-152.
- Jaiswal, A., Banerjee, S., Mani, R. and Chattopadhyaya, M.C. (2013) Synthesis, characterization and application of goethite mineral as an adsorbent. *Journal of Environmental Chemical Engineering* 1(3), 281-289.
- Körbahti, B.K. (2007) Response surface optimization of electrochemical treatment of textile dye wastewater. *Journal of Hazardous Materials* 145(1–2), 277-286.
- Khataee, A.R., Fathinia, M., Aber, S. and Zarei, M. (2010) Optimization of photocatalytic treatment of dye solution on supported TiO₂ nanoparticles by central

- composite design: Intermediates identification. *Journal of Hazardous Materials* 181(1–3), 886-897.
- Kusic, H., Peternel, I., Koprivanac, N. and Loncaric Bozic, A. (2011). Iron-activated persulfate oxidation of an azo dye in model wastewater: Influence of iron activator type on process optimization. *Journal of Environmental Engineering* 137(6), 454-463.
- Liang, C., Wang, Z.-S. and Bruell, C.J. (2007) Influence of pH on persulfate oxidation of TCE at ambient temperatures. *Chemosphere* 66(1), 106-113.
- Lin, H., Wu, J. and Zhang, H. (2013) Degradation of bisphenol A in aqueous solution by a novel electro/Fe³⁺/peroxydisulfate process. *Separation and Purification Technology* 117, 18-23.
- Lin, H., Wu, J. and Zhang, H. (2014) Degradation of clofibric acid in aqueous solution by an EC/Fe³⁺/PMS process. *Chemical Engineering Journal* 244, 514-521.
- McIntyre, N.S. and Zetaruk, D.G. (1977) X-ray photoelectron spectroscopic studies of iron oxides. *Analytical Chemistry* 49(11), 1521-1529.
- Nidheesh, P.V. and Gandhimathi, R. (2014) Removal of Rhodamine B from aqueous solution using graphite–graphite electro-Fenton system. *Desalination and Water Treatment* 52(10-12), 1872-1877.
- Nie, Y., Hu, C., Qu, J. and Zhao, X. (2009) Photoassisted degradation of endocrine disruptors over CuO_x–FeOOH with H₂O₂ at neutral pH. *Applied Catalysis B: Environmental* 87(1–2), 30-36.
- Özcan, A., Oturan, M.A., Oturan, N. and Şahin, Y. (2009) Removal of Acid Orange 7 from water by electrochemically generated Fenton's reagent. *Journal of Hazardous Materials* 163(2–3), 1213-1220.
- Saien, J., Soleymani, A.R. and Sun, J.H. (2011) Parametric optimization of individual and hybridized AOPs of Fe²⁺/H₂O₂ and UV/S₂O₈²⁻ for rapid dye destruction in aqueous media. *Desalination* 279(1–3), 298-305.
- Wahba, N., El Asmar, M.F. and El Sadr, M.M. (1959) Iodometric Method for Determination of Persulfates. *Analytical Chemistry* 31(11), 1870-1871.
- Wu, J., Zhang, H., Oturan, N., Wang, Y., Chen, L. and Oturan, M.A. (2012a)

- Application of response surface methodology to the removal of the antibiotic tetracycline by electrochemical process using carbon-felt cathode and DSA (Ti/RuO₂-IrO₂) anode. *Chemosphere* 87(6), 614-620.
- Wu, J., Zhang, H. and Qiu, J. (2012b) Degradation of Acid Orange 7 in aqueous solution by a novel electro/Fe²⁺/peroxydisulfate process. *Journal of Hazardous Materials* 215–216, 138-145.
- Zhang, H., Fu, H. and Zhang, D. (2009) Degradation of C.I. Acid Orange 7 by ultrasound enhanced heterogeneous Fenton-like process. *Journal of Hazardous Materials* 172(2–3), 654-660.
- Zhang, H., Li, Y., Wu, X., Zhang, Y. and Zhang, D. (2010) Application of response surface methodology to the treatment landfill leachate in a three-dimensional electrochemical reactor. *Waste Management* 30(11), 2096-2102.
- Zhang, H., Li, Y., Zhong, X. and Ran, X. (2011). Application of experimental design methodology to the decolorization of Orange II using low iron concentration of photoelectro-Fenton process. *Water Science Technology* 63(7), 1373-1380.
- Zhao, J., Zhang, Y., Quan, X. and Chen, S. (2010) Enhanced oxidation of 4-chlorophenol using sulfate radicals generated from zero-valent iron and peroxydisulfate at ambient temperature. *Separation and Purification Technology* 71(3), 302-307.
- Zinatizadeh, A.A.L., Mohamed, A.R., Abdullah, A.Z., Mashitah, M.D., Hasnain Isa, M. and Najafpour, G.D. (2006) Process modeling and analysis of palm oil mill effluent treatment in an up-flow anaerobic sludge fixed film bioreactor using response surface methodology (RSM). *Water Research* 40(17), 3193-3208.

**Chapter 7 Decolorization of Orange II in water by
electro/Fe₃O₄/PDS process**

7.1 Introduction

In this part, Orange II was degraded by electrochemical process combined with Fe₃O₄ activated PDS process (EC/Fe₃O₄/PDS process). The effect of various reaction parameters such as initial pH, current density, PDS concentration and Fe₃O₄ dosage on the removal of Orange II was investigated. The X-ray photoelectron spectroscopy (XPS) was applied to investigate the surface properties of Fe₃O₄ before and after reaction. Gas chromatography–mass spectrometry (GC–MS) was applied to identify the intermediates and the degradation pathway of Orange II is proposed accordingly. The mineralization of Orange II in terms of TOC removal was also investigated. The change of acute toxicity during the treatment was investigated by activated sludge inhibition test.

7.2 Materials and methods

7.2.1 Materials

Orange II (4-(2-hydroxynaphthylazo) benzenesulfonic acid sodium salt) with reagent purity grade was obtained from Sinopharm Chemical Reagent Co., Ltd. (China) and used without further purification. Fe₃O₄ used in this study was from Prolabo Co. (Paris, France). Sodium peroxydisulfate (Na₂S₂O₈, 98%) and anhydrous sodium sulfate (Na₂SO₄, 99%) were purchased from Sinopharm Chemical Reagent Co., Ltd. (Shanghai, China) and of analytical grade.

7.2.2 Experimental

The experimental set-up used for this study is illustrated in Fig. 7-1. Bulk electrolyses were carried out in undivided glass beaker with a capacity of 250 mL. A plate mixed metal oxide (DSA, Ti/RuO₂–IrO₂) anode (5.0 cm × 11.9 cm) is served as the anode and a plate of stainless steel with the same dimensions is used as cathode. The gap between the electrodes was 4.0 cm. The reactor was immersed in a water bath to

keep the temperature constant at 25 °C. A Model RYI-3010 direct current (DC) power supply from Shenzhen Yizhan Source, Co., Ltd. (China) was employed to provide the constant current.

Before each run, a fresh stock solution of Orange II was prepared in deionised water and the initial concentration (C_0) was kept at 25 mg/L. Sodium sulfate (50 mM) was added as a background electrolyte. The initial pH (pH_0) of Orange II solutions was measured with a Mettler-Toledo FE20 pH-meter (Mettler-Toledo Instruments Co., Ltd., Shanghai) and adjusted by sulfuric acid or sodium hydroxide. Before the beginning of electrolysis, a certain amount of PDS and Fe_3O_4 were added into 200 mL of Orange II solution with constant stirring by using a mechanical stirrer (RW 20, IKA, Germany).

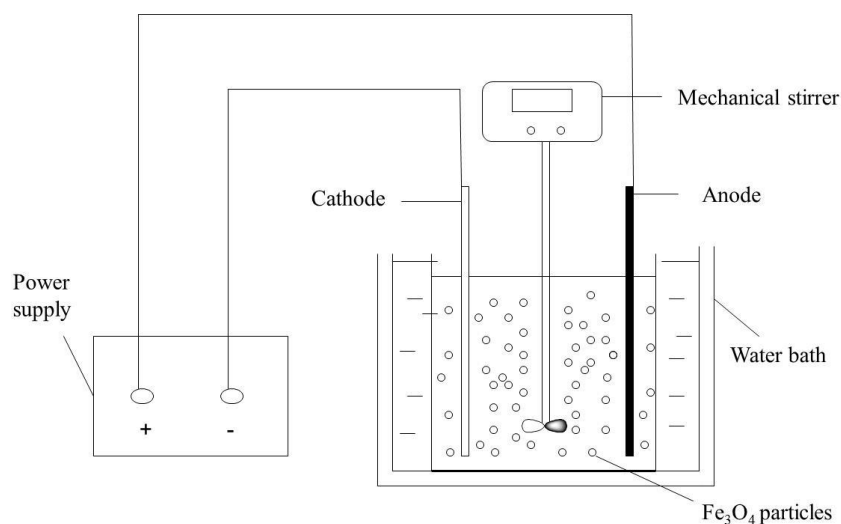


Fig. 7-1 Schematic of the experimental setup employed in the present study

7.2.3 Analysis

The absorbance of Orange II was measured at $\lambda_{max} = 485$ nm using a Rayleigh UV-9100 spectrophotometer (Rayleigh Co., China). Decolorization efficiency was calculated according to Eq. (7-1),

$$\text{Decolorization efficiency (\%)} = \frac{A_0 - A}{A_0} \times 100 \quad (7-1)$$

where the A_0 and A were the absorbance of the sample at time 0 and t , respectively. The concentration of residual PDS was measured by an iodometric titration method (Wahba *et al.* 1959). The quantification of the dissolved iron ions concentration in the solution

was systematically evaluated by Atomic Absorption Spectroscopy (AAS, Perkin Elmer AAnalyst 800). XPS was operated on a KRATOS XSAM800 spectrometer equipped with MgK α X-ray source. GC–MS (VARIAN 450–GC/320–MS) was employed to determine the intermediates. Before analysis, Orange II solution was extracted with dichloromethane for ten times, and then the extracts were concentrated by rotary evaporator at 40 °C to about 1 mL (Zhong *et al.* 2011a; Zhong *et al.* 2011b). A VF–5 MS capillary column (30 m length \times 0.25 mm ID \times 0.25 μ m film thickness) was employed for GC separation. The GC equipments were operated in a temperature programmed mode with an initial temperature of 35 °C held for 2 min, then ramped to 280 °C with a 10 °C/min rate. Helium was used as the carrier gas. Electronimpact (EI) mass spectra were scanned from 0 to 550 m/z.

The TOC of the samples were determined by an Analytik Jena Multi N/C 3100 analyzer with non dispersive infra red absorption detector (NDIR). The carrier gas was oxygen with a flow rate of 158 mL/min. The acute toxicity of intermediates generated during the treatment was assessed by means of activated sludge inhibition test (Olmez-Hanci *et al.* 2009). The activated sludge used as the heterotrophic biomass was obtained from a municipal wastewater treatment located in Wuhan. The mixed liquor suspended solids (MLSS) concentration used in the activated sludge inhibition experiments was adjusted to 1800 mg/L. To conduct the activated sludge inhibition test, 80 mL activated sludge was aerated 5 min and mixed with 20 mL treated wastewater at room temperature. The dissolved oxygen (DO) concentration of the mixed solution was measured by HQ30d (HACH) oxygen meter at selected time intervals. Oxygen uptake rate (OUR) was measured through the slope of the DO concentration versus time (Wu *et al.* 2012a):

$$\text{OUR} = \Delta\text{DO}/\Delta t \quad (7-2)$$

Specific oxygen uptake rate (SOUR) was determined by dividing OUR to the MLSS concentration:

$$\text{SOUR} = \text{OUR}/\text{MLSS} \quad (7-3)$$

where the MLSS were measured by filtration and evaporation the solution at 105 °C for 2 h.

7.3 Results and discussion

7.3.1 Decolorization of Orange II under different systems

To evaluate the decolorization efficiency of Orange II under different systems, the following blank experiments were conducted: Fe₃O₄ alone, PDS alone, Fe₃O₄/PDS process, EC alone, EC/Fe₃O₄ process, EC/PDS process and EC/Fe₃O₄/PDS process. The results are shown in Fig. 7-2a. It can be obviously seen that no appreciable Orange II decolorization was observed when Fe₃O₄ was added into the Orange II solution alone, indicating the effect of adsorption on Orange II decolorization was not obvious under the condition investigated. Little decolorization also occurred when PDS alone was applied. PDS is stable at ambient temperature and its oxidation power was limited ($E^0 = 2.01$ V) (Zhao *et al.* 2010b; Wu *et al.* 2012b), which could hardly degrade Orange II. The remaining percentage of PDS after 60 min reaction in the PDS alone process was 98.0% (Fig. 7-2b), indicating almost no PDS decomposed in this case. The concentration of Orange II was hardly decreased in Fe₃O₄/PDS process and the remaining percentage of PDS was 90%. This may due to the lack of Fe(II) on the surface of Fe₃O₄ particles. When treated by EC alone, 61.1% of 25 mg/L Orange II was decolorized due to a certain amount of hydroxyl radicals (M([•]OH)) formed as intermediate of water discharge on DSA anode (M) (Eq. (7-4)) (Özcan *et al.* 2009).

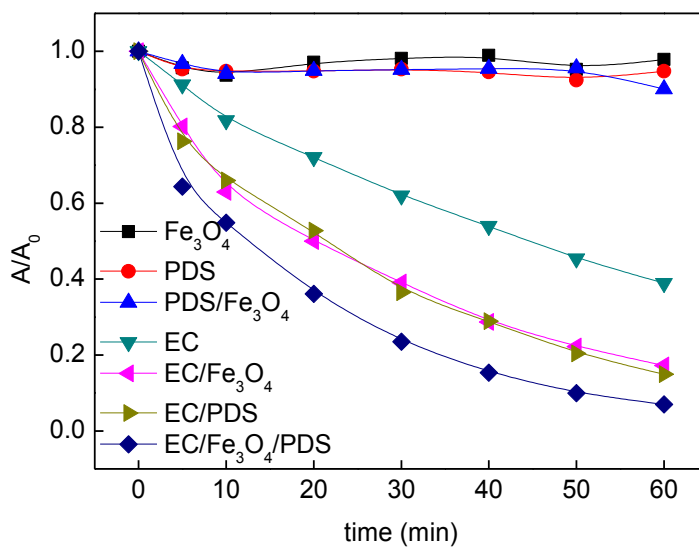


When 0.5 g/L Fe₃O₄ was employed to the electrolytic reactor, the decolorization efficiency of Orange II increased to 82.8%. It can be explained that in EC/Fe₃O₄ process, Fe₃O₄ was used as particle electrodes and could increase mass transfer coefficient and reduce energy consumption (Lin *et al.* 2013). The decolorization efficiency slightly improved to 85.1% in EC/PDS process, which might be attributed to sulfate radicals produced via Eq. (7-5). 54.4% of PDS was decomposed in this case (Fig. 7-2b).

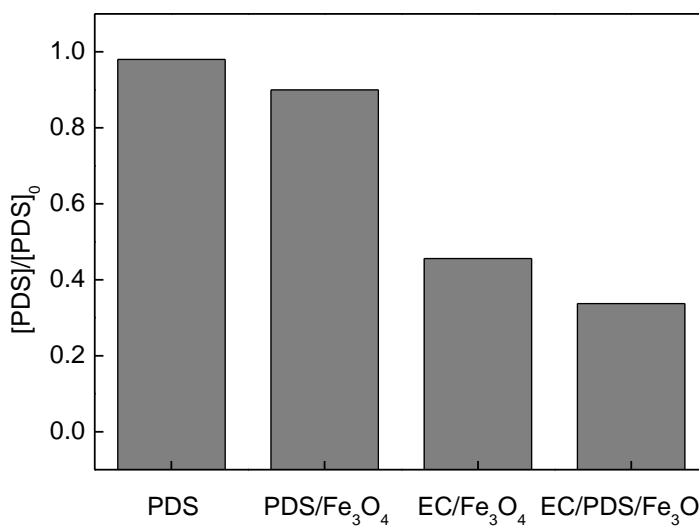


The decolorization efficiency of Orange II was 93.0% and the remaining percentage of PDS was 33.7% in the process of EC/Fe₃O₄/PDS, indicating Fe(II) can be

generated by the cathodic reduction of Fe(III) (Eq. (7-6)), thus more sulfate radicals can be formed by Fe(II) activating PDS reaction.



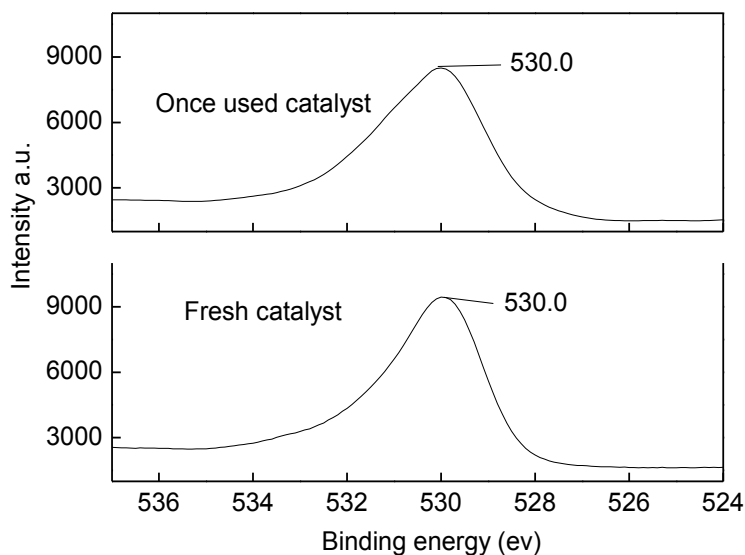
(a)



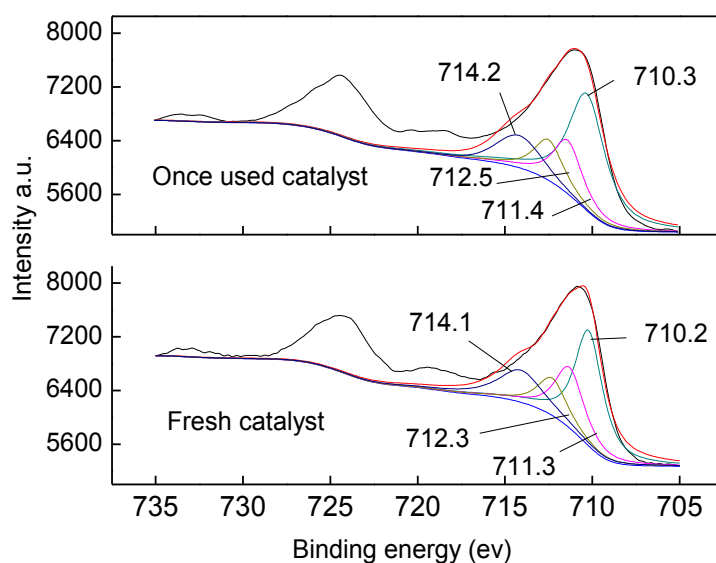
(b)

Fig. 7-2 Decolorization of Orange II (a) and remaining percentage of PDS (b) after 60 min of reaction under different systems ($C_0 = 25 \text{ mg/L}$, $[\text{PDS}] = 20 \text{ mM}$, $[\text{Fe}_3\text{O}_4] = 0.5 \text{ g/L}$, $j = 8.4 \text{ mA/cm}^2$, $\text{pH}_0 = 3.0$, $[\text{Na}_2\text{SO}_4] = 50 \text{ mM}$)

To verify the enhancement of the conversion of Fe(III) into Fe(II) in the process of EC/Fe₃O₄/PDS, the X-ray photoelectron spectroscopy was applied to characterize Fe₃O₄ before and after reaction. The domain peak for O 1s at 530.0 eV is characteristic of oxygen in a metal oxide (Zhao *et al.* 2012). The peak of Fe 2p spectrum at 710.6 and 724.4 eV represent Fe 2p_{3/2} and 2p_{1/2}, respectively, indicated the existence of Fe₃O₄ (Huang *et al.* 2012). As can be seen from Fig. 7-3(a), no significantly change was observed about O 1s XPS spectra before and after reaction. Before the reaction, the Fe2p_{3/2} spectrum fitted to four peaks located at binding energies (BE): 710.2, 711.3, 712.3 and 714.1 eV (Guo *et al.* 2010; Zhao *et al.* 2012). The peak at 710.2 eV could be assigned to the formation of ferrous oxide, where other peaks would be considered as the Fe(III) oxide (Fig. 7-3(b)). The ratio of Fe(II)/Fe(III) on the surface of Fe₃O₄ adsorbent increased from 0.75 to 1.09 after 60 min reaction. This implied more Fe(II) was generated on the surface of Fe₃O₄ particles in the electrochemical reactor (Eq. (7-6)).



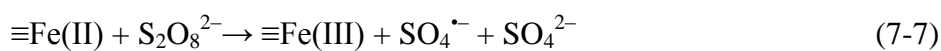
(a)



(b)

Fig. 7-3 O 1s (a) and Fe2p (b) XPS spectra of fresh and used Fe₃O₄ after the reaction

Based on the results and the literature (Liang *et al.* 2007; Özcan *et al.* 2009; Yan *et al.* 2011; Lin *et al.* 2013), the mechanism of EC/Fe₃O₄/PDS process was indicated in Fig. 7-4. Fe(II) was generated by the reduction and transformation of Fe(III) on the surface of Fe₃O₄ due to the direct electron transfer (Eq. (7-6)), and then Fe(II) activated PDS to release sulfate radicals via Eq. (7-7)). Meanwhile, hydroxyl radicals were generated both by water discharge on DSA anode (Eq. (7-4)) and the reaction between sulfate radicals and H₂O or OH⁻ (Eqs. (7-8) and (7-9)). Orange II was degraded by both sulfate radicals and hydroxyl radicals.



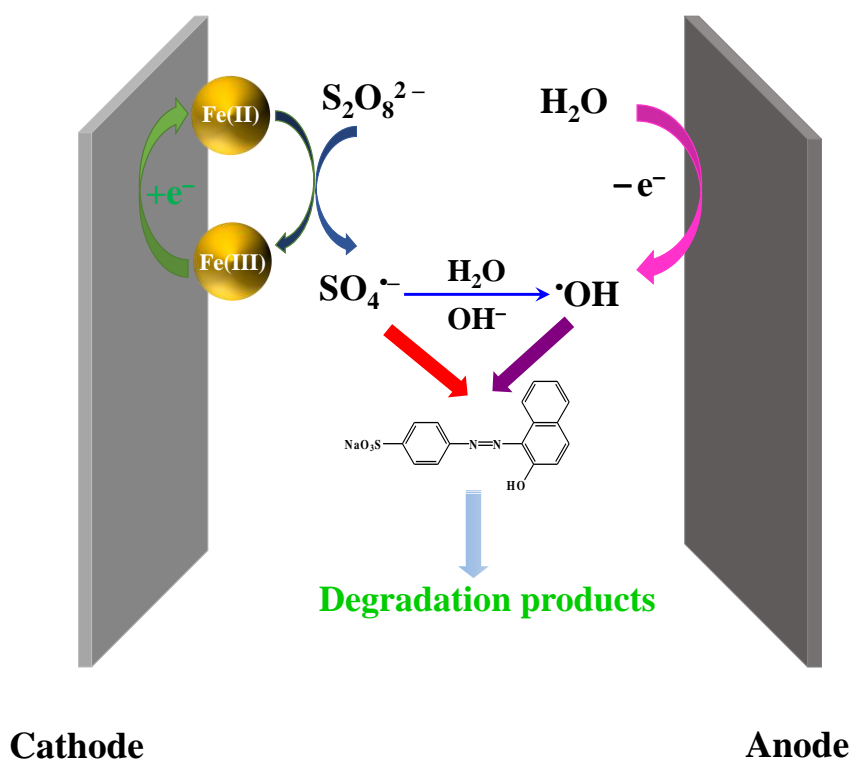


Fig. 7-4 Proposed mechanism of EC/ Fe_3O_4 /PDS process

The degradation kinetics of different systems was investigated and the results were summarized in Table 7-1. It can be seen that the decolorization of 25 mg/L Orange II by EC, EC/ Fe_3O_4 , EC/PDS and EC/ Fe_3O_4 /PDS process followed apparent first order kinetics and the apparent rate constants (k_{app}) were 0.015, 0.028, 0.030 and 0.043 min^{-1} , respectively, at pH 3.0.

Table 7-1 Kinetic coefficients and residual concentrations of PDS under various operating conditions

| Run | pH ₀ | Current density (mA/cm ²) | [PDS] (mM) | [Fe ₃ O ₄] (g/L) | k_{app} (min ⁻¹) | R ² | Residual [PDS] (mM) |
|-----|-----------------|---------------------------------------|------------|---|---------------------------------------|----------------|---------------------|
| 1 | 3.0 | 8.40 | 0 | 0 | 0.015 | 0.998 | – |
| 2 | 3.0 | 8.40 | 0 | 0.5 | 0.028 | 0.996 | – |
| 3 | 3.0 | 8.40 | 20 | 0 | 0.030 | 0.993 | 9.12 |
| 4 | 3.0 | 8.40 | 20 | 0.5 | 0.043 | 0.992 | 6.74 |

| | | | | | | | |
|----|-----|------|----|-----|-------|-------|-------|
| 5 | 6.0 | 8.40 | 20 | 0.5 | 0.039 | 0.995 | 7.56 |
| 6 | 9.0 | 8.40 | 20 | 0.5 | 0.037 | 0.996 | 7.14 |
| 7 | 6.0 | 3.36 | 20 | 0.5 | 0.027 | 0.988 | 11.60 |
| 8 | 6.0 | 16.8 | 20 | 0.5 | 0.071 | 0.989 | 4.04 |
| 9 | 6.0 | 25.2 | 20 | 0.5 | 0.117 | 0.973 | 2.92 |
| 10 | 6.0 | 8.40 | 5 | 0.5 | 0.030 | 0.998 | 1.45 |
| 11 | 6.0 | 8.40 | 10 | 0.5 | 0.053 | 0.994 | 2.70 |
| 12 | 6.0 | 8.40 | 10 | 0.2 | 0.029 | 0.991 | 2.92 |
| 13 | 6.0 | 8.40 | 10 | 0.8 | 0.057 | 0.969 | 2.10 |
| 14 | 6.0 | 8.40 | 10 | 1.2 | 0.049 | 0.976 | 2.10 |

7.3.2 Effect of initial pH

The effect of initial pH was observed when Orange II concentration was 25 mg/L, PDS concentration was 20 mM, Fe₃O₄ dosage was 0.5 g/L, Na₂SO₄ solution concentration was 50 mM and the electrical density was 8.4 mA/cm². As can be seen from Fig. 7-5, the decolorization efficiencies of Orange II were 93.0%, 91.2% and 92.1% at initial pH 3.0, 6.0 and 9.0, respectively. When initial pH ranged from 3.0 to 9.0, the rate constants varied slightly from 0.037 to 0.043 min⁻¹ (Table 7-1). Sulfate radicals generated in EC/Fe₃O₄/PDS process could react with H₂O or OH⁻ to produce hydroxyl radicals (Liang *et al.* 2007; Saien *et al.* 2011). Either H⁺ could be generated or OH⁻ could be consumed (Eqs. (7-8) and (7-9)), which resulted in the reduction of solution pH. Moreover, the dissociation of HSO₄⁻ (Eq. (7-10)), which was formed through Eq. (7-11), would further release H⁺ and decrease the solution pH (Kusic *et al.* 2011).



Therefore, the pH of Orange II solution after 60 min at different initial pH was almost the same (about 2.3). As a result, the decolorization efficiency of Orange II and the decomposition of PDS (Table 7-1) were similar at different initial pH values. This

proved that the EC/Fe₃O₄/PDS process could be successfully applied at a wide range of initial pH from 3.0 to 9.0. Since pH₀ 6.0 was the natural pH of 25 mg/L Orange II solution, it was selected in the following experiments.

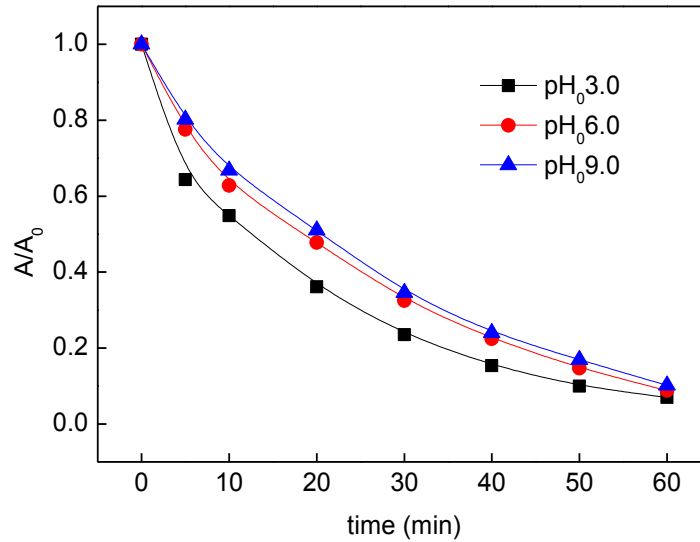


Fig. 7-5 The effect of initial pH on the oxidation efficiency of Orange II ($C_0 = 25$ mg/L, [PDS] = 20 mM, [Fe₃O₄] = 0.5 g/L, $j = 8.4$ mA/cm², [Na₂SO₄] = 50 mM)

7.3.3 Effect of current density

Fig. 7-6 illustrated the effect of current density with initial Orange II concentration of 25 mg/L, PDS concentration 20 mM, Fe₃O₄ dosage 0.5 g/L, Na₂SO₄ solution concentration 50 mM and the initial pH 6.0. The decolorization efficiency and apparent rate constant were 80.3% and 0.027 min⁻¹ (Table 7-1) in a 60 min reaction when current density was 3.4 mA/cm². When current density increased to 25.2 mA/cm², the decolorization efficiency was nearly 100% in 30 min reaction and the rate constant increased to 0.117 min⁻¹ (Table 7-1). On the one hand, when current density increased, more hydroxyl radicals would be formed on anode surface (Eq. (7-4)) and more sulfate radicals would be generated via electron transfer reaction (Eq. (7-5)). On the other hand, the increase of current density favored the cathodic reduction of Fe(III) (Eq. (7-6)), and more PDS would be activated to generate sulfate radicals via Eq. (7-7). Meanwhile, Table 7-1 demonstrated that the increase of current density from 3.34 to 25.2 mA/cm²

did cause the increase of PDS decomposition. This also suggested more sulfate radicals would be generated when current density increased.

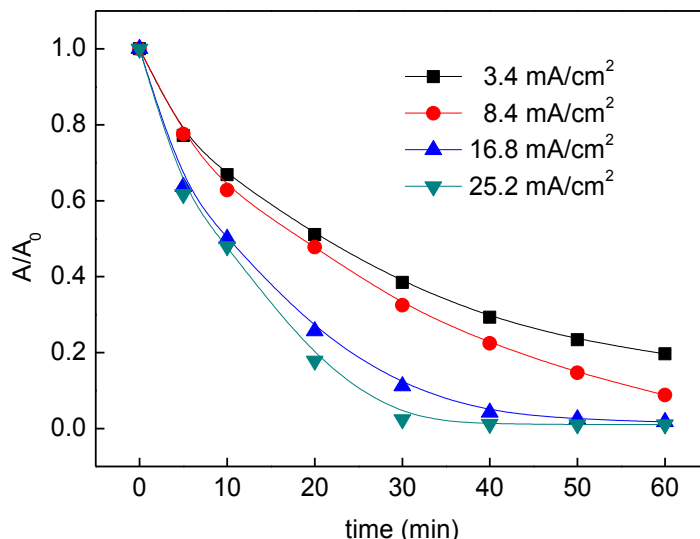


Fig. 7-6 The effect of current density on the oxidation efficiency of Orange II ($C_0 = 25$ mg/L, [PDS] = 20 mM, $[\text{Fe}_3\text{O}_4] = 0.5$ g/L, $\text{pH}_0 = 6.0$, $[\text{Na}_2\text{SO}_4] = 50$ mM)

7.3.4 Effect of PDS concentration

As the source of sulfate radicals, PDS plays a significant role in EC/ Fe_3O_4 /PDS process. The effect of PDS concentration was investigated by varying the concentration of PDS from 5 to 20 mM when Orange II concentration was 25 mg/L, Fe_3O_4 dosage was 0.5 g/L, Na_2SO_4 solution concentration was 50 mM, initial pH was 6.0 and the electrical density was 8.4 mA/cm². As can be seen from Fig. 7-7, when PDS concentration increased from 5 to 10 mM, the Orange II decolorization efficiency and apparent rate constants over a 60 min reaction increased from 84.1% to 95.8% and the rate constants increased from 0.030 to 0.053 min⁻¹ (Table 7-1). Meanwhile, the amount of PDS decomposed also increased, indicating more reactive radicals would be generated to degrade Orange II at higher PDS concentration. When PDS concentration increased to 20 mM, the Orange II decolorization efficiency and rate constants after 60 min declined slightly to 91.2% and 0.039 min⁻¹ (Table 7-1). This was due to the fact that the side reaction between $\text{S}_2\text{O}_8^{2-}$ and $\text{SO}_4^{\bullet-}$ became more significant (Eq. (7-12))

when PDS concentration was excessive (Hori *et al.* 2005; Wu *et al.* 2012b).



Therefore, 10 mM was selected as the optimal initial PDS concentration and used in the following experiments.

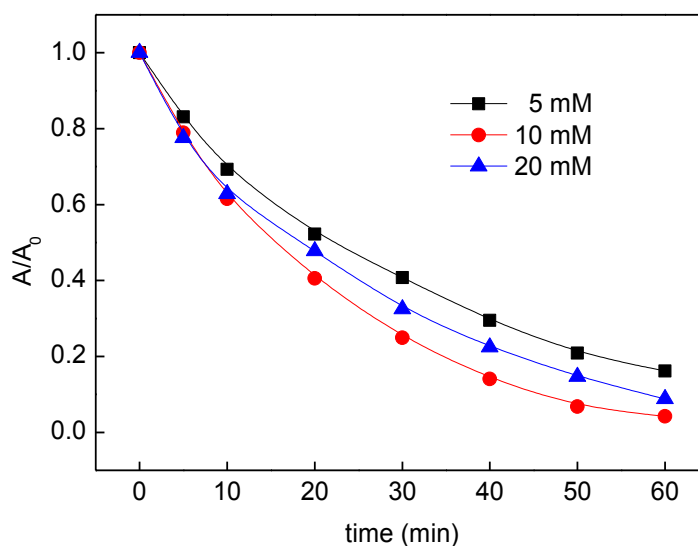
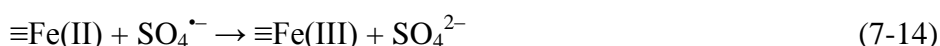


Fig. 7-7 The effect of PDS concentration on the oxidation efficiency of Orange II ($C_0 = 25$ mg/L, $[\text{Fe}_3\text{O}_4] = 0.5$ g/L, $\text{pH}_0 = 6.0$, $j = 8.4$ mA/cm², $[\text{Na}_2\text{SO}_4] = 50$ mM)

7.3.5 Effect of Fe_3O_4 dosage

The comparison of Orange II decolorization efficiency under different Fe_3O_4 dosage was investigated with initial Orange II concentration 25 mg/L, PDS concentration 10 mM, Na_2SO_4 solution concentration 50 mM, the initial pH 6.0 and the electrical density 8.4 mA/cm². The results were shown in Fig. 7-8. When Fe_3O_4 dosage varied from 0.2 to 0.8 g/L, the decolorization efficiency of Orange II within 60 min reaction increased from 83.9% to 97.6% and apparent rate constants increased from 0.029 to 0.057 min⁻¹ (Table 7-1). At higher Fe_3O_4 dosage, more Fe(II) could be generated through Eq. (7-5), and then a considerable amount of sulfate radicals would be produced via Eq. (7-6). These sulfate radicals reacted immediately with Orange II, leading to a fast increase of the Orange II decolorization. When Fe_3O_4 dosage further increased to 1.2 g/L, the Orange II decolorization efficiency declined slightly to 96.0%

and apparent rate constants decreased to 0.049 min^{-1} (Table 7-1). When Fe_3O_4 particles were added in excess, an excess of sulfate radicals would be generated, resulting in considerable disappearance of sulfate radicals without the degradation of Orange II due to the combination between sulfate radicals themselves (Eq. (7-13)). Moreover, the interaction between excess Fe(II) on the surface of Fe_3O_4 particles and sulfate radicals might directly quench sulfate radicals via Eq. (7-14) (Yan *et al.* 2011).



As a result, the decomposition of PDS increased with an increase in Fe_3O_4 dosage of up to 0.8 g/L (Table 7-1), and the highest decolorization efficiency of Orange II was obtained at Fe_3O_4 dosage of 0.8 g/L. This value was chosen as the optimal Fe_3O_4 dosage and applied in the following experiments.

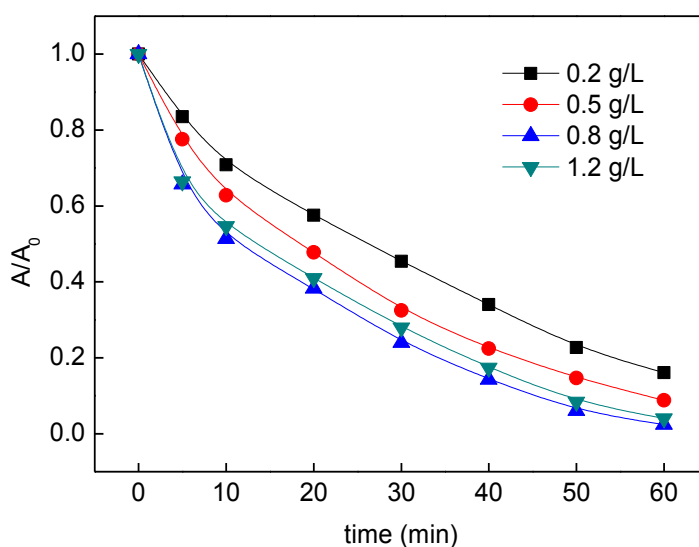
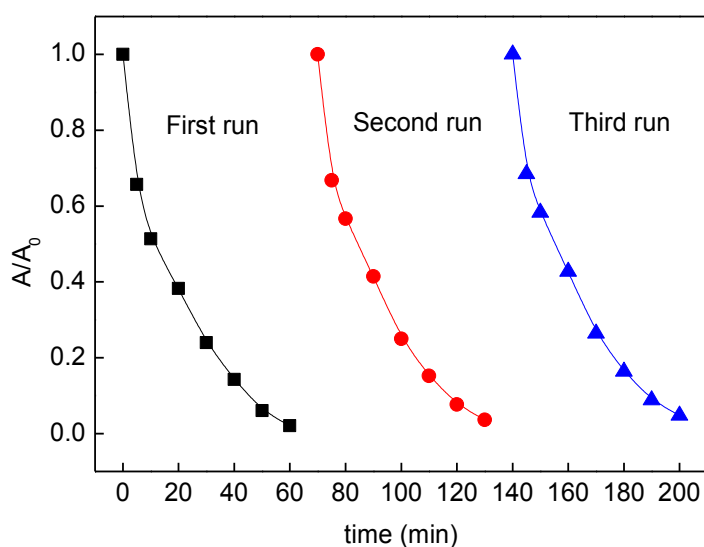


Fig. 7-8 The effect of Fe_3O_4 dosage on the oxidation efficiency of Orange II ($C_0 = 25 \text{ mg/L}$, $[\text{PDS}] = 10 \text{ mM}$, $\text{pH}_0 = 6.0$, $j = 8.4 \text{ mA/cm}^2$, $[\text{Na}_2\text{SO}_4] = 50 \text{ mM}$)

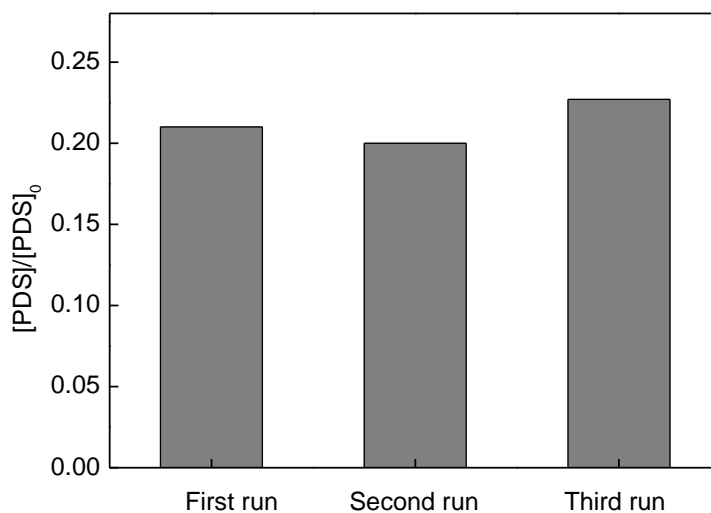
7.3.6 Stability of Fe_3O_4

The recycle experiments were performed to investigate the stability of Fe_3O_4 . The solid was easily removed from the electrochemical reactor after each repetitive oxidation process, then washed by deionised water, dried in the vacuum oven and stored

at ambient temperature. The initial concentration of Orange II solution was fixed at 25 mg/L, PDS concentration was 10 mM, Fe₃O₄ dosage was 0.8 g/L, Na₂SO₄ solution concentration was 50 mM, initial pH was 6.0 and the electrical density was 8.4 mA/cm². As shown in Fig. 7-9a, the decolorization efficiencies of Orange II during three reaction cycles ranged from 98.0% to 95.3%. The remaining percentages of PDS in each recycle experiment were similar (Fig. 7-9b). The metal leaching level was not obviously changed after three recycle time, with a Fe content in the solution at the end of the test almost constant at 13.05-32.72 mg/L. This indicated Fe₃O₄ is stable and can be reused.



(a)



(b)


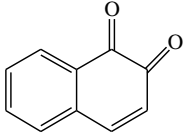
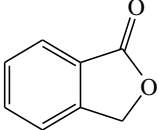
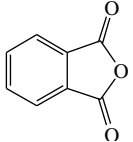
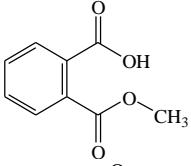
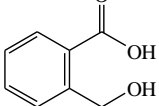
Fig. 7-9 Recycling study of the degradation of Orange II (a) and remaining percentage of PDS (b)

($C_0 = 25 \text{ mg/L}$, $[\text{PDS}] = 10 \text{ mM}$, $[\text{Fe}_3\text{O}_4] = 0.8 \text{ g/L}$, $\text{pH}_0 = 6.0$, $j = 8.4 \text{ mA/cm}^2$, $[\text{Na}_2\text{SO}_4] = 50 \text{ mM}$)

7.3.7 The degradation pathway of Orange II

GC–MS was employed to identify the intermediate products formed during EC/Fe₃O₄/PDS process. The main intermediate products detected were illustrated in Table 7-2 and a plausible degradation pathway was proposed (Fig. 7-10) based on the results and previous studies (Özcan *et al.* 2009; Zhao *et al.* 2010a; Zhong *et al.* 2011b). The cleavage of –N=N– of Orange II caused by electron transfer of sulfate radicals (Yuan *et al.* 2011) leads to the formation of sodium sulfanilamide and 1-amino-2-naphthol. Sodium sulfanilamide is thermally stable and highly soluble in water, whereas 1-amino-2-naphthol is oxygen sensitive and may be decomposed under aerobic conditions (Zhao *et al.* 2010a; Zhong *et al.* 2011b). Therefore, neither of these two intermediates was detected during GC–MS analysis. Afterwards, sodium sulfanilamide was subsequently oxidized to 1,4-benzoquinone (A). 1-amino-2-naphthol was firstly oxidized to 1,2-naphthalenedione (B). 1,2-naphthalenedione (B) was subsequently oxidized to the quinoid structures, resulting in the formation of 1(3H)-isobenzofuranone (C), phthalic anhydride (D), methyl hydrogen phthalate (E) and 2-(hydroxymethyl) benzoic acid (F) (Özcan *et al.* 2009, Zhao *et al.* 2010a)[1,50]. Further oxidation resulted in aromatic ring cleavage and generation of carboxylic acids and finally converted to CO₂ and H₂O.

Table 7-2 GC-MS identified reaction intermediates during EC/Fe₃O₄/PDS process

| Compound | Retention time (min) | Chemical name | Chemical structure |
|----------|----------------------|--------------------------------|---|
| A | 6.03 | 1,4-benzoquinone |  |
| B | 16.02 | 1,2-naphthalenedione |  |
| C | 12.75 | 1(3H)-isobenzofuranone |  |
| D | 12.24 | phthalic anhydride |  |
| E | 12.26 | methyl hydrogen phthalate |  |
| F | 12.83 | 2-(hydroxymethyl) benzoic acid |  |

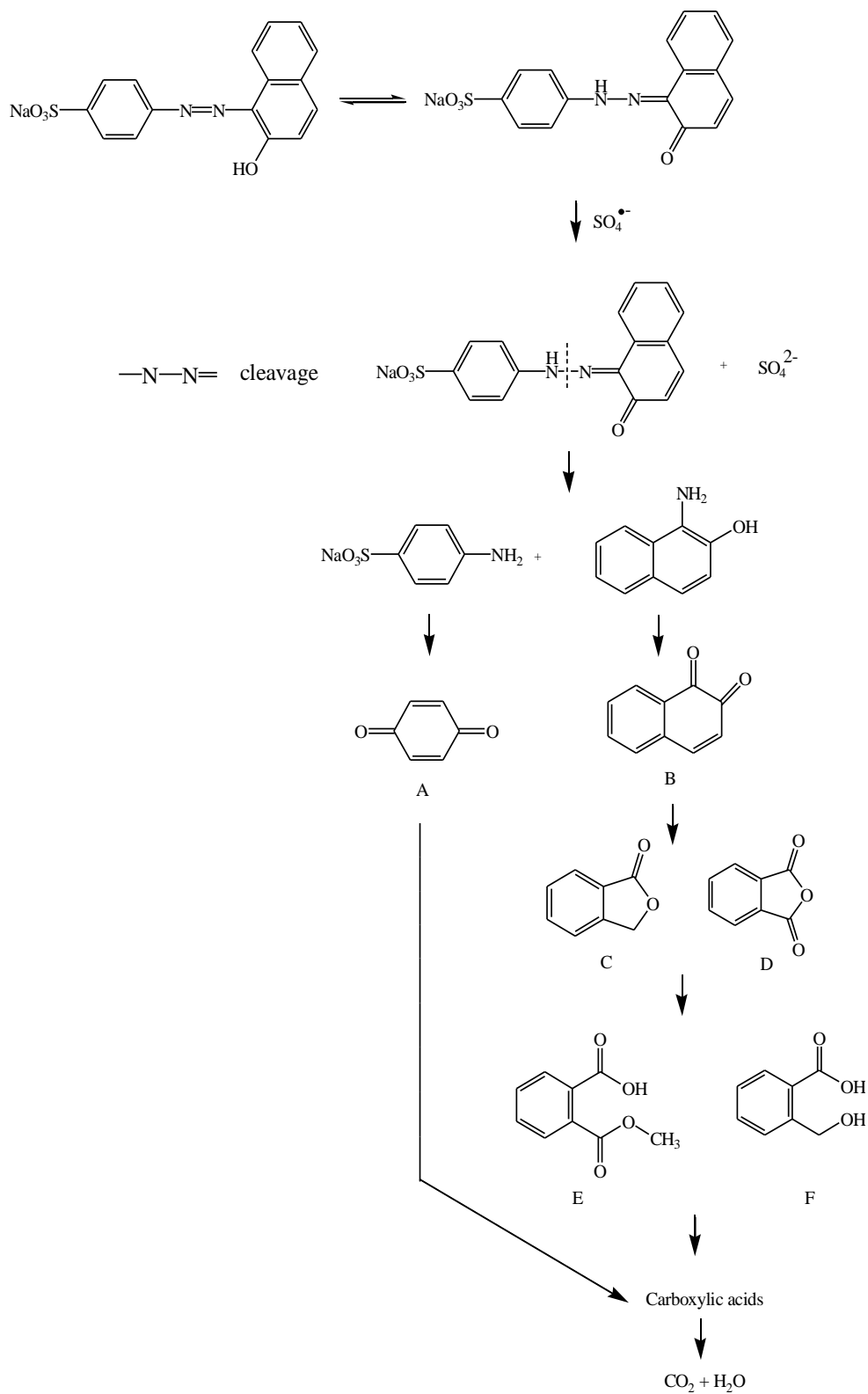


Fig. 7-10 Proposed pathway for the oxidation of Orange II by EC/Fe₃O₄/PDS process

7.3.8 The changes of TOC and toxicity with reaction time

In order to clarify the mineralization efficiency of Orange II in EC/Fe₃O₄/PDS

process, the changes of TOC were investigated with initial Orange II concentration 25 mg/L, PDS concentration 10 mM, Fe₃O₄ dosage 0.8 g/L, Na₂SO₄ solution concentration 50 mM, initial pH value 6.0 and the current density 16.8 mA/cm². As can be seen in Fig. 7-11, Orange II was almost completely removed after a 60 min reaction, but the TOC removal efficiency was only 19.6%. Further prolong of reaction time to 90 min, the TOC removal efficiency achieved 30.0%. This indicated part of Orange II was converted to smaller intermediates. The variation of acute toxicity in EC/Fe₃O₄/PDS process was monitored by oxygen uptake (Olmez-Hanci *et al.* 2009; Olmez-Hanci *et al.* 2010,). As indicated in Fig.7-11, the SOUR value decreased at the beginning of the reaction, indicating more toxic products were generated. It has been illustrated in Section 7.3.7 that the main intermediates formed at the early stage of the treatment are 1,4-benzoquinone (A) and 1,2-naphthalenedione (B). Therefore, the higher toxicity observed at the beginning of EC/Fe₃O₄/PDS process can be attributed to the formation of these intermediates, because the toxicity of quinones is well-known (Hammami *et al.* 2008). After 30 to 90 min reaction, the value of SOUR increased gradually. This means further treatment could convert these intermediates to less toxic products and mineralization led to the detoxification of treated solution.

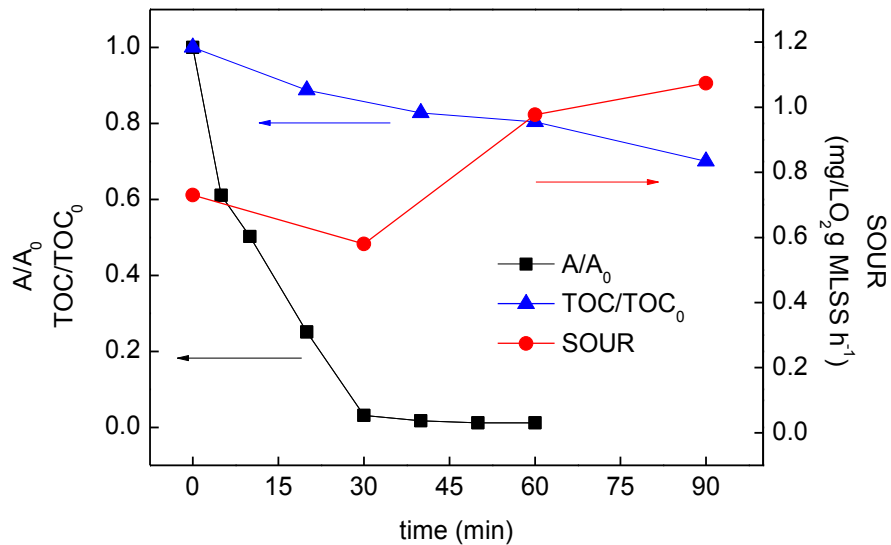


Fig. 7-11 The changes of TOC, Orange II concentration and SOUR with reaction time ($C_0 = 25$ mg/L, [PDS] = 10 mM, [Fe₃O₄] = 0.8 g/L, $j = 16.8$ mA/cm², pH₀ 6.0, [Na₂SO₄] = 50 mM)

7.3.9 Electrical energy consumption estimation

In order to evaluate the energy consumption of EC/Fe₃O₄/PDS process, an electrical energy consumption per order of magnitude (EE/O) was employed. EE/O is defined as the number of kilowatt hours of electrical energy required for bringing about the degradation of a pollutant by one order of magnitude (90%) in 1 m³ of contaminated water (Daneshvar *et al.* 2007; Sadik 2007a; Sadik 2007b; Behnajady *et al.* 2009).

$$EE/O \text{ (kWh m}^{-3} \text{ order}^{-1}\text{)} = \frac{U_{cell}It}{V \log(A_0/A)} \quad (7-15)$$

where U_{cell} is the average cell voltage (V), I is the current (A), t is the electrolysis time (h) and V is the volume (L).

The electrical energy consumption for Orange II degradation under different reaction systems were summarized in Table 7-3. It can be seen from Table 7-3 that the electrocatalysis processes were more energy saving than the photocatalysis processes. For example, EE/O value was 273.9 (kWh m⁻³ order⁻¹) for UV/TiO₂ process, while EC/Fe₃O₄ process only needed 19.65 (kWh m⁻³ order⁻¹) electrical energy consumption. What's more, the presence of oxidant (H₂O₂ or PDS) could improve electrocatalysis and photocatalysis, and the associated electrical energy consumption decreased. Table 4 indicated that the EE/O value of EC/Fe₃O₄/PDS process was less than one-half of EC/Fe₃O₄ process.

Table 7-3 Comparison of electrical consumption under the different reaction system

| Method | Operating parameters | EE/O (kWh m ⁻³ order ⁻¹) | Ref. |
|--|---|---|---------------------------|
| UV/TiO ₂ | [Orange II] ₀ = 17.5 mg/L, [TiO ₂] = 0.5 g/L, pH ₀ 6.1 43 W UV lamp | 273.9 | Sadik 2007b |
| EC/Fe ₃ O ₄ | [Orange II] ₀ = 25 mg/L, [Fe ₃ O ₄] = 0.5 g/L, $j = 8.$ mA/cm ² , pH ₀ 3.0, [Na ₂ SO ₄] = 50 mM | 19.65 | Lin <i>et al.</i> 2013 |
| UV/TiO ₂ /H ₂ O ₂ | [Orange II] ₀ = 17.5 mg/L, [H ₂ O ₂] = 71 mM, [TiO ₂] = 0. g/L, , pH ₀ 6.1, 43 W UV lamp | 40.45 | Sadik 2007b |
| UV/TiO ₂ +ZnO/PDS | [Orange II] ₀ = 17.5 mg/L, [PDS] = 8.5 mM, [TiO ₂ +ZnO | 18.08 | Sadik |

= 0.25 g/L, , pH₀ 6.1, 43 W UV lamp

2007a

EC/Fe₃O₄/PDS [Orange II]₀ = 25 mg/L, [PDS] = 10 mM, [Fe₃O₄] = 0.8 g/L, *j* = 8.4 mA/cm², pH₀ 6.0, [Na₂SO₄] = 50 mM 8.69 this study

7.4 Conclusions

Aqueous solutions of Orange II have been degraded effectively in the EC/Fe₃O₄/PDS process, in which Fe₃O₄-activated PDS process is enhanced by the electrochemical process. The effect of initial pH, current density, PDS concentration and Fe₃O₄ dosage, on the Orange II decolorization was investigated. The results indicated that Orange II can be totally decolorized in a 60 min reaction when initial Orange II concentration was 25 mg/L, PDS concentration was 10 mM, Fe₃O₄ dosage was 0.8 g/L, current density was 8.4 mA/cm² and initial pH was 6.0. Recycle experiments showed Fe₃O₄ particles were stable and can be reused. XPS spectrum indicated Fe(II) was generated on the surface of Fe₃O₄ particles after reaction. The main intermediates were separated and identified by GC–MS technique and a plausible degradation pathway of Orange II was proposed.

References

- Behnajady, M.A., Modirshahla, N., Shokri, M. and Vahid, B. (2009). Design equation with mathematical kinetic modeling for photooxidative degradation of C.I. Acid Orange 7 in an annular continuous-flow photoreactor. *Journal of Hazardous Materials* 165(1–3), 168-173.
- Daneshvar, N., Rasoulifard, M.H., Khataee, A.R. and Hosseinzadeh, F. (2007). Removal of C.I. Acid Orange 7 from aqueous solution by UV irradiation in the presence of ZnO nanopowder. *Journal of Hazardous Materials* 143(1–2), 95-101.
- Guo, L., Chen, F., Fan, X., Cai, W. and Zhang, J. (2010). S-doped α -Fe₂O₃ as a highly active heterogeneous Fenton-like catalyst towards the degradation of acid orange 7 and phenol. *Applied Catalysis B: Environmental* 96(1–2), 162-168.
- Hammami, S., Bellakhal, N., Oturan, N., Oturan, M.A. and Dachraoui, M. (2008). Degradation of Acid Orange 7 by electrochemically generated \cdot OH radicals in acidic aqueous medium using a boron-doped diamond or platinum anode: A mechanistic study. *Chemosphere* 73(5), 678-684.
- Lin, H., Hou L., Zhang, H (2013). Degradation of Orange II in aqueous solution by a novel electro/Fe₃O₄ process. *Water Science and Technology* 68 (11), 2441-2447.
- Hori, H., Yamamoto, A., Hayakawa, E., Taniyasu, S., Yamashita, N., Kutsuna, S., Kiatagawa, H. and Arakawa, R. (2005). Efficient decomposition of environmentally persistent perfluorocarboxylic acids by use of persulfate as a photochemical oxidant. *Environmental Science & Technology* 39(7), 2383-2388.
- Huang, R., Fang, Z., Yan, X. and Cheng, W. (2012). Heterogeneous sono-Fenton catalytic degradation of bisphenol A by Fe₃O₄ magnetic nanoparticles under neutral condition. *Chemical Engineering Journal* 197, 242-249.
- Kusic, H., Peternel, I., Ukic, S., Koprivanac, N., Bolanca, T., Papic, S. and Bozic, A.L. (2011). Modeling of iron activated persulfate oxidation treating reactive azo dye in water matrix. *Chemical Engineering Journal* 172(1), 109-121.
- Liang, C., Wang, Z.S. and Bruell, C.J. (2007). Influence of pH on persulfate oxidation of TCE at ambient temperatures. *Chemosphere* 66(1), 106-113.
- Lin, H., Wu, J. and Zhang, H. (2013). Degradation of bisphenol A in aqueous solution

- by a novel electro/ Fe^{3+} /peroxydisulfate process. *Separation and Purification Technology* 117, 18-23.
- Olmez-Hanci, T., Dalmaz, B., Arslan-Alaton, I., Kabdaşlı, I. and Tünay, O. (2010). Kinetic modeling and toxicity assessment of diethyl phthalate treated by H_2O_2 /UV-C process. *Ozone: Science & Engineering* 32(4), 238-243.
- Olmez-Hanci, T., Imren, C., Arslan-Alaton, I., Kabdasl, I. and Tunay, O. (2009). H_2O_2 /UV-C oxidation of potential endocrine disrupting compounds: a case study with dimethyl phthalate. *Photochemical & Photobiological Sciences* 8(5), 620-627.
- Özcan, A., Oturan, M.A., Oturan, N. and Şahin, Y. (2009). Removal of Acid Orange 7 from water by electrochemically generated Fenton's reagent. *Journal of Hazardous Materials* 163(2–3), 1213-1220.
- Sadik, W.A. (2007a). Decolourization of an azo dye by heterogeneous photocatalysis. *Process Safety and Environmental Protection* 85(6), 515-520.
- Sadik, W.A. (2007b). Effect of inorganic oxidants in photodecolourization of an azo dye. *Journal of Photochemistry and Photobiology A: Chemistry* 191(2–3), 132-137.
- Saien, J., Soleymani, A.R. and Sun, J.H. (2011). Parametric optimization of individual and hybridized AOPs of $\text{Fe}^{2+}/\text{H}_2\text{O}_2$ and UV/ $\text{S}_2\text{O}_8^{2-}$ for rapid dye destruction in aqueous media. *Desalination* 279(1–3), 298-305.
- Wahba, N., El Asmar, M.F. and El Sadr, M.M. (1959). Iodometric method for determination of persulfates. *Analytical Chemistry* 31(11), 1870-1871.
- Wu, J., Liu, F., Zhang, H., Zhang, J. and Li, L. (2012a). Decolorization of CI Reactive Black 8 by electrochemical process with/without ultrasonic irradiation. *Desalination and Water Treatment* 44(1-3), 36-43.
- Wu, J., Zhang, H. and Qiu, J. (2012b). Degradation of Acid Orange 7 in aqueous solution by a novel electro/ Fe^{2+} /peroxydisulfate process. *Journal of Hazardous Materials* 215–216, 138-145.
- Yan, J., Lei, M., Zhu, L., Anjum, M.N., Zou, J. and Tang, H. (2011). Degradation of sulfamonomethoxine with Fe_3O_4 magnetic nanoparticles as heterogeneous activator of persulfate. *Journal of Hazardous Materials* 186(2–3), 1398-1404.
- Yuan, R., Ramjaun, S.N., Wang, Z. and Liu, J. (2011). Effects of chloride ion on

- degradation of Acid Orange 7 by sulfate radical-based advanced oxidation process: Implications for formation of chlorinated aromatic compounds. *Journal of hazardous materials* 196, 173-179.
- Zhao, H.-Z., Sun, Y., Xu, L.-N. and Ni, J.-R. (2010a). Removal of Acid Orange 7 in simulated wastewater using a three-dimensional electrode reactor: Removal mechanisms and dye degradation pathway. *Chemosphere* 78(1), 46-51.
- Zhao, H., Wang, Y., Wang, Y., Cao, T. and Zhao, G. (2012). Electro-Fenton oxidation of pesticides with a novel Fe₃O₄@Fe₂O₃/activated carbon aerogel cathode: High activity, wide pH range and catalytic mechanism. *Applied Catalysis B: Environmental* 125, 120-127.
- Zhao, J., Zhang, Y., Quan, X. and Chen, S. (2010b). Enhanced oxidation of 4-chlorophenol using sulfate radicals generated from zero-valent iron and peroxydisulfate at ambient temperature. *Separation and Purification Technology* 71(3), 302-307.
- Zhong, X., Royer, S., Zhang, H., Huang, Q., Xiang, L., Valange, S. and Barrault, J. (2011a). Mesoporous silica iron-doped as stable and efficient heterogeneous catalyst for the degradation of C.I. Acid Orange 7 using sono-photo-Fenton process. *Separation and Purification Technology* 80(1), 163-171.
- Zhong, X., Xiang, L., Royer, S., Valange, S., Barrault, J. and Zhang, H. (2011b). Degradation of C.I. Acid Orange 7 by heterogeneous Fenton oxidation in combination with ultrasonic irradiation. *Journal of Chemical Technology & Biotechnology* 86(7), 970-977.

Chapter 8 General conclusion and future perspectives

8.1 General conclusion

In this paper, electro-Fenton and electro-Fenton-like processes were used to degrade artificial sweeteners and azo dyes. The results obtained during this thesis work concern the removal efficiency, the oxidation mechanism, degradation pathway and toxicity evolution of target pollutants.

(1) Electro-Fenton process was an effective method for the degradation of ASP in water. The oxidative degradation rate and mineralization efficiency were affected mainly by the catalyst (Fe^{2+}) concentration and applied current. The absolute rate constant of hydroxylation reaction of ASP was found as to be $(5.23 \pm 0.02) \times 10^9 \text{ M}^{-1} \text{ s}^{-1}$. Short-chain aliphatic acids such as oxalic, oxamic and maleic acid were identified as aliphatic intermediates in the electro-Fenton process. The bacteria luminescence inhibition showed the toxicity of ASP solution decreased, during the treatment, after reaching a maximum during the first period of the oxidation reaction.

(2) Artificial sweetener SAC could be degraded effectively by electro-Fenton process with a DSA, Pt or BDD anode. However, the using of BDD anode could accelerate the mineralization of SAC. The optimal conditions for SAC removal were SAC concentration 0.2 mM, Fe^{2+} concentration 0.2 mM, Na_2SO_4 concentration 50 mM, applied current 200 mA and initial pH 3.0. Oxalic, formic, and maleic acids were observed as aliphatic by-products of SAC during electro-Fenton process. The bacteria luminescence inhibition showed the toxicity of SAC solution increased at the beginning of electrolysis, and then it declined until the end of the reaction.

(3) Artificial sweetener SUC could be completely mineralized in a 360 min reaction by electro-Fenton process with a Pt or BDD anode. The mineralization rate was affected mainly by the Fe^{2+} concentration and applied current. The mineralization current efficiency (MCE) decreased with rising applied current from 100 to 500 mA with both Pt and BDD anodes. Oxalic, pyruvic, formic and glycolic acids were detected during the oxidation of SUC.

(4) Orange II was effectively decolorized by EC/ α -FeOOH/PDS process. The initial pH of Orange II solution had little effect on the decolorization of Orange II. RSM

based on Box-Behnken statistical experiment design was applied to analyze the experimental variables. The response surface methodology models were derived based on the results of the pseudo-first-order decolorization rate kinetics and the response surface plots were developed accordingly. The results indicated that the applied current showed a positive effect on the decolorization rate constant of Orange II. The interaction of α -FeOOH dosage and PDS concentration were significant. The ANOVA results confirmed that the proposed models were accurate and reliable for the analysis of the variables of EC/ α -FeOOH/PDS process. The catalyst α -FeOOH showed good structural stability and could be reused.

(5) Aqueous solutions of Orange II have been degraded effectively in the EC/Fe₃O₄/PDS process. The decolorization rate was affected by the initial pH of Orange II solution, current density, PDS concentration and Fe₃O₄ dosage. Orange II can be totally decolorized in a 60 min reaction time when initial Orange II concentration was 25 mg/L, PDS concentration was 10 mM, Fe₃O₄ dosage was 0.8 g/L, current density was 8.4 mA/cm² and initial pH was 6.0. Recycle experiments showed that Fe₃O₄ particles were stable and can be reused. XPS spectrum indicated that Fe(II) was generated on the surface of Fe₃O₄ particles after reaction. The main reaction intermediates of Orange II were separated and identified by GC–MS technique and a plausible degradation pathway was proposed.

8.2 Future perspectives

Further studies can be developed as follows:

(1) Finding out the suitable method to detect the intermediate products of artificial sweeteners and then obtain the degradation pathway;

(2) In the sulfate radical-based electro-Fenton-like process, persulfate is remained in the solution after the reaction. Moreover, persulfate can be decomposed to SO₄⁻ and H⁺, resulting the decline of the pH value. So it is important to separate persulfate and SO₄⁻ from the treated solution.

(3) Both sulfate radicals and hydroxyl radicals are contributed to the degradation

of organic contaminants in the sulfate radical-based electro-Fenton-like process. When attacking organic compounds, hydroxyl radicals are more likely to do through hydrogen abstraction or addition reactions, while sulfate radicals participate in electron transfer reaction. Therefore, further investigation can focus on the different by-products generated under the attack of these two radicals.

(4) All the solutions contained organic pollutants are synthetic wastewaters which were prepared in the lab. In the future, we can use eletro-Fenton and sulfate radical-based electro-Fenton-like processes to degrade target pollutants in actual wastewater.

Publications

- [1] **Heng. Lin**, Hui. Zhang, Liwei. Hou, Degradation of C. I. Acid Orange 7 in aqueous solution by a novel electro/Fe₃O₄/PDS process, *Journal of Hazardous Materials*, 276 (2014) 182-191.
- [2] **Heng. Lin**, Jie. Wu, Hui. Zhang, Degradation of clofibrac acid in aqueous solution by an EC/Fe³⁺/PMS process, *Chemical Engineering Journal*, 244 (2014) 514-521.
- [3] **Heng. Lin**, Jie. Wu, Hui. Zhang, Degradation of bisphenol A in aqueous solution by a novel electro/Fe³⁺/peroxydisulfate process, *Separation and Purification Technology*, 117 (2013) 18-23.
- [4] **Heng. Lin**, Hui. Zhang, Xue. Wang, Ligu. Wang, Jie. Wu, Electro-Fenton removal of Orange II in a divided cell: Reaction mechanism, degradation pathway and toxicity evolution, *Separation and Purification Technology*, 122 (2014) 533-540.
- [5] **Heng. Lin**, Liwei. Hou, Hui. Zhang, Degradation of Orange II in aqueous solution by a novel electro/Fe₃O₄ process, *Water Science and Technology*, 68 (2013) 2441-2447.
- [6] **Heng Lin**, Hui Zhang, Treatment of organic pollutants using electro-Fenton and electro-Fenton-like process in aqueous solution, *Progress in Chemistry*, accepted.